AD_____

Award Number: DAMD17-02-1-0001

TITLE: Genetic Radiotherapy of Prostate Cancer

PRINCIPAL INVESTIGATOR: Donald J. Buchsbaum, Ph.D.

CONTRACTING ORGANIZATION: The University of Alabama at Birmingham
Birmingham, Alabama 35294-0111

REPORT DATE: December 2004

TYPE OF REPORT: Final

PREPARED FOR: U.S. Army Medical Research and Materiel Command
Fort Detrick, Maryland 21702-5012

DISTRIBUTION STATEMENT: Approved for Public Release;
Distribution Unlimited

REPORT DOCUMENTATION PAGE

Form Approved
OMB No. 074-0188

1. AGENCY USE ONLY (Leave blank)	2. REPORT DATE	3. REPORT TYPE AND DATES COVERED
	December 2004	Final (1 Dec 2001 - 30 Nov 2004)

4. TITLE AND SUBTITLE
Genetic Radiotherapy of Prostate Cancer

5. FUNDING NUMBERS
DAMD17-02-1-0001

6. AUTHOR(S)
Donald J. Buchsbaum, Ph.D.

7. PERFORMING ORGANIZATION NAME(S) AND ADDRESS(ES)
The University of Alabama at Birmingham
Birmingham, Alabama 35294-0111

E-Mail: djb@uab.edu

8. PERFORMING ORGANIZATION REPORT NUMBER

9. SPONSORING / MONITORING AGENCY NAME(S) AND ADDRESS(ES)
U.S. Army Medical Research and Materiel Command
Fort Detrick, Maryland 21702-5012

10. SPONSORING / MONITORING AGENCY REPORT NUMBER

11. SUPPLEMENTARY NOTES

12a. DISTRIBUTION / AVAILABILITY STATEMENT
Approved for Public Release; Distribution Unlimited

12b. DISTRIBUTION CODE

13. ABSTRACT (Maximum 200 Words)

The goal to achieve a high intratumoral concentration of 5-fluorouracil (5-FU) *via* molecular chemotherapy employing adenoviral (Ad) vectors encoding the genes for somatostatin receptor subtype 2 (SSTr2) and cytosine deaminase (CD) which converts the prodrug 5-fluorocytosine (5-FC) to 5-FU under control of the cyclooxygenase-2 (Cox-2) tumor-specific promoter was achieved. We evaluated novel two-gene Ad vectors: (1) a native fiber Ad (AdCMVCDCMVSSTr2) and (2) Ad under control of the Cox-2 promoter expressing CD and SSTr2. We produced several vectors including AdCox-2LCDCox-2LSSTr2, AdCox-2LSSTr2Cox-2LCD, AdRGDCox-2LCDCox-2LSSTr2, and AdRGDCox-2LCDCox-2LSSTr2. The vectors were tested for SSTr2 and CD expression employing membrane receptor binding *in vitro* with ^{125}Isomatostatin and ^{99m}Tc-P2045 that binds to SSTr2, conversion of 5-FC to 5-FU, and cytotoxicity against Ad infected cells in the presence of 5-FC. The vectors were evaluated *in vivo* for SSTr2 expression and CD expression. Efforts to produce RGD modified vectors expressing CD and SSTr2 under control of the Cox-2L promoter were not successful. We identified chimeric Ad5/3 virus with the Cox-2L promoter driving CD and SSTr2 to have therapeutic efficacy against prostate cancer xenografts, and identified that Ad virus expressing CDUPRT was more efficacious than CD in combination with 5-FC and radiation therapy.

14. SUBJECT TERMS
Prostate cancer, gene therapy, molecular chemotherapy, transcriptional targeting, cytosine deaminase, somatostatin receptor, brachytherapy

15. NUMBER OF PAGES
105

16. PRICE CODE

17. SECURITY CLASSIFICATION OF REPORT	18. SECURITY CLASSIFICATION OF THIS PAGE	19. SECURITY CLASSIFICATION OF ABSTRACT	20. LIMITATION OF ABSTRACT
Unclassified	Unclassified	Unclassified	Unlimited

TABLE OF CONTENTS

INTRODUCTION

The objective of this project was to develop novel two gene adenovirus (Ad) vectors expressing human somatostatin receptor subtype 2 (SSTr2) and cytosine deaminase (CD) under control of the cyclooxygenase-2 (Cox-2) promoter for radiolabeled peptide therapy/molecular chemotherapy of prostate cancer. The tumor specific promoter Cox-2 was selected based on the fact that it is active in prostate cancer, and the liver is Cox-2 negative and is the predominant site of Ad vector localization after systemic administration. Thus, the Ad may infect normal liver cells but no transgene expression would occur.

Two forms of the Cox-2 promoter were compared to the cytelomegalovirus (CMV); a "long" form (Cox-2L) and a truncated "medium" form (Cox-2M). It was shown that the Cox-2L promoter resulted in greater CD activity than the Cox-2M promoter so we focused on the Cox-2L promoter. However, the level of CD conversion of 5-fluorocytosine (5-FC) to 5-fluorouracil (5-FU) was lower than with CMV. This led to an investigation of alternative promoters including flt-1 and survivin. Another goal was to determine if transductional targeting with the RGD peptide in the HI-loop of the knob of the Ad vector would result in greater SSTr2 and CD expression. It was determined that the RGD modified vectors were not more effective than the non-RGD modified Ad. Thus, we pursued a second transductional modification in which the Ad3 fiber was genetically expressed in the Ad5 virus since there is minimal or absent expression of the Ad5 coxsackie and adenovirus receptor (CAR) on cancer cells. This proved to be the more useful approach. The new vectors were evaluated *in vivo* for SSTr2, CD expression, and antitumor efficacy using prostate cancer xenograft models. Based upon these results, we investigated expression of the fusion protein CD:uracil phosphoribosyl transferase (CDUPRT) to overcome 5-FU resistance.

BODY

Statement of Work (SOW) Specific Aim 1 Task 1 and Task 2: To develop, validate, and evaluate genetically modified Ad vectors that will selectively express both SSTr2 and CD in the context of prostate cancer compared to normal tissues (especially liver where systemically injected Ad vectors localize) and our first generation AdCMVSSTr2 and AdCMVCD vectors. Cellular Cox-2 mRNA status and promoter activity was determined in LNCap, DU145, and PC3 human prostate cancer cells using Ad vectors expressing luciferase. DU145 and PC3 cells expressed Cox-2 mRNA and their Cox-2L promoter activity was 70% and 100% of CMV promoter activity (**Figure 1**). However, LNCap cells did not express COX-2 mRNA.

SOW Specific Aim 1 Task 2 and Specific Aim 2 Task 1: The vectors that we developed were tested for magnitude of SSTr2 expression employing membrane receptor binding *in vitro*. Seven vectors expressing CD and/or SSTr2 were developed and evaluated using the prostate cancer cell lines DU145 and PC3: AdCox-2LCDCox-2LSSTr2, AdCox-2LSSTr2Cox-2LCD, AdRGDCox-2LCDCox-2LSSTr2, AdCMVCDCMVSSTr2, AdCMVCD, AdRGDCMVCD, and AdRGDCMVCDCMVSSTr2. Somatostatin binding and internalization assays were performed by incubating infected cells with ^{99m}Tc-P2045, a peptide specific for SSTr2, and gamma camera imaging of cells in plates 5 min after addition of peptide and 20 min later after removing the excess peptide and stripping the peptide bound to SSTr2 on the cell surface.[1,2] As shown in **Figure 2**, DU145 prostate cancer cells infected with AdCMVSSTr2, AdCox-2LCDCox-2LSSTr2, or AdCox-2LSSTr2Cox-2LCD showed binding and internalization of ^{99m}Tc-P2045, demonstrating that the vectors all induced SSTr2 expression, although the Cox-2L vectors produced less SSTr2 expression than the CMV vector. In addition, AdCox-2LSSTr2Cox-2LCD produced more SSTr2 expression than AdCox-2LCDCox-2LSSTr2.

SOW Specific Aim 2 Task 1, Task 2 and Task 3: Athymic nude mice bearing DU145 prostate cancer xenografts were injected intratumorally with AdCMVSSTr2 or AdCox-2LSSTr2 followed 2 days later by *i.v.* injection of ^{99m}Tc-P2045. As shown in **Figures 3** and **4**, there was less accumulation of ^{99m}Tc-P2045 in tumors injected with AdCox-2LSSTr2 compared to AdCMVSSTr2. Scatchard analysis demonstrated higher SSTr2 expression in DU145 and PC3 cells infected with the RGD modified AdRGDCMVCDCMVSSTr2 than following infection with AdCMVCDCMVSSTr2 or AdCMVSSTr2 (**Figure 5** and **Table 1**). These results indicate that the Cox-2 vectors produced less SSTr2 expression than the CMV vector both *in vitro* and *in vivo*, and indicate the importance of producing RGD modified Cox-2 vectors.

Table 1. Binding of ^{125}I-somatostatin to human prostate cancer cell lines 48 h after infection with 100 MOI of each virus.

	DU145		PC3	
	B_{max}	fmol/μg	B_{max}	fmol/μg
AdCMVSSTr2	364913	4.4	125852	1.5
AdCMVCDCMVSSTr2	238182	2.7	93592	1.1
AdRGDCMVCDCMVSSTr2	501701	5.6	276868	3.1

SOW Specific Aim 1 Task 1 and Task 2: CD conversion assays were performed with lysates from infected cells with the addition of ^{3}H-5-fluorocytosine (5-FC) at various time points, and separation on thin layer chromatography plates in butanol and water.[3] Spots containing 5-FC and 5-fluorouracil (5-FU) were cut out, put into scintillation fluid, and counted in a liquid scintillation counter. Cytotoxicity assays were performed using the MTS assay (Promega) as described in the manufacturer's protocol. CD expression in tumor xenografts was detected by immunohistochemistry. CD conversion assays were also performed with lysates from prostate cancer xenografts. Tumors were homogenized and lysed, and CD conversion assays performed as described for cellular lysates.

The vectors expressing CD and SSTr2 were next tested to determine their conversion of 5-FC to 5-FU following infection of DU145 and PC3 human prostate cancer cell lines. The results from two or three independent experiments with different lots of virus are presented in **Table 2.**[3] They indicate that AdCox-2LCD, AdCox-2LCDCox-2LSSTr2, and AdCox-2LSSTr2Cox-2LCD produced a lower level of conversion of 5-FC to 5-FU in DU145 and PC3 cells than AdCMVCD and AdCMVCDCMVSSTr2. Furthermore, AdRGDCMVCD produced a level of conversion that was significantly greater than AdCMVCD. The highest level of CD expression in DU145 tumor xenografts occurred following infection with AdCMVCD as compared to AdCox-2LCDCox-2LSSTr2 or AdCox-2LSSTr2Cox-2LCD (**Figure 6**). These results support earlier ones that the CMV promoter is stronger than the Cox-2 promoter, although less specific. Moreover, the RGD modified CMV viruses produced the highest level of conversion, whereas the RGD modified Cox-2L viruses (AdRGDCox-2LCD and AdRGDCox-2LCDCox-2LSSTr2) did not produce CD, suggesting a problem in their design. Efforts to redesign the RGD modified COX-2L viruses were unsuccessful, and we were not able to identify the problem.

Table 2. Conversion of 5-FC to 5-FU in pmol/min/mg measured over a 1 h period at 48 h after infection of DU145 and PC3 human prostate cancer cell lines with 100 MOI of each virus.

Vector	DU145 (pmol/min/mg)	PC3 (pmol/min/mg)
Uninfected	-0.01	0.00
AdCMVCD	25.6	8.1
AdCMVSSTr2	0.04	-0.02
AdCMVCDCMVSSTr2	7.5, 7.8	2.5, 4.5
AdCox-2LCD	2.1	1.0
AdCox-2LCDCox-2LSSTr2	3.0, 1.2, 2.7	1.2, 4.3, 4.5
AdCox-2LSSTr2Cox-2LCD	2.5	0.9
AdRGDCMVCD	150.4	194.0
AdRGDCMVCDCMVSSTr2	38.5, 29.1, 13.2	35.6, 28.5, 53.9
AdRGDCox-2LCD	1.1	0.5
AdRGDCox-2LCDCox-2LSSTr2	0.1, -0.2, -0.8	0.04, 1.1, 1.6

In the next set of studies, we evaluated the cytotoxicity of the various vectors after infection of DU145 cells with 10 MOI (plaque forming units/cell) of virus. The 5-FC IC_{50} values are shown in **Table 3.** The results indicate that AdCox-2LCDCox-2LSSTr2 produced equivalent cytotoxicity compared to AdCMVCD, whereas AdCMVCDCMVSSTr2, AdRGDCMVCD, and AdRGDCMVCDCMVSSTr2 produced the greatest degree of cytotoxicity. The level of cytotoxicity was lowest in the AdRGDCox-2LCD and AdRGDCox-2LCDCox-2LSSTR2 infected cells. These results are consistent with the conversion results shown in **Table 2**, and again suggest a problem with the RGDCox-2L vectors.

Table 3. Cytotoxicity of Ad infected DU145 human prostate cancer cells (10 MOI) exposed to 5-FC expressed as IC_{50} (nM).

Vector	DU145
Uninfected	165.9
AdCMVCD	31.0
AdCMVCDCMVSSTr2	3.4
AdRGDCMVCD	2.2
AdCox-2LCDCox-2LSSTr2	30.4
AdRGDCox-2LCD	114.9
AdRGDCMVCDCMVSSTr2	0.9
AdRGDCox-2LCDCox-2LSSTr2	128.1

Thus, we pursued a second transductional modification in which the Ad3 fiber was genetically expressed in the Ad5 virus to eliminate the need of the Ad5 coxsackie adenovirus receptor (CAR) binding for virus entry. The SSTr2 expression and CD results with the fiber chimeric Ad5/3 virus are shown in **Tables 4** and **5** and **Figure 7**. They show a higher rate of CD conversion *in vitro* compared to the unmodified Cos-2L viruses.

Table 4. Conversion of 5-FC to 5-FU in pmol/min/mg measured over a 1 h period at 48 h after infection of DU145 and PC3 human prostate cancer cell lines with 100 MOI of Ad.

Vector	DU145 (pmol/min/mg)	PC3 (pmol/min/mg)
Ad5/3Cox-2LCDCox-2LSSTr2	1.9	3.1
Ad5Cox-2LCDCox-2LSSTr2	2.7	4.5

Table 5. Binding of ^{125}I-somatostatin to human prostate cancer cells infected with Ad vectors and blocked with cold octreotide.

Vector	DU145		PC3	
	+	Block (-)	+	Block (-)
Uninfected	8.0	8.3	7.1%	6.5%
Ad5Cox-2LCDCox-2LSSTr2 (1,000VP)	7.8%	7.0%	7.6%	6.6%
Ad5/3Cox-2LCDCox-2LSSTr2 (1,000VP)	8.6%	7.6%	10.4%	6.9%
Ad5/3Cox-2LCDCox-2LSSTr2 (100 MOI)	10.2%	7.7%	14.9%	6.7%

SOW Specific Aim 2 Task 2 and Task 3 and Specific Aim 3 Task 1: We evaluated CD and SSTr2 two-gene vectors in *in vivo* tumor models after intratumoral delivery of the vector. The transduction of the tumor nodules was evaluated by radiolabeled peptide uptake in the tumor and other normal tissues.[4-6] Gamma camera imaging of ^{99m}Tc-P2045 showed localization in a DU145 *s.c.* tumor injected with AdCox-2LSSTr2.[4] On the basis of the results with the chimeric Ad5/3Cox-2L vector, an *in vivo* therapy study was carried out in athymic nude mice bearing established *s.c.* PC3 xenografts which were injected intratumorally with $5x10^6$ viral particles (VP) of Ad5Cox-2LCDCox-2LSSTr2, Ad5/3Cox-2LCDCox-2LSSTr2, or Ad5Luc and treated with 5-FC (400 mg/kg 2x/day x7) and ^{60}Co radiation (5x2 Gy). The results are shown in **Figure 8**. There was greater tumor growth inhibition with the chimeric Ad5/3Cox-2L vector than the Ad5Cox-2L vector. However, there were no complete regressions.

SOW Specific Aim 1 Task 2: Based on these results, we investigated Flt-1 as an alternative promoter.[7] Flt-1 (VEGF receptor) occurs in various types of tumors, including prostate carcincoma. The Flt-1 promoter exhibits a "liver off" phenotyhpe when used in Ad vectors. To evaluate the ability of the Flt-1 promoter to drive cell-specific gene expression, analysis of ß-galactosidase production from AdFlt-LacZ Ad infection was performed. Since the efficiency of gene transfer differs between cell types, infectivity for each cell type was normalized to a positive control, *LacZ* gene delivery driven by the CMV promoter (AdCMV-LacZ). This normalization is expressed as a ratio of the transfection effectiveness of AdFlt-LacZ to AdCMV-LacZ, where transfection efficiency is defined as the percentage of cells expressing *LacZ* gene out of the entire population. Forty-eight h after AdFlt-LacZ or AdCMV-LacZ infection cells were harvested and ß-galactosidase activity was analyzed by ß-galactosidase enzyme assay (**Figure 9A**). As expected, the highest levels of Flt-1 driven LacZ expression were observed in HUVEC human and SVEC4-10 murine endothelial cells and were relatively high in hormone-independent DU145 (p53-mutant) and PC3 (p53-negative) human prostate cancer cells in comparison with normal human bronchial epithelial BEAS-2B cells.

We hypothesized that the activity of the Flt-1 promoter would correlate to the relative levels of Flt-1

mRNA expression in the tested cell lines. Flt-1 and GAPDH (as control) mRNA levels were assessed by RT-PCR. The comparative levels of the LacZ expression of prostate cancer cells correlated with VEGF receptor mRNA expression. DU145 prostate cancer cells demonstrated detectable levels of Flt-1 mRNA expression in comparison with BEAS-2B control cells, whereas PC3 cells showed low level Flt-1 mRNA expression (**Figure 9B**). Comparing the Flt-1 promoter with CMV promoter driven reporter expression, specificity of Flt-1 promoter for HUVEC endothelial cells and prostate cancer cells was demonstrated.

Ionizing radiation has an important role in localized prostate cancer treatment. We further sought to determine whether ionizing radiation alters Flt-1 promoter activity. Radiation treatment at 3 Gy increased LacZ expression driven by the Flt-1 promoter by 61% in DU145 prostate cancer cells and 34% in HUVEC endothelial cells *in vitro* (**Figure 9C**). To test whether VEGF protein expression modulates Flt-1 promoter activity in combination with ionizing radiation, DU145 prostate cancer cells and HUVEC cells were infected with AdFlt-Luc Ad vector, exposed to ionizing radiation and incubated with recombinant human VEGF (rhVEGF). As shown in **Figure 9D**, incubation in presence of rhVEGF alone and in combination with radiation treatment significantly increased ($p<0.05$) Flt-1-driven Luc expression in HUVEC endothelial cells (220 and 282%, respectively) in comparison with AdFlt-Luc-infected DU145 prostate cancer cells (139 and 151%). These data provide evidence of relatively high levels of Flt-1 promoter activity in human endothelial cells and prostate cancer cells *in vitro*.

A major factor limiting 5-FU-based therapy and potentially CD/5-FC molecular chemotherapy for prostate cancer is 5-FU resistance, which is due in part to intratumoral 5-FU catabolism to inactive metabolites by the enzyme dihydropyrimidine dehydrogenase (DPD). One strategy to overcome high intratumoral expression of DPD involves expression of the enzyme uracil phosphoribosyltransferase (UPRT). This enzyme converts 5-FU to 5-fluorouracil monophosphate (5-FUMP), the next metabolite in the 5-FU anabolism pathway. Coexpression of CD and UPRT as a fusion protein (CDUPRT) has been shown to sensitize human tumor cells to both 5-FC and 5-FU *in vitro*, and to greatly augment CD/5-FC efficacy *in vivo*. Based upon these results, we hypothesized that Ad-mediated CDUPRT/5-FC may be useful as an adjunct to radiation therapy in the management of prostate cancer.

5-FC cytotoxicity to cells infected with either AdCMVCD or AdCMVCDUPRT at various MOI (10-300) was determined after 5 days of continuous exposure.[8] As shown in **Table 6**, 5-FC cytotoxicity to prostate cancer cell lines after viral infection was variable. LNCaP cells were the most susceptible to 5-FC after infection with either AdCMVCD or AdCMVCDUPRT, PC3 cells displayed an intermediate level of sensitivity, and DU145 cells were the least sensitive. However, in all 3 cells lines, coexpression of CD and UPRT from AdCMVCDUPRT rendered cells much more sensitive to 5-FC (range 6-125 fold) than CD expression alone from AdCMVCD. The magnitude of enhancement in 5-FC sensitivity between AdCMVCDUPRT and AdCMVCD varied among cell lines, with LNCaP>PC3>DU145 cells in order of decreasing sensitivity (increasing IC_{50}). These data demonstrate a significant enhancement in 5-FC cytotoxicity to prostate cancer cells after Ad-mediated expression of CDUPRT versus CD alone.

Table 6. AdCMVCD versus AdCMVCDUPRT mediated 5-FC cytotoxicity to human prostate cancer cells *in vitro*

Cell Line	MOI (pfu/cell)	5-FC IC_{50} (μg/ml)		Enhancement
		AdCMVCD	AdCMVCDUPRT	
DU145	10	>200	20.3 ± 1.6 (3)	>10
	100	24.8 ± 0.6 (3)	0.7 ± 0.7 (4)	34
	300	15.4 ± 15.4 (2)	0.3 ± 0.01 (2)	56
LNCaP	1	15.8 (1)	ND	
	10	3.9 ± 0.7 (3)	0.03 ± 0.01 (4)	125
	100	1.0 ± 0.4 (3)	0.01 ± 0.001 (4)	108
PC3	1	>200 34.4 (1)	>6	
	10	26.6 ± 0.02 (2)	1.6 ± 0.7 (3)	17
	100	5.7 ± 1.9 (4)	0.2 ± 0.2 (3)	24
	300	4.6 ± 1.5 (2)	0.1 (1)	46

Mean ± SEM 5-FC IC_{50} determined by piecewise linear regression from log-linear dose-response curves (6 replicates at 10 separate drug concentrations) from 1-4 separate experiments. ND, not determined.

To determine whether the AdCMVCDUPRT-mediated enhancement of 5-FC cytotoxicity was due to UPRT expression, 5-FU cytotoxicity to PC3 cells was determined after infection with AdCMVCDUPRT versus AdCMVCD. Compared to treatment with 5-FU alone, no change in 5-FU sensitivity was seen after infection with a high dose of AdCMVCD (100 pfu/cell, IC_{50} 0.22 versus 0.15, $p>0.05$). However, a significant decrease in 5-FU cytotoxicity was apparent after infection with either 10 or 30 pfu/cell of AdCMVCDUPRT (IC_{50} 0.005 versus 0.003, respectively, $p<0.001$). These data suggest that the enhanced cytotoxicity of CDUPRT/5-FC was due to UPRT mediated conversion of 5-FU to its downstream toxic metabolite 5-FUMP.

SOW Specific Aim 3 Task 1: The efficacy of AdCMVCDUPRT/5-FC/XRT therapy in local tumor control was assessed using a subcutaneous xenograft model of DU145 in nude mice. The effect of coexpression of CD and UPRT was assessed by comparing the efficacy of AdCMVCD/5-FC versus AdCMVCDUPRT/5-FC with or without XRT (**Figure 10**). In general, AdCMVCDUPRT-containing regimens achieved an increased level of growth inhibition compared to AdCMVCD-containing regimens.

SOW Specific Aim 4: No evidence for uptake of Ad vectors in tumor xenografts following systemic *i.v.* injection was obtained either in terms of targeting of ^{99m}Tc-P2045 or by CD expression. The bulk of gene expression and targeting occurred in the liver. This problem has been universal for all investigators using Ad vectors. Based on the results presented, it appears that the Flt-1 promoter driving CDUPRT and SSTr2 would be a good choice for future studies because the promoter is expressed in prostate cancer but not hepatocytes, its expression is increased by radiation, and CDUPRT showed greater efficacy compared to CD. Retargeting of the Ad vector to vascular endothelial targets might result in selective gene expression following systemic injection.

KEY RESEARCH ACCOMPLISHMENTS

- Validated the expression of SSTr2 and CD in tumor cells and xenografts after infection with Ad vectors expressing SSTr2 and CD under control of Cox-2L promoter.
- Identified Flt-1 promoter as being active in prostate cancer cell lines.
- Validated expression of SSTr2 in prostate cancer cells after infection with chimeric Ad5/3Cox-2L vector.
- Determined the conversion of 5-FC to 5-FU in prostate cancer cells and tumor xenografts.
- Demonstrated cytotoxicity of prostate cancer cells infected with Ad vectors under control of Cox-2L promoter expressing CD and exposed to 5-FC.
- Demonstrated localization of ^{99m}Tc-P2045 which binds to SSTr2 in tumor xenografts infected with SSTr2 expressing Ad vectors.
- Showed that AdCMVCDUPRT and 5-FC produced increased cytotoxicity of prostate cancer cells compared to AdCMVCD and 5-FC.
- Determined therapeutic efficacy of chimeric Ad5/3Cox-2LCDCox-2LSSTr2 in combination with 5-FC and radiation therapy against prostate cancer xenografts.
- Showed that AdCMVCDUPRT/5-FC and radiation produced greater growth inhibition of prostate cancer xenografts than AdCMVCD/5-FC and radiation.

REPORTABLE OUTCOMES

Developed new Ad vectors expressing both SSTr2 and CD under control of CMV and Cox-2L promoters. Developed new Ad vector expressing CDUPRT under control of CMV.

CONCLUSIONS

In conclusion, the combination of the therapeutic genes CD and SSTr2 with the Cox-2L or FLt-1 promoter should provide specificity for tumor uptake of radiolabeled peptides that bind to SSTr2 and selective 5-FC molecular chemotherapy. Transductional targeting with the chimeric Ad5/3 virus enhanced infectivity in human prostate carcinoma. The most promising approach involves the Flt-1 promoter which is increased by radiation in combination with the CDUPRT and SSTr2 genes in an Ad vector.

ABBREVIATIONS

Ad	adenoviral
CD	cytosine deaminase
CDUPRT	cytosine deaminase uracil phosphoribosyl transferase
Cox-2	cyclooxygenase-2
CMV	cytomegalovirus
DPD	dihydropyrimidine dehydrogenase
5-FC	5-fluorocytosine
5-FU	5-fluorouracil
Flt-1	vascular endothelial growth factor receptor
SSTr2	somatostatin receptor subtype 2

REFERENCES

1. Zinn KR, Chaudhuri TR, Buchsbaum DJ, Mountz JM, and Rogers BE. Simultaneous evaluation of dual gene transfer to adherent cells by gamma-ray imaging. Nucl Med Biol, *28:* 135-144, 2001.
2. Zinn KR, Chaudhuri TR, Buchsbaum DJ, Mountz JM, and Rogers BE. Detection and measurement of *in vitro* gene transfer by gamma camera imaging. Gene Ther, *8:* 291-299, 2001.
3. Della Manna DL, Yamamoto M, Krasnykh V, Zinn KR, Davydova J, Chiz S, and Buchsbaum DJ. New adenoviral vectors for molecular chemotherapy of prostate cancer. Mol Ther, *7:* S315-S316, 2003.
4. Buchsbaum DJ, Chaudhuri TR, Yamamoto M, and Zinn KR. Gene expression imaging with radiolabeled peptides. Ann Nucl Med, *18:* 275-283, 2004.
5. Buchsbaum DJ, Chaudhuri TR, and Zinn KR. Radiotargeted gene therapy. J Nucl Med Suppl In press, 2004.
6. Buchsbaum DJ. Imaging and therapy of tumors induced to express somatostatin receptor by gene transfer using radiolabeled peptides and single chain antibody constructs. Semin Nucl Med, *34:* 32-46, 2004.
7. Kaliberov SA, Kaliberova L, Stockard CR, Grizzle WE, and Buchsbaum DJ. Adenovirus-mediated flt-1 targeted proapoptotic gene therapy of human prostate cancer. Mol Ther, *10:* 1059-1070, 2004.
8. Williams CR, Buchsbaum DJ, and Miller CR. Adenovirus-mediated cytosine deaminase/5-fluorocytosine gene therapy of experimental human prostate cancer is enhanced by uracil phosphoribosyltransferase. Submitted, 2004.

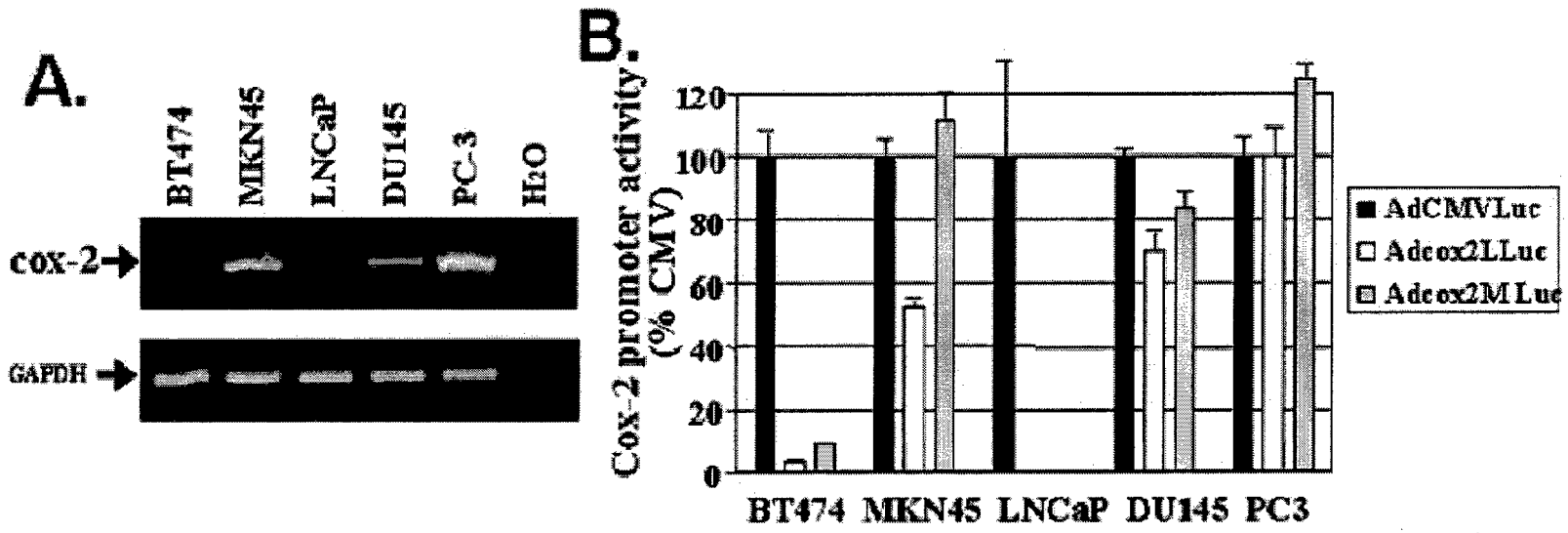

Figure 1. Cellular Cox-2 mRNA status and promoter activity in prostate cancer cells.

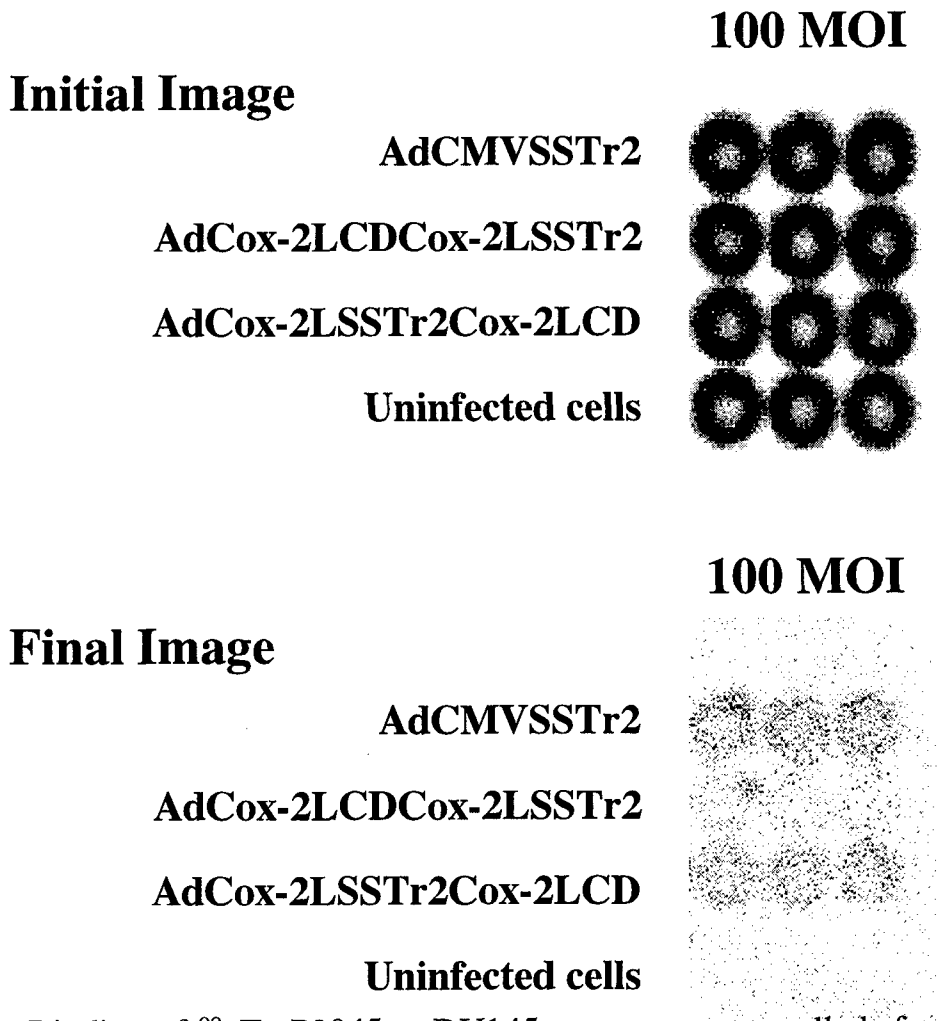

Figure 2. Binding of ^{99m}Tc-P2045 to DU145 prostate cancer cells before (initial) and after (final) washing of cells detected by gamma camera imaging.

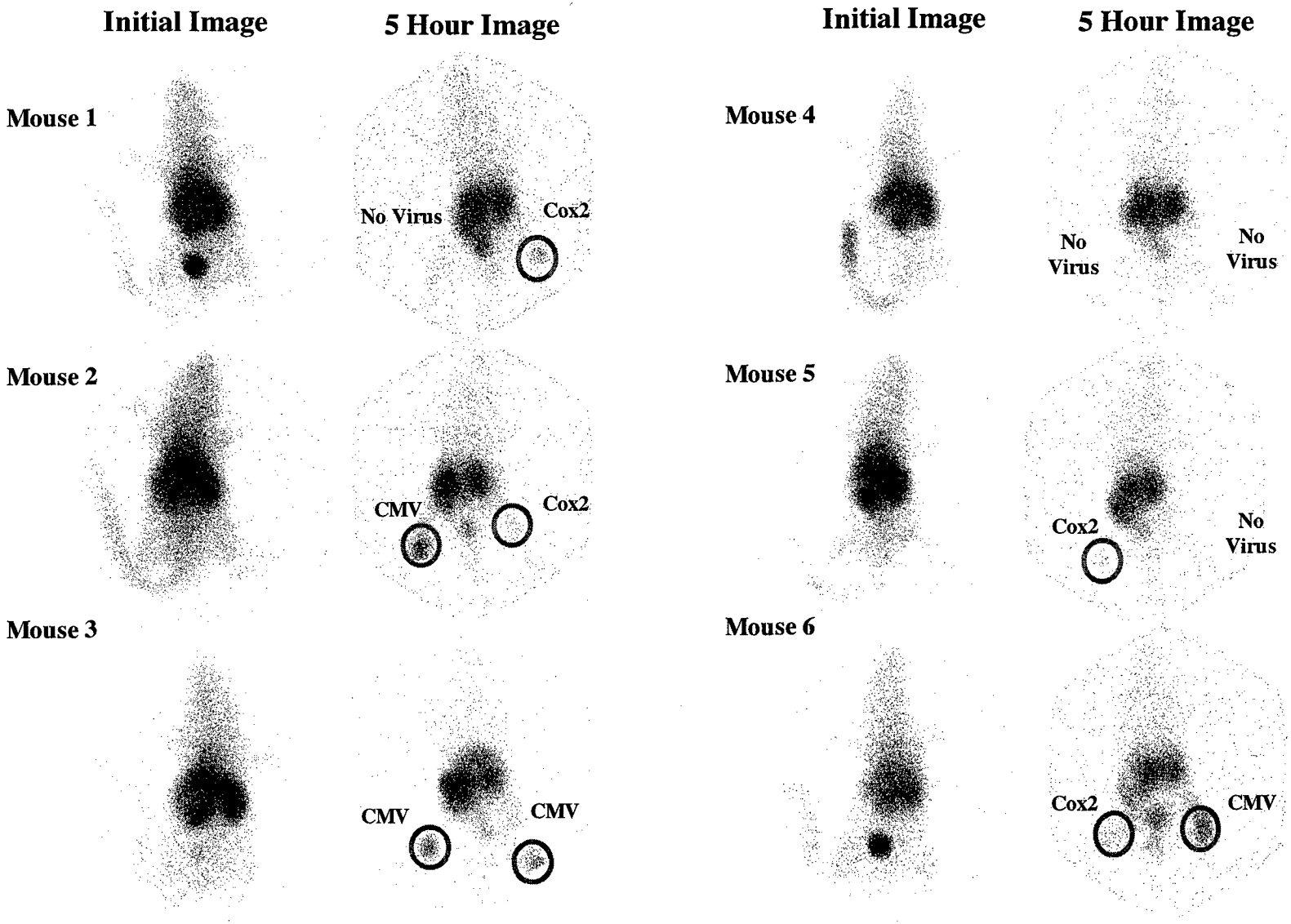

Figure 3. Gamma camera images of mice bearing DU145 prostate cancer xenografts injected intratumorally with AdCMVSSTr2 or AdCox-2LSSTr2 followed 2 days later by *i.v.* administration of ^{99m}Tc-P2045.

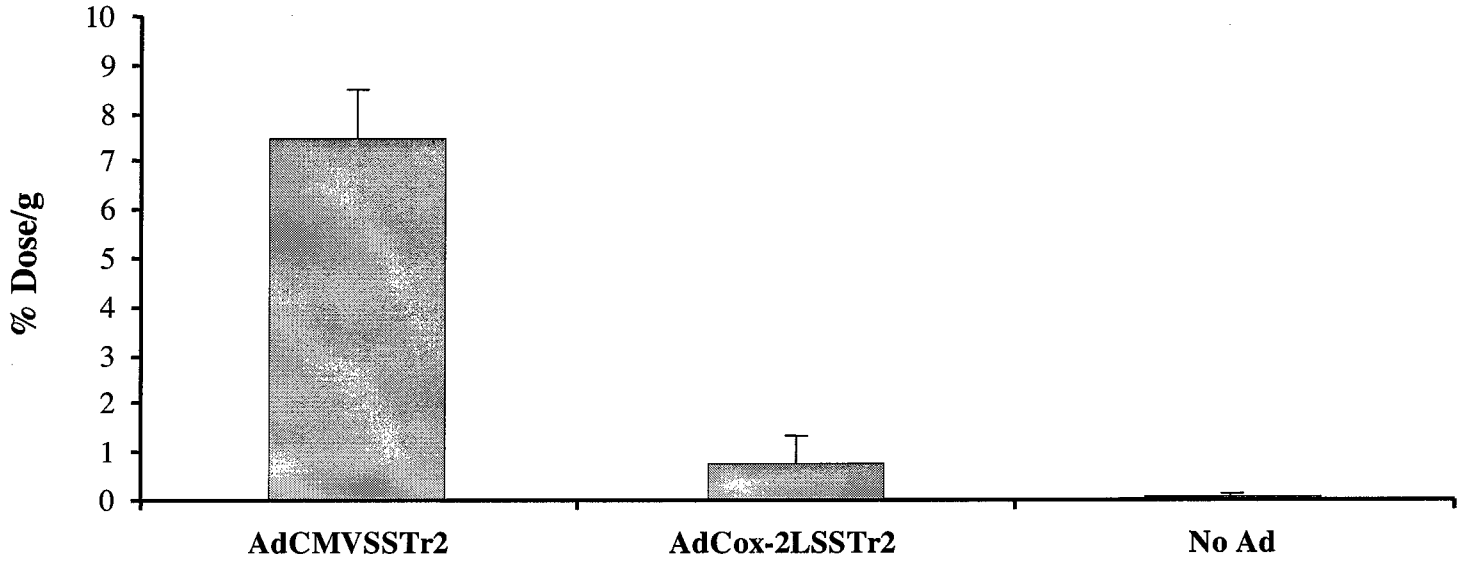

Figure 4. ^{99m}Tc-P2045 localization in DU145 prostate cancer xenografts injected intratumorally with AdCMVSSTr2 or AdCox-2LSSTr2.

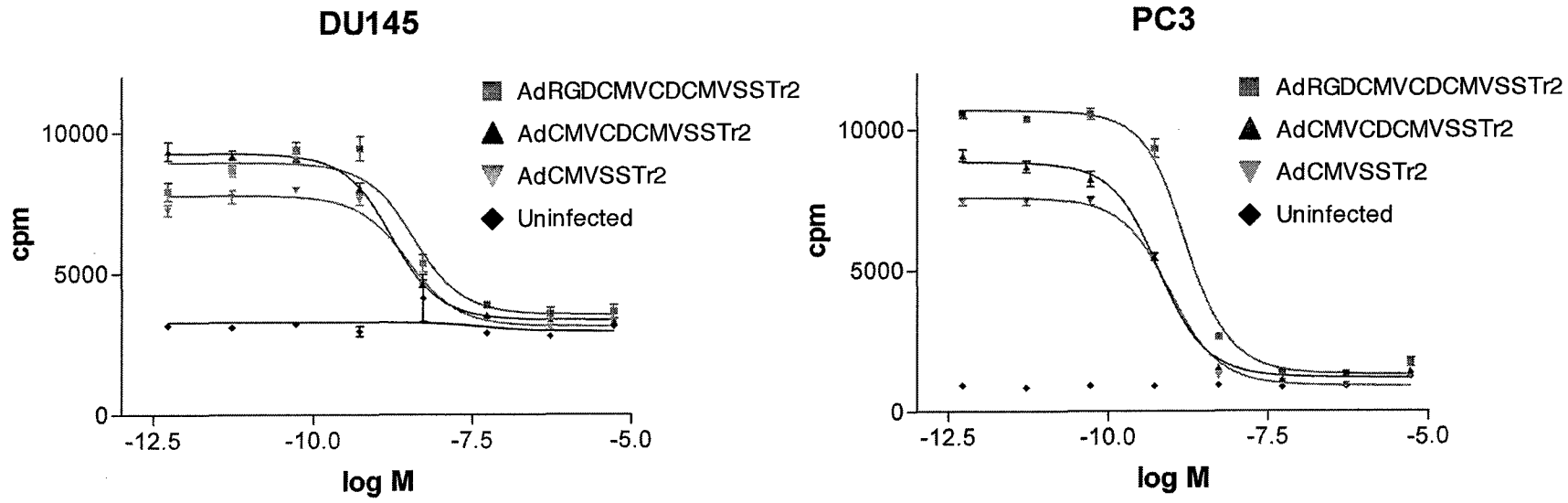

Figure 5. Scatchard analysis of DU145 and PC3 human prostate cancer cells 48 h after infection determined with ^{125}I-somatostatin.

AdCMVCD

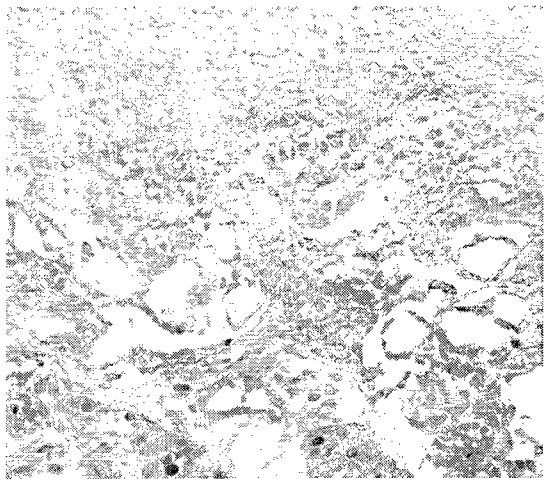

AdCox-2LCDCox-2LSSTr2

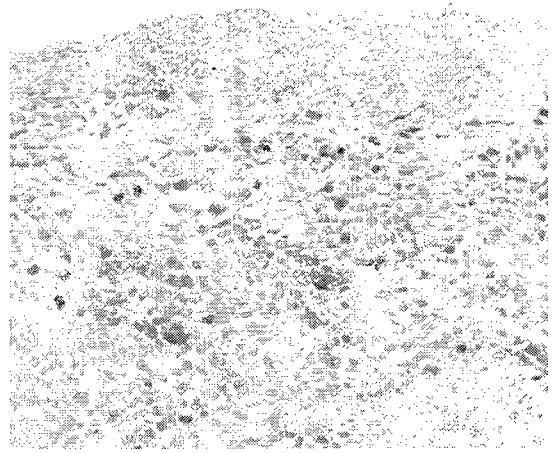

AdCox-2LSSTr2Cox-2LCD

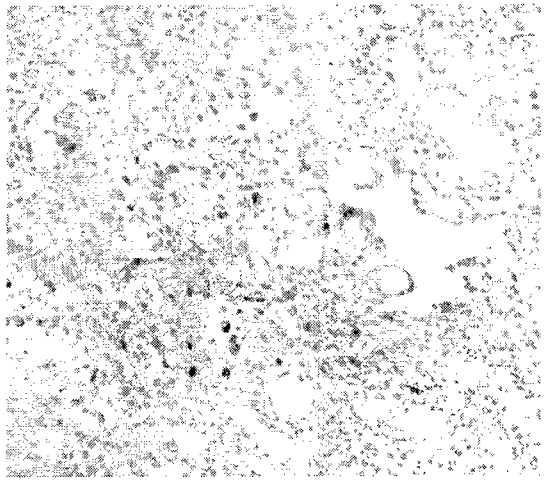

Figure 6. Expression of CD in DU145 prostate cancer xenografts after infection with several Ad vectors.

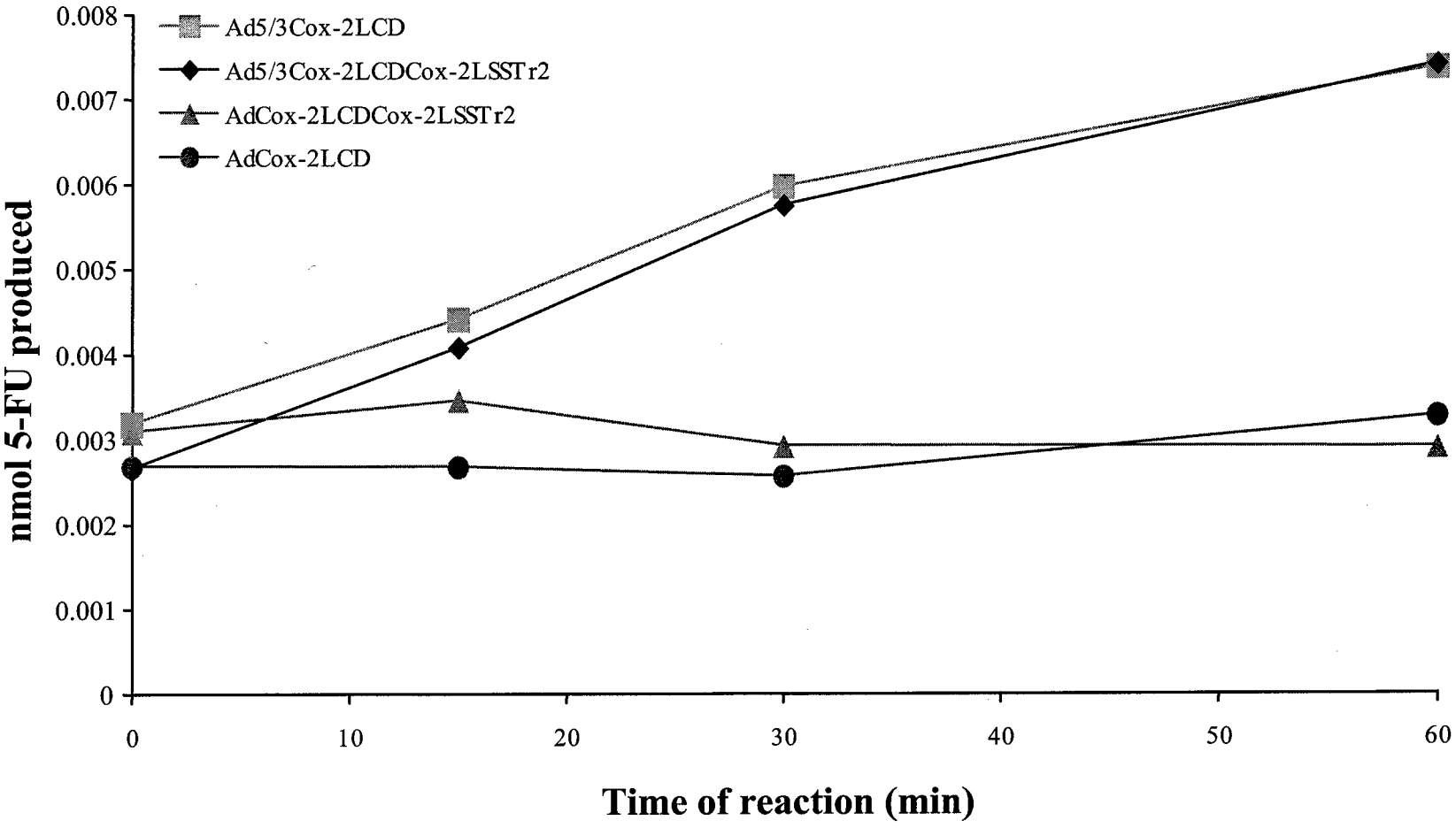

Figure 7. CD conversion in PC3 cells infected with Cox-2 viruses at 1000 VP.

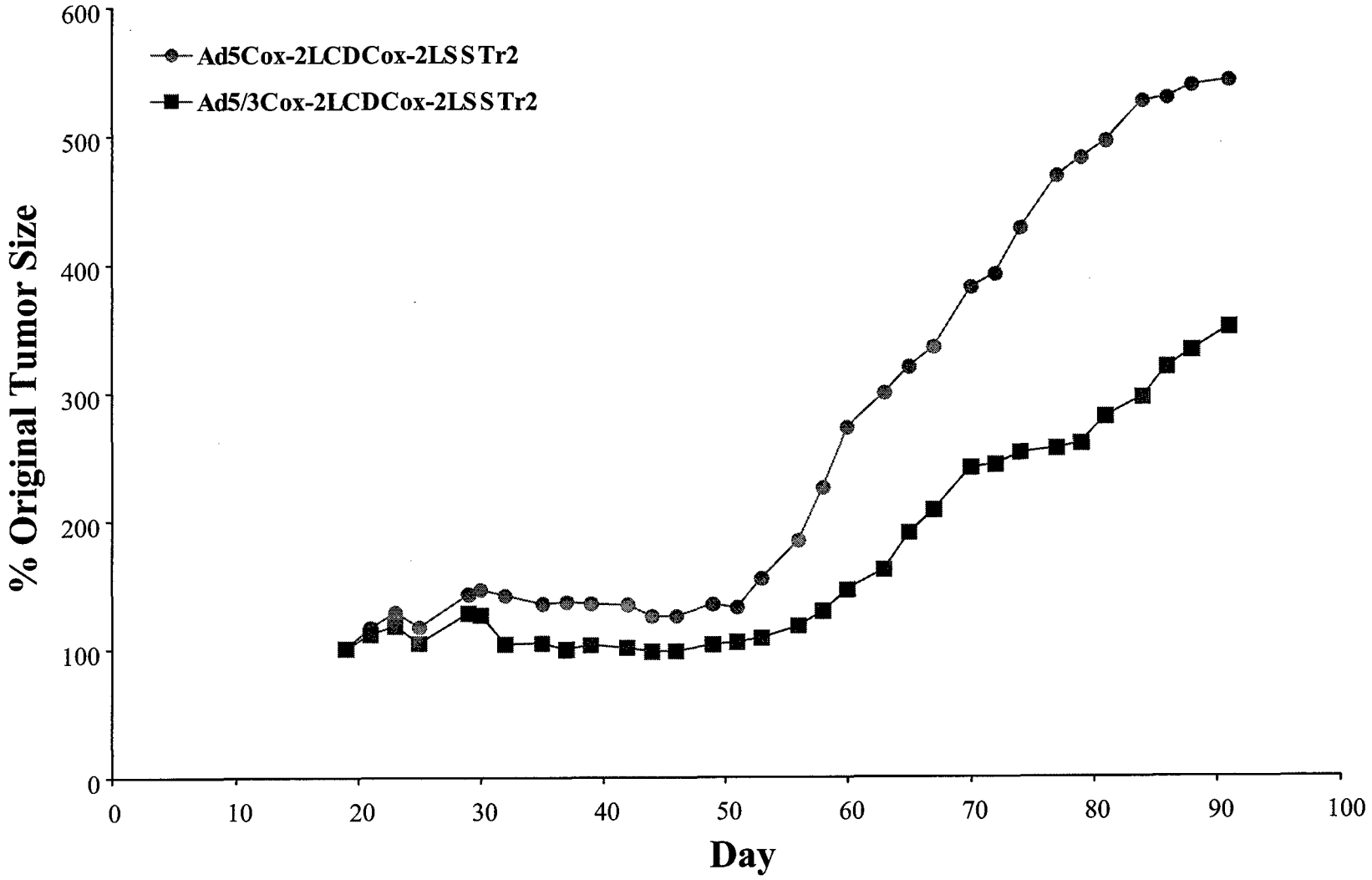

Figure 8. Athymic nude mice were injected *s.c.* with $2x10^7$ PC3 cells and Matrigel (1:1). On day 19, the tumors were injected with $5x10^{10}$ viral particles of Ad5Cox-2LCDCox-2LSSTr2 or Ad5/3Cox-2LCDCox-2LSSTr2. The animals received 400 mg/kg 5-FC (2x/day x7) beginning on the day of viral injection, and 5 daily fractions of 2 Gy ^{60}Co radiation starting 2 days after viral injection. The average change in tumor size relative to the starting size at day 19 is shown (n=8 mice/group).

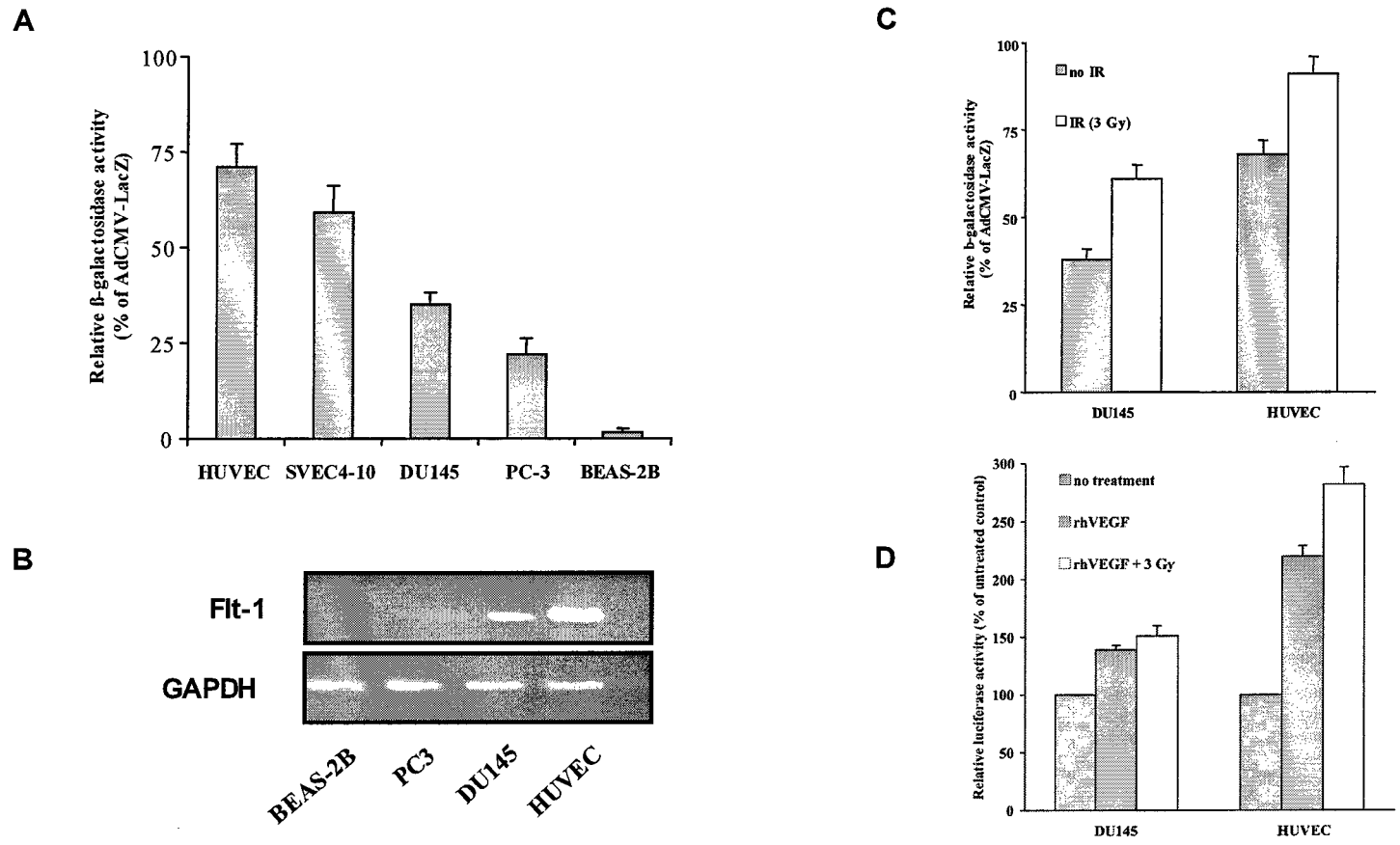

Figure 9. Flt-1 promoter activity in prostate cancer and endothelial cells. (**A**) LacZ expression in prostate cancer and endothelial cell lines. Cells were infected with AdFlt-LacZ or AdCMV-LacZ (control of infectivity) recombinant Ad at 100 MOI. LacZ expression was analyzed at 48 h after infection by ß-galactosidase enzyme assay system. Presented are mean values ± standard deviations of three independent experiments, each performed in triplicate. (**B**) The levels of Flt-1 mRNA in prostate cancer cells and endothelial cells. (**C**) Enhanced Flt-1 promoter activity following ionizing radiation treatment of human prostate cancer and endothelial cells. Cells were infected with the AdFlt-LacZ or AdCMV-LacZ (control) recombinant Ad at 100 MOI. At 24 h after infection, cells were ^{60}Co irradiated (I R) at 3 Gy. LacZ expression was analyzed at 48 h after radiation treatment. Presented are mean values ± standard deviations of three independent experiments, each performed in triplicate. **(D)** VEGF overexpression increases Flt-1 promoter activity. DU145 and HUVEC cells were infected with 100 MOI AdFlt-Luc or AdCMV-Luc recombinant Ad. Twenty-four h later cells were exposed to ionizing radiation at 3 Gy. Immediately after radiation treatment 50 ng/ml rhVEGF was added to the cell culture media. After 48 h incubation, cells were collected and relative luciferase activity was determined. Presented are mean values ± standard deviations of four independent experiments, each performed in six replicates.

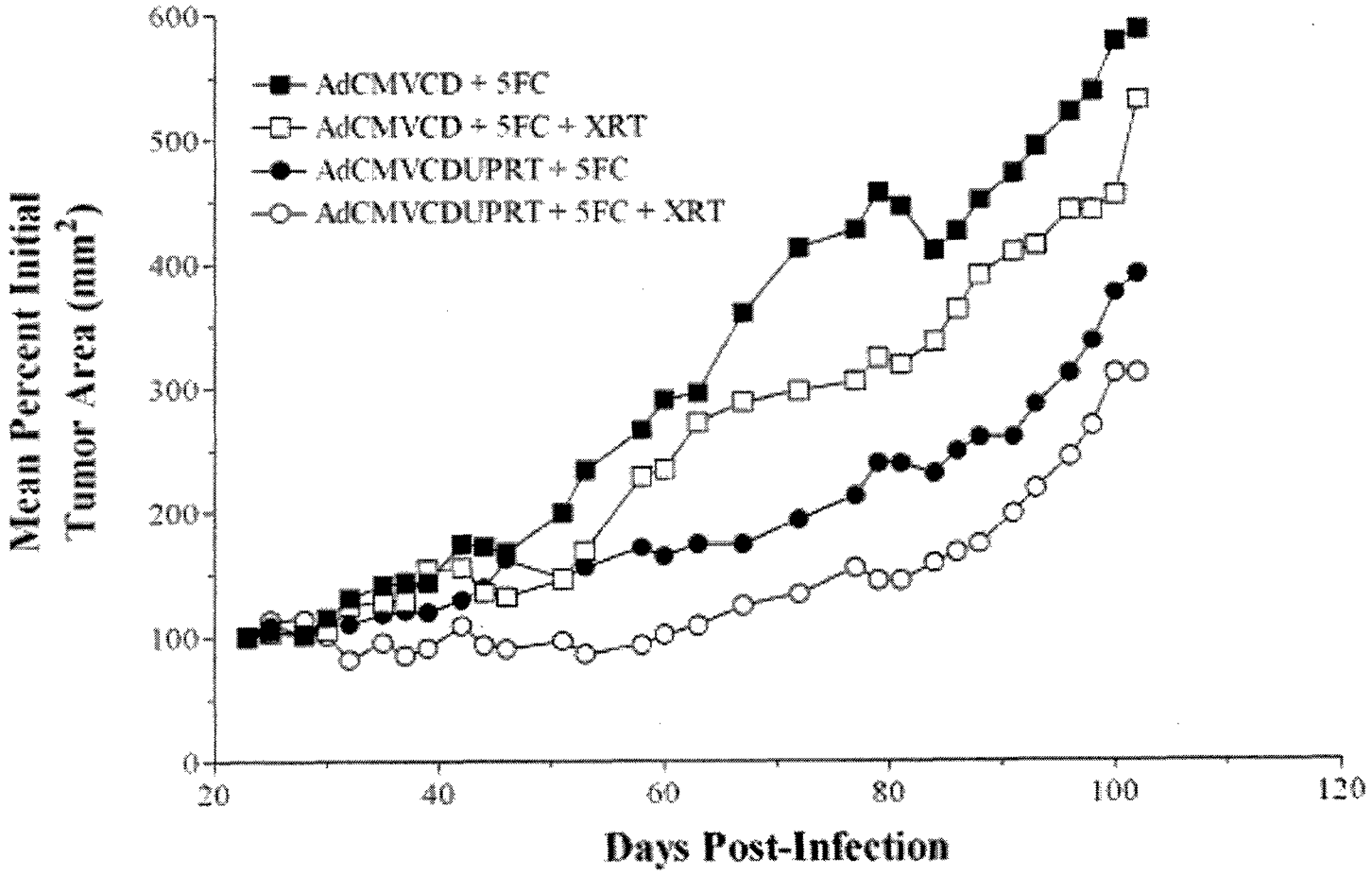

Figure 10. AdCMVCD *vs.* AdCMVCDUPRT plus systemic 5-FC and XRT therapy of subcutaneous human DU145 prostate xenografts in nu/nu mice. Flank tumors were established (63±8 mm^2, range 20-168 mm^2, p=0.97 among groups) and treated with a single injection of 10^9 pfu AdCMVCD or 10^9 pfu AdCMVCDUPRT. Animals in the XRT groups received 6 Gy 2 days post-infection. 400 mg/kg 5-FC was given bid for 7 days beginning at 2 days post-infection. Data presented as the mean percent change in initial tumor area (n = 5 per group). A representative of 2 separate experiments is shown comparing AdCMVCDUPRT *vs.* AdCMVCD regimens.

doi:10.1016/j.ymthe.2004.08.024

ARTICLE

Adenovirus-Mediated *FLT1*-Targeted Proapoptotic Gene Therapy of Human Prostate Cancer

Sergey A. Kaliberov,[1] Lyudmila N. Kaliberova,[1] Cecil R. Stockard,[2] William E. Grizzle,[2] and Donald J. Buchsbaum[1,*]

[1]*Department of Radiation Oncology and* [2]*Department of Pathology, University of Alabama at Birmingham, Birmingham, AL 35294, USA*

**To whom correspondence and reprint requests should be addressed. Fax: +1 205 975 7060. E-mail: djb@uab.edu.*

Available online 2 October 2004

Tumor necrosis factor-related apoptosis-inducing ligand (TRAIL/Apo2L) is of particular interest in the development of prostate carcinoma therapeutics as it preferentially induces apoptosis of tumor cells. To employ adenoviral vectors for highly efficient and specific *TRAIL* gene transfer into cancer cells could overcome some potential problems for recombinant TRAIL. The vascular endothelial growth factor receptor FLT-1 is involved in regulation of angiogenesis and tumor growth, invasion, and metastasis of prostate carcinoma. FLT-1 expression is observed in both tumor endothelial cells and prostate cancer cells. We developed an adenoviral vector encoding the *TRAIL* gene under control of the *FLT1* promoter (AdFlt-TRAIL), which produced endothelial and prostate cancer cell death. The combination of ionizing radiation and adenovirus-driven TRAIL expression overcame human prostate cancer cell resistance to TRAIL. Furthermore, *in vivo* administration of AdFlt-TRAIL at the site of tumor growth in combination with radiation treatment produced significant suppression of the growth of DU145 human prostate tumor xenografts in athymic nude mice. Our results suggest that specific TRAIL delivery employing the *FLT1* promoter can effectively inhibit tumor growth and demonstrate the advantage of combination radiotherapy and gene therapy for the treatment of prostate cancer.

Key Words: antiangiogenesis gene therapy, prostate cancer, TRAIL, radiation, FLT-1, adenoviral vector

INTRODUCTION

Prostate cancer is the most frequently diagnosed, noncutaneous neoplasm and second to lung cancer in cancer-related deaths [1]. Thus, surgical, radiation, or hormonal therapy as monotherapy or in combination does not appear to be adequate to control prostate cancer, which ultimately leads to distant metastasis and morbidity [2]. Because androgen-independent prostate cancer cells eventually lead to death, successful strategies to modify the biological behavior of these cells may potentially have the most significant clinical impact [3]. Clearly other novel treatment approaches to advanced/recurrent disease are desperately needed to achieve long-term local control and particularly to develop effective systemic therapy for metastatic prostate cancer [4].

The interaction between tumor cells and their microenvironment is a promising area for the development of novel therapeutic anti-cancer modalities. The formation of new blood vessels is an important step in prostate cancer progression. The angiogenic switch occurs early in tumorigenesis and allows for expansion of the tumor mass, favoring acquisition of additional malignant properties and metastatic dissemination [5]. In prostate cancer, the degree of tumor vascularization correlates with the development of metastatic disease. The newly formed tumor vasculature remarkably differs from mature vessels in normal tissues. Observations of human cancers and animal models argue that vascular endothelial growth factor (VEGF) receptors are up-regulated in new blood vessels [6]. A variety of studies have shown that overexpression of VEGF and its cognate receptor FLT-1 and KDR occurs in various types of tumors, in contrast to low levels in normal tissues [7]. VEGF has been implicated in the angiogenesis and growth of prostate carcinoma [8]. Recently, VEGF receptor expression was demonstrated not only in microvascu-

1525-0016/$30.00

doi:10.1016/j.ymthe.2004.08.024

lar cells but also in a variety of tumor cells, including prostate carcinoma [9,10].

Antiangiogenesis therapy is a particularly attractive antitumor modality with many potential targets, considering that the regulation of tumor angiogenesis is profoundly multifactorial. Strategies to inhibit tumor angiogenesis include targeting molecules involved in blood vessel formation, as well as targeting endothelial cell survival [11]. Gene therapy is a promising approach for the treatment of prostate carcinoma. Recombinant adenoviral vectors are effective tools for gene delivery because of their superior *in vivo* gene transfer efficiency in a wide spectrum of both dividing and nondividing cell types. The employment of gene therapy using antiangiogenesis genes has shown promise in preclinical models in mice [12]. The most important obstacles for adenoviral gene therapy are low selectivity of the existing vectors and low efficiency of gene transfer. Thus, new strategies for targeting regional or systemic disease are required. The use of targeted viral vectors to localize gene transfer to specific cell types holds many advantages over conventional, nontargeted vectors currently used in gene therapy. Utilization of tumor/tissue-specific promoters can reduce toxicity, increase safety, and improve the therapeutic index [13]. Recent studies have demonstrated promising results using the *FLT1* promoter in gene therapy. Furthermore, the *FLT1* promoter exhibits a "liver off" phenotype when used in adenoviral vectors [14].

Clonal expansion and tumor growth are the result of the deregulation of the balance between cell proliferation and apoptosis. This imbalance is a major factor in the multistep process of tumorigenesis, and inhibition of apoptosis is the main cause of this phenomenon. Thus, specific induction of programmed cell death is a rational approach for cancer therapy. The extrinsic pathway of apoptosis can be induced by members of the tumor necrosis factor (TNF) family of cytokines, which includes the TNF-related apoptosis-inducing ligand (TRAIL/Apo2L) [15]. TRAIL is of particular interest in the development of cancer therapeutics as it preferentially induces apoptosis of tumor cells, with little or no effect on normal cells [16]. TRAIL can trigger caspase activation and result in rapid apoptosis through binding of specific proapoptotic receptors [17].

Induction of cytotoxicity via selective expression of the proapoptotic *TRAIL* gene in tumor microvasculature and prostate cancer cells may improve antitumor therapy alone and in combination with radiation therapy of prostate cancer xenografts. The central hypothesis of this study was that selective transcriptional targeting of adenoviral vectors encoding the *TRAIL* gene under control of the *FLT1* promoter could increase specificity and efficiency of human prostate cancer therapy in combination with ionizing radiation. The results of the present study demonstrated that overexpression of the apoptosis-inducing *TRAIL* gene in combination with ionizing radiation may be an effective approach for the treatment of prostate cancer.

Results and Discussion

FLT1 Promoter Activity in Prostate Cancer Cell Lines

Development of efficient and selective gene therapy vectors for cancer cells will increase the efficacy and safety of gene-based cancer therapeutics. Transcriptional targeting could add a further level of safety to regulate transgene expression selectively in target cells by using specific promoters for gene therapy. Ideally, promoters should provide high-level transgene expression in tumor cells but be silent in normal tissues, particularly hepatocytes. In an attempt to enhance the selectivity for prostate cancer gene therapy several adenoviral vectors were developed using well-characterized prostate cancer-specific promoters such as PSA and PSMA (for more details see reviews [18,19]). Over the past decades, numerous studies have demonstrated the importance of tumor angiogenesis in cancer development. High levels of VEGF production in prostate cancer cells and robust expression of its cognate receptors in tumor-associated blood microvessels as well as prostate carcinoma suggest that VEGF/VEGF receptor expression plays an important role in prostate tumor angiogenesis [6,7,9,10]. Recently, a fragment of the promoter for the VEGF receptor gene *FLT1* has been demonstrated to be transcriptionally silent in human hepatocytes *in vitro* and mouse and rat hepatocytes *in vivo* [20,21].

To evaluate the ability of the *FLT1* promoter to drive cell-specific gene expression, we performed an analysis of β-galactosidase production from AdFlt-LacZ adenovirus infection. Since the efficiency of gene transfer differs between cell types, we normalized infectivity for each cell type to a positive control, *LacZ* gene delivery driven by the CMV promoter (AdCMV-LacZ). This normalization is expressed as a ratio of the transfection effectiveness of AdFlt-LacZ to AdCMV-LacZ, where transfection efficiency is defined as the percentage of cells expressing *LacZ* out of the entire population. Forty-eight hours after AdFlt-LacZ or AdCMV-LacZ infection, we harvested the cells and analyzed β-galactosidase activity by β-galactosidase enzyme assay (Fig. 1A). As expected, the highest levels of *FLT1*-driven LacZ expression were observed in HUVEC human and SVEC4-10 murine endothelial cells and were relatively high in hormone-independent DU145 (p53-mutant) and PC3 (p53-negative) human prostate cancer cells in comparison with normal human bronchial epithelial BEAS-2B cells.

Transcriptional activity of cell-specific promoters typically correlates with the level of expression of the corresponding endogenous gene. Thus, we hypothesized that the activity of the *FLT1* promoter would correlate with the relative levels of *FLT1* mRNA expression in the

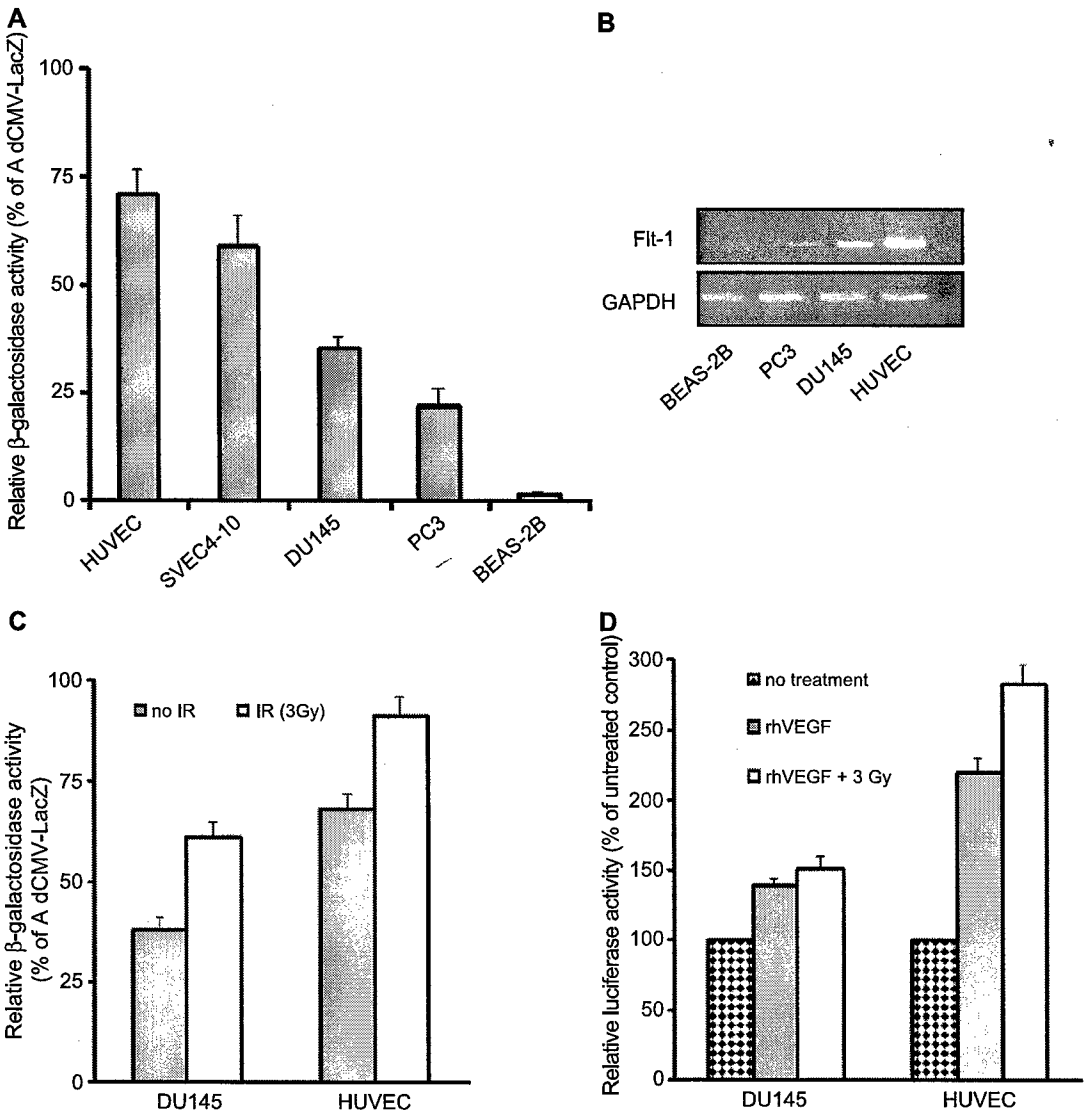

FIG. 1. *FLT1* promoter activity in prostate cancer and endothelial cells. (A) LacZ expression in prostate cancer and endothelial cell lines. DU145 and PC3 human prostate cancer cells, BEAS-2B normal human bronchial epithelial cells (negative control), SVEC4-10 small vessel murine endothelial cells, and HUVEC human umbilical vein endothelial cells (positive control) were infected with AdFlt-LacZ or AdCMV-LacZ (control for infectivity) recombinant adenoviruses at an m.o.i. of 100. LacZ expression was analyzed at 48 h after infection using a β-galactosidase enzyme assay system. *FLT1* promoter activity is presented as a percentage of CMV promoter activity. Presented are mean values ± standard deviations of three independent experiments, each performed in triplicate. (B) The levels of *FLT1* mRNA in prostate cancer cells and endothelial cells. BEAS-2B (negative control), PC3, and DU145 prostate cancer cells and HUVEC (positive control) were collected and total RNA was extracted. The levels of *FLT1* and *GAPDH* (loading control) expression were determined using RT-PCR. One representative of three different experiments is shown. (C) Enhanced *FLT1* promoter activity following ionizing radiation treatment of human prostate cancer and endothelial cells. DU145 prostate cancer cells and HUVEC endothelial cells were infected with the AdFlt-LacZ or AdCMV-LacZ (control) recombinant adenoviruses at an m.o.i. of 100. At 24 h after infection, cells were ^{60}Co irradiated at 3 Gy. LacZ expression was analyzed at 48 h after radiation treatment using a β-galactosidase enzyme assay system. *FLT1* promoter activity is presented as a percentage of CMV promoter activity. Presented are mean values ± standard deviations of three independent experiments, each performed in triplicate. (D) VEGF overexpression increases *FLT1* promoter activity. DU145 and HUVEC cells were infected with an m.o.i. of 100 AdFlt-Luc or AdCMV-Luc recombinant adenoviruses. Twenty-four hours later cells were exposed to ionizing radiation at 3 Gy. Immediately after radiation treatment 50 ng/ml rhVEGF was added to the cell culture medium. After 48 h incubation, cells were collected and relative luciferase activity was determined using a luciferase assay. Presented are mean values ± standard deviations of four independent experiments, each performed in six replicates.

tested cell lines. We assessed *FLT1* and glyceraldehyde-3-phosphate dehydrogenase (*GAPDH*) (as control) mRNA levels by reverse transcriptase polymerase chain reaction (RT-PCR). The comparative levels of the LacZ expression of prostate cancer cells correlated with VEGF receptor mRNA expression. DU145 prostate cancer cells demon-

doi:10.1016/j.ymthe.2004.08.024

strated detectable levels of *FLT1* mRNA expression in comparison with BEAS-2B control cells, whereas PC3 cells showed a low level *FLT1* mRNA expression (Fig. 1B). Comparing the *FLT1* promoter with CMV promoter-driven reporter expression, the specificity of the *FLT1* promoter for HUVEC endothelial cells and prostate cancer cells was demonstrated.

Ionizing radiation has an important role in localized prostate cancer treatment. Identification of compounds that will enhance the efficacy of radiation treatment is an essential goal for multimodality therapy. We further sought to determine whether ionizing radiation alters *FLT1* promoter activity. Radiation treatment at 3 Gy increased LacZ expression driven by the *FLT1* promoter by 61% in DU145 prostate cancer cells and 34% in HUVEC endothelial cells *in vitro* (Fig. 1C). Studies with a number of tumors have identified both *FLT1* and *VEGF* gene expression in malignant cells, suggesting the presence of an autocrine stimulatory loop promoting tumor cell growth in addition to the more commonly recognized effects of VEGF on tumor angiogenesis. Additionally, exposure of prostate cancer to ionizing radiation increased the secretion of VEGF by tumor cells that may enhance the angiogenic response and play a role in the protection against radiation damage [22].

To test whether VEGF protein expression modulates *FLT1* promoter activity in combination with ionizing radiation, we infected DU145 prostate cancer cells and HUVEC cells with AdFlt-Luc adenoviral vector, exposed them to ionizing radiation, and incubated them with recombinant human VEGF (rhVEGF). As shown in Fig. 1D, incubation in the presence of rhVEGF alone and in combination with radiation treatment significantly increased ($P < 0.05$) *FLT1*-driven Luc expression in HUVEC endothelial cells (220 and 282%, respectively) in comparison with AdFlt-Luc-infected DU145 prostate cancer cells (139 and 151%). These data provide evidence of relatively high levels of *FLT1* promoter activity in human endothelial cells and prostate cancer cells *in vitro*.

Tumor growth is critically dependent on blood supply and cancer cells can induce the formation of new blood vessels. Increased angiogenic activity, based on microvessel density counts of preserved tissues, has been linked to a more aggressive phenotype in studies of human prostate cancer [23,24]. High levels of VEGF have been observed in aggressive variants of human prostate cancer lines in comparison to less malignant variants [25]. Increased levels of VEGF were also identified specifically in patients with metastatic prostate cancer in comparison to prostate cancer patients with localized disease [26]. These observations indicate that increased production of VEGF may be associated specifically with the emergence of an aggressive phenotype in prostate cancer progression. Studies in model systems have shown that high levels of VEGF are likely to promote angiogenesis through paracrine mediation of endothelial cell migration and proliferation. Recent studies of prostate carcinoma have shown that FLT-1 was detected in carcinoma cells in 100% of the specimens evaluated. FLT-1 was also expressed in benign areas adjacent to the tumors [9,10].

Although it was assumed that the two VEGF receptors are expressed almost exclusively on vascular endothelial cells, recent studies have demonstrated both KDR and FLT-1 expression in tumor cells, including those derived from neuroblastoma and prostate and pancreatic cancers [9,10,27]. In this study, we used DU145 and PC3 cell lines, which were derived from brain and bone metastases, respectively, and thus these cells would be expected to be differentiated prostate cancer cells. This agrees with observations that VEGF receptor expression is increased in prostate intraepithelial neoplasia and malignant cells from well and moderately differentiated prostate cancer, in comparison with normal glands and poorly differentiated cancer [28].

The results of our experiments are in an agreement with these findings and suggest the possibility that tumor cell-derived VEGF might play an autocrine role in prostate cancer spread in addition to its known paracrine activity. Also, VEGF overexpression and ionizing radiation increased *FLT1* promoter activity in prostate carcinoma. According to current literature, these data are the first demonstration of the ability of ionizing radiation to increase *FLT1* promoter activity.

Induction of Proapoptotic TRAIL Protein Overexpression Causes Prostate Cancer Cell Death

Failure to undergo programmed cell death has been implicated in tumor development and resistance to prostate cancer therapy [29]. Promotion of apoptosis in prostate cancer cells may lead to the regression and improved prognosis of refractory disease. Apoptosis can be achieved through the exploitation of certain cellular pathways such as death receptors and caspases. TRAIL is able to induce p53-independent apoptosis in a variety of tumor cell types, and it appeared not to induce toxicity in normal cells [30].

To determine the susceptibility of cells to TRAIL-mediated killing, we incubated DU145 and PC3 prostate cancer cells and HUVEC endothelial cells with soluble TRAIL (sTRAIL) at various concentrations and measured relative cell viability using the crystal violet staining assay (Fig. 2A). The results reveal that prostate cancer cells were resistant to sTRAIL protein. Cell viability of DU145 and PC3 cells, following incubation for 96 h with sTRAIL at 400 ng/ml, was 75 and 77%, respectively. HUVEC endothelial cells demonstrated a high level of resistance to sTRAIL treatment. Several potential problems for sTRAIL as an anti-cancer agent have been identified. Large amounts of sTRAIL were required to inhibit tumor development, as most of the protein was cleared within several hours after intravenous injection in murine models. Furthermore, the antitumor activity of sTRAIL

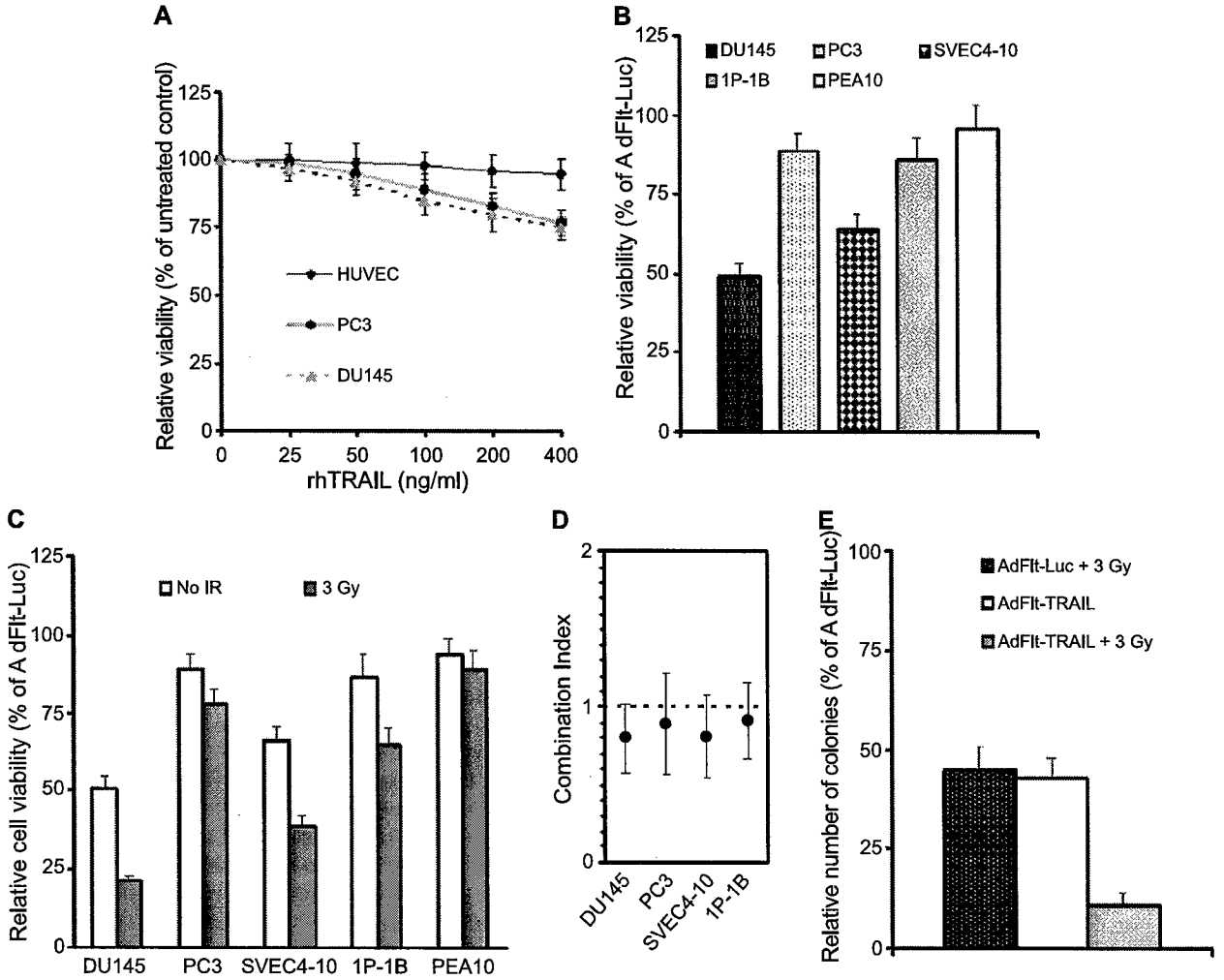

FIG. 2. Induction of proapoptotic TRAIL overexpression causes prostate cancer cell death. (A) Prostate cancer cells are resistant to sTRAIL. DU145 and PC3 prostate cancer cells and HUVEC were incubated with sTRAIL at various concentrations. Cell viability was determined at 72 h by using the crystal violet staining assay. Presented are mean values ± standard deviations of three independent experiments, each performed in 10 replicates. (B) AdFlt-TRAIL infection induces cytotoxicity in prostate cancer cells and endothelial cells. DU145 and PC3 human prostate cancer cells, SVEC4-10 and 1P-1B mouse endothelial cells, and PEA10 normal fibroblasts were infected with AdFlt-TRAIL or AdFlt-Luc recombinant adenoviruses at an m.o.i. of 100. Cell viability was determined at 72 h by using the crystal violet staining assay. Data shown represent relative cell viability following AdFlt-TRAIL infection compared to AdFlt-Luc viral control. Presented are mean values ± standard deviations of three independent experiments, each performed in 10 replicates. (C) Induction of TRAIL expression combined with ionizing radiation resulted in increased prostate cancer cell death. Prostate cancer cells, endothelial cells, and fibroblasts were infected with AdFlt-TRAIL or AdFlt-Luc (viral control) recombinant adenoviruses at an m.o.i. of 100. At 24 h after infection, cells were ^{60}Co irradiated at 3 Gy. Cell viability was determined at 96 h after radiation treatment using the crystal violet staining assay. Presented are mean values ± standard deviations of three to four independent experiments, each performed in 10 replicates. (D) Mean combination index values for AdFlt-TRAIL infection and radiation treatment combinations with human prostate cancer and mouse endothelial cell lines. DU145, PC3, SVEC4-10, and 1P-1B cells were treated with different m.o.i. of AdFlt-TRAIL or AdFlt-Luc and 24 h later cells were irradiated at different doses. The m.o.i. of AdFlt-TRAIL and AdFlt-Luc ranged from 12 to 400 $TCID_{50}$ per cell, and the radiation dose ranged from 1 to 6 Gy. Mean values were derived from three replicate dose ranges sufficient to inhibit growth of tested cells by 5–95%. Error bars indicate the 95% confidence intervals of the mean value. Combination index values were derived from parameters of the median effect plots, and statistical tests were used to determine whether the mean combination index values at multiple effect levels (IC_5–IC_{95}) were significantly different from combination index values equal to 1. (E) Clonogenic survival assay of DU145 prostate cancer cells. AdFlt-TRAIL- or AdFlt-Luc-infected cells (m.o.i. of 50) were exposed to ionizing radiation at 3 Gy. Cells were fixed and colonies were counted at 15 days after radiation treatment. Data are presented as percentage of number of colonies in comparison with AdFlt-Luc-infected mock-irradiated controls. Presented are mean values ± standard deviations of three independent experiments, each performed in 6 replicates.

was highest when given shortly after tumor implantation [31,32]. Also, the reported cytotoxicity against normal human hepatocytes of some forms of sTRAIL could limit the effectiveness of this anti-cancer agent [33,34]. Because of these issues, the development of alternative approaches to specific TRAIL protein delivery may

doi:10.1016/j.ymthe.2004.08.024

increase specificity and efficacy of treatment. One way to overcome these limitations is to employ adenoviral vectors for highly efficient and specific TRAIL gene transfer into cancer cells *in vitro* and *in vivo* [34–36].

We constructed a replication-deficient recombinant adenoviral vector encoding the human *TRAIL* gene under control of the human *FLT1* promoter element (AdFlt-TRAIL). We detected TRAIL protein expression following AdFlt-TRAIL infection in cell lysates using an immunoblotting technique (data not shown). To determine the susceptibility of prostate cancer cell and endothelial cell lines to TRAIL-mediated killing, we infected cells with AdFlt-TRAIL and AdFlt-Luc at various multiplicities of infection (m.o.i.). There was a dose-dependent correlation in cell killing measured by crystal violet staining assay (results not shown). A major advantage of using AdFlt-TRAIL would be transcriptional targeting of *TRAIL* gene expression in FLT-1-positive endothelial cells. Therefore, it was critical to determine whether murine endothelial cells would be sensitive to AdFlt-TRAIL infection before examining the effects of *FLT1*-driven *TRAIL* gene therapy *in vivo*. We infected prostate cancer cells, murine endothelial cells, and fibroblasts with AdFlt-TRAIL or AdFlt-Luc at an m.o.i. of 100 and determined cell viability using the crystal violet staining assay (Fig. 2B). AdFlt-TRAIL produced increased cytotoxicity to DU145 cells ($P < 0.05$) in comparison with the PC3 cell line. SVEC4-10 murine endothelial cells were sensitive to AdFlt-TRAIL infection, in contrast to the 1P-1B mouse endothelial cell line and PEA10 normal mouse fibroblasts. Thus, treatment using the *TRAIL* gene driven by the *FLT1* promoter produced prostate cancer and endothelial cell killing. Several studies recently demonstrated that adenoviral-driven *TRAIL* gene expression can overcome an impaired response to sTRAIL, with induction of cytotoxicity and apoptotic bystander effects in lung, colon, ovary, and prostate cancer cells [37–39]. However, the transduction of primary human hepatocytes revealed a high number of apoptotic cells [40]. These data imply that adenoviral-driven *TRAIL* administration *in vivo* must be restricted to tumor tissue and controlled by a specific promoter to avoid liver damage in human trials.

Additive Effect of TRAIL Overexpression in Combination with Ionizing Radiation in the Production of Prostate Cancer Cell Death

Surgical extirpation and external beam radiotherapy are potentially curative treatment options for clinically localized prostate cancer. The development of new therapeutic strategies for the treatment of hormone refractory metastatic prostate cancer is imperative. It appears that a combination treatment approach will be required to control metastatic disease. Combined radiotherapy and gene therapy is a novel therapeutic approach for prostate cancer [41,42].

To test whether combined *TRAIL* expression and treatment with ionizing radiation can increase cytotoxicity, we infected DU145 and PC3 human prostate cancer cells and SVEC4-10 and 1P-1B murine endothelial cells with AdFlt-TRAIL or AdFlt-Luc (as control) adenoviruses and exposed them to ionizing radiation. As shown in Fig. 2C, irradiation produced increased AdFlt-TRAIL cytotoxicity to DU145 cells ($P < 0.05$) in comparison to the PC3 cell line. Treatment with radiation enhanced the AdFlt-TRAIL-induced SVEC4-10 and 1P-1B endothelial cell killing in comparison with PEA10 normal fibroblasts (Fig. 2C), and the cytotoxic effect improved as the m.o.i. of AdFlt-TRAIL was increased (data not shown).

As shown in Fig. 2D, the combination of AdFlt-TRAIL infection with ionizing radiation treatment of prostate cancer cells and mouse endothelial cells resulted in combination index values of 0.80, with a confidence interval ($CI_{95\%}$) from 0.58 to 1.02 and P value (indicates level of statistical significance compared with a combination index value of 1.0) of 0.05 for DU145, 0.89 ($CI_{95\%}$ = 0.46 to 1.32, P = 0.41) for PC3, 0.81 ($CI_{95\%}$ = 0.54 to 1.08, P = 0.06) for SVEC4-10, and 0.91 ($CI_{95\%}$ = 0.67 to 1.15, P = 0.46) for 1P-1B cells. The mean combination index values, resulting from separate experiments at multiple effect levels, were not significantly different from 1.0, which indicates an additive effect of the combined therapy for these cell lines (Fig. 2D).

We confirmed the additive interaction observed between AdFlt-TRAIL infection and radiation treatment in DU145 cells using a long-term clonogenic survival assay. The day after infection with an m.o.i. of 50 AdFlt-TRAIL or AdFlt-Luc (viral control), we exposed DU145 prostate cancer cells to ionizing radiation and subjected them to clonogenic survival assay. Radiation alone caused a dose-dependent reduction in cell survival of uninfected cells (results not shown). AdFlt-Luc-infected DU145 cells showed a reduction in the number of colonies by 55% after 3 Gy in comparison with unirradiated cells and AdFlt-TRAIL-infected cells had a 57% reduction in the number of colonies in comparison with AdFlt-Luc-infected cells (Fig. 2E). There was a significantly greater reduction ($P < 0.05$) in the number of AdFlt-TRAIL-infected DU145 colonies (89% after 3 Gy) in comparison with AdFlt-Luc-infected cells. Thus, treatment with AdFlt-TRAIL and radiation enhanced cell killing, and the cytotoxic effect improved as the m.o.i. of AdFlt-TRAIL was increased (data not shown). Combination treatment with ionizing radiation and specific proapoptotic gene transfer, two therapies with different toxicity profiles, has several potential benefits. Gene therapy may cause radiosensitization and enhanced cell killing [43]. Theoretical mechanisms of the enhanced antitumor effects from this combined approach may be that ionizing radiation improves transfection or transduction of a therapeutic gene [44]. On the other hand, radiation treatment may enhance the efficacy of TRAIL-

induced apoptosis through up-regulation of death receptor expression and/or p53-mediated transcriptional activation of Bax, Bak, or similar proapoptotic Bcl-2 family members [45].

To confirm that the tumor cell killing following AdFlt-TRAIL infection was mediated through an apoptotic mechanism, we analyzed caspase-like activity and alteration of cell membrane (Table 1). We detected increased caspase-3-like activity in the ionizing radiation-treated DU145 cells, AdFlt-TRAIL-infected DU145 cells, and cells that received combined treatment, which in comparison with AdFlt-Luc-infected cells were 3.6-, 5.3-, and 8.1-fold greater, respectively. Since caspase-3 and -7 share the same target substrate sequence, it is difficult to assess the cleavage activity attributed to caspase. The activation of caspases is the hallmark of apoptosis. The initiator caspases-8 and -9 are activated by two alternative pathways and thereby activate downstream, effector caspase-3. This caspase is ultimately involved in proteolytic cleavage of a variety of cellular proteins that leads to apoptotic cell death [46].

The loss of plasma membrane asymmetry is an early event in apoptosis and could result in the exposure of phosphatidylserine residues at the outer plasma membrane leaflet. Annexin V, a phospholipid binding protein, specifically binds to phosphatidylserine residues. The results from an annexin V–FITC binding assay showed that the higher proportion of annexin V-positive cells was observed in both AdFlt-TRAIL-infected and AdFlt-TRAIL plus radiation-treated groups, with values of 38 and 61%, respectively. These values were statistically greater than in AdFlt-Luc-infected or ionizing radiation-treated cells alone ($P < 0.05$) (Table 1). Additionally, DU145 prostate cancer cells showed an increased percentage of necrotic (propidium iodide (PI)-positive) cells following combined AdFlt-TRAIL infection and radiation treatment (data not shown).

These data demonstrated that AdFlt-TRAIL produced cytotoxicity in endothelial and prostate cancer cells through activation of the apoptosis pathway. Also, AdFlt-TRAIL infection plus ionizing radiation produced additive cell killing.

TABLE 1: The effects of combined treatment with AdFlt-TRAIL and ionizing radiation on the apoptosis of DU145 prostate cancer cells

Treatment	Fluorescence intensity (DEVD-AFC)	% of annexin V-positive cells
AdFlt-Luc (control)	350 ± 140	5 ± 3
Radiation treatment (3 Gy)	1250 ± 230*	8 ± 4
AdFlt-TRAIL	1840 ± 401*	38 ± 12**
AdFlt-TRAIL + 3 Gy	2825 ± 360**	61 ± 24**

* $P < 0.05$ in comparison with AdFlt-Luc control.
** $P < 0.05$ in comparison with AdFlt-Luc control or radiation treatment alone.

Combined *TRAIL* Gene Delivery with Ionizing Radiation Increased Cytotoxicity to Prostate Tumor Xenografts

Multimodality therapy has been widely used in cancer treatment for enhancing efficacy, reducing toxicity, and preventing or delaying development of resistance. There is increasing evidence that certain chemotherapeutic agents and ionizing radiation synergize with TRAIL-mediated apoptosis of cancer cells [47,48]. TRAIL triggers apoptosis even in cells resistant to apoptosis in response to radiation, since ionizing radiation induces apoptosis by a pathway different from death ligands, although an overlapping set of molecules is involved [45]. Combination of both modalities has been shown to induce additive or synergistic apoptotic effects and eradication of clonogenic tumor cells. In tumors that retain some responsiveness to conventional therapy, TRAIL overexpression in combination with ionizing radiation might lead to synergistic apoptosis activation, as well as reducing the probability that tumor cells resistant to either type of agent will emerge. In tumors that have lost p53 function, death receptor targeting might help circumvent resistance to radiotherapy. In mouse models, combinations of TRAIL and certain DNA-damaging drugs or radiotherapy exerted synergistic antitumor xenograft activity [47,48].

To investigate the effects of the combination of AdFlt-TRAIL infection and ionizing radiation treatment on tumor growth *in vivo,* we injected DU145 cells subcutaneously into the flank of athymic nude mice. Before treatment, the mean tumor sizes in groups of 10–12 mice at baseline were not significantly different between treatment groups ($P > 0.05$), and the within-treatment variances were not significantly different ($P > 0.05$). The baseline mean and standard deviation for tumor sizes was 97 ± 39 mm^3. We initiated *in vivo* tumor therapy on Day 0, which corresponded to 22 days post-tumor cell injection. We injected animals intratumorally with AdFlt-TRAIL or AdFlt-Luc recombinant adenoviruses on Days 0 and 7. Two groups of mice received radiation treatment at 2 Gy on Days 1 and 8. We noted an inhibition of tumor growth in groups of mice treated with AdFlt-Luc plus radiation, AdFlt-TRAIL alone, and AdFlt-TRAIL in combination with ionizing radiation versus the AdFlt-Luc-injected control group (Fig. 3A). There were no significant differences in tumor growth between groups that received AdFlt-TRAIL alone versus AdFlt-TRAIL in combination with ionizing radiation or AdFlt-Luc plus radiation treatment versus AdFlt-TRAIL alone ($P > 0.05$). Comparisons of mean tumor volumes of the AdFlt-Luc in combination with ionizing radiation treatment group versus AdFlt-TRAIL in combination with radiation showed significant differences between the groups ($P < 0.05$). This difference in tumor size was evident at day 38 and persisted for the duration of the experiment. On day 56, the average tumor size was 101 ± 38 mm^3 in mice treated with AdFlt-TRAIL in

doi:10.1016/j.ymthe.2004.08.024

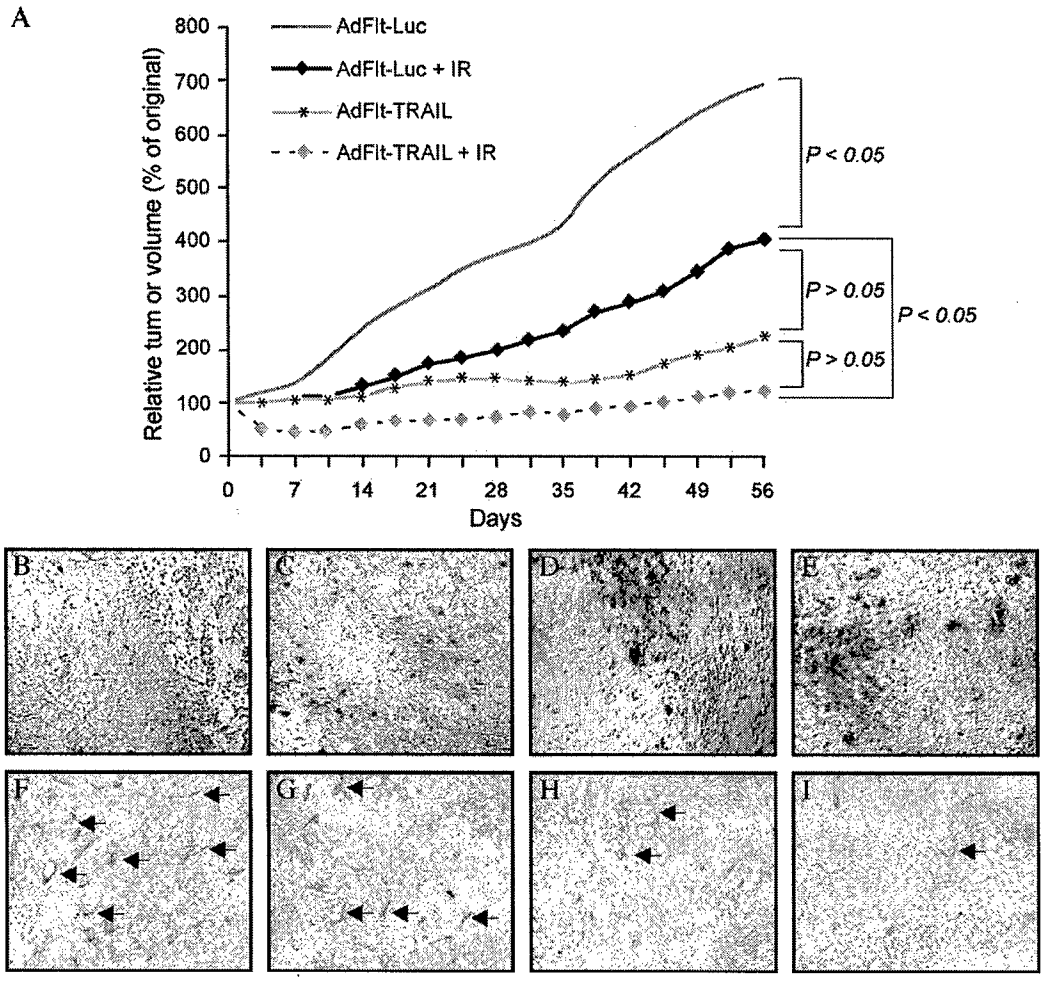

FIG. 3. The effects of AdFlt-TRAIL and radiation treatment on tumor growth in athymic nude mice bearing prostate cancer xenografts. (A) Growth of DU145 prostate cancer xenografts treated with AdFlt-TRAIL in combination with ionizing radiation. Treatment was started at the time of established tumor growth, 22 days postinjection. Animals were injected intratumorally with 1×10^9 $TCID_{50}$ AdFlt-TRAIL or AdFlt-Luc (control) on Days 0 and 7 and irradiated with 2 Gy on Days 3 and 9. Data points represent the mean change in tumor volume relative to Day 0 for each group of animals. On the last day of the study, the average tumor size was 101 ± 38 mm^3 in mice treated with AdFlt-TRAIL in combination with ionizing radiation ($n = 10$), 193 ± 41 mm^3 in mice injected with AdFlt-TRAIL alone ($n = 12$), and 368 ± 129 mm^3 in mice treated with AdFlt-Luc plus radiation therapy ($n = 11$) versus 703 ± 207 mm^3 in AdFlt-Luc control ($n = 12$) mice ($P = 0.015$, 0.028, and 0.04, respectively). (B–E) TUNEL assay of DU145 prostate cancer xenografts. Representative areas of a DU145 xenograft tumor from an animal treated with AdFlt-Luc as control (B), ionizing radiation only (C), AdFlt-TRAIL alone (D), and AdFlt-TRAIL plus ionizing radiation (E). (F–I) Vascular staining in DU145 xenograft tumors. Photomicrographs of immunocytochemistry staining of tumors from nude mice with DU145 human prostate cancer xenografts, stained with an anti-CD31 antibody (arrows). Representative areas of a DU145 xenograft tumor from an animal treated with AdFlt-Luc as viral control (F), ionizing radiation alone (G), AdFlt-TRAIL alone (H), and AdFlt-TRAIL in combination with ionizing radiation (I). Original magnification ×200.

combination with ionizing radiation, 193 ± 41 mm^3 in mice injected with AdFlt-TRAIL alone, and 368 ± 129 mm^3 in mice treated with AdFlt-Luc plus radiation therapy versus 703 ± 207 mm^3 in AdFlt-Luc control mice ($P = 0.015$, 0.028, and 0.04, respectively). The mean times to tumor doubling for control, AdFlt-Luc plus radiation, and AdFlt-TRAIL alone treatment groups were 12, 32, and 54 days, respectively; in animals that received AdFlt-TRAIL in combination with ionizing radiation tumors had not doubled by day 56, the last day of the study.

To assess the *in vivo* effects of AdFlt-TRAIL on apoptosis and angiogenesis, we analyzed the tumor samples by terminal deoxynucleotidyl transferase-mediated dUTP nick end labeling (TUNEL) and CD31 staining. DU145 xenograft-bearing mice received 2 weeks of treatment with AdFlt-TRAIL or AdFlt-Luc alone (every 7 days for three injections), radiation therapy (every 7 days for three treatments), and AdFlt-TRAIL plus radiation therapy (every 7 days for three injections plus 2 Gy the day after the adenoviral injection). At 3 days after the last

treatment, we excised the tumors, fixed them in alcoholic formalin, and stained them for apoptosis and CD31 by the procedures described under Materials and Methods. Microscopic examination of TUNEL-stained tumor sections showed that, compared to AdFlt-Luc-injected control mice (Fig. 3B) and ionizing radiation alone (Fig. 3C), AdFlt-TRAIL injection alone (Fig. 3D) or in combination with radiation (Fig. 3E) increased TdT-positive (brown-stained) cells. The quantitative evaluation of apoptosis showed that, in DU145 prostate tumor xenografts treated with AdFlt-TRAIL alone and in combination with radiation, the percentage of TUNEL-positive cells increased by 4.6- and 6.5-fold ($P < 0.05$), respectively, over that of AdFlt-Luc control tumor (Table 2). The positive control, in which TACS-nuclease was used to generate DNA fragments with free 3′-OH ends, showed positive staining in all the nuclei, whereas in the negative control, in which labeling buffer was used instead of TdT, there was not considerable positive staining (data not shown).

To determine whether the inhibitory effect of AdFlt-TRAIL on tumor growth is associated with the suppression of tumor angiogenesis, we examined the distribution of the endothelial cell-specific antigen CD31 (Table 2). The negative control, in which only blocking buffer was used instead of anti-CD31 antibody, did not show positive staining (data not shown). Immunohistochemical analysis of DU145 tumors by staining endothelial cells with anti-CD31 antibody showed fewer stained endothelial cells and reduced microvessel density ($P < 0.05$) in a cross section of tumor from mice treated with AdFlt-TRAIL alone (Fig. 3H) and AdFlt-TRAIL in combination with ionizing radiation (Fig. 3I) compared with radiation treatment alone (Fig. 3F) and AdFlt-Luc-injected tumor control (Fig. 3G), demonstrating the antiangiogenesis efficacy of AdFlt-TRAIL against endothelial cells *in vivo*.

These *in vivo* tumor therapy studies demonstrated significant inhibition of DU145 tumor growth in animals that received AdFlt-TRAIL alone and in combination with radiation treatment in comparison with PBS control tumors. Moreover, in the group treated with AdFlt-TRAIL alone (12 mice), 5 of the tumors underwent complete regression and 2 eventually recurred. In contrast, the group treated with AdFlt-TRAIL in combination with ionizing radiation showed 3/10 regressions without recurrence.

TABLE 2: The effects of combined treatment with AdFlt-TRAIL and ionizing radiation on apoptosis and tumor microvessel density of DU145 prostate cancer xenografts

Treatment	TUNEL-positive cells (%)	CD31-positive vessel density/100× field
AdFlt-Luc	1.8 ± 0.8	35 ± 3.8
Ionizing radiation (2 Gy)	2.9 ± 1.2	29 ± 2.4
AdFlt-TRAIL	8.4 ± 1.5*,**	21 ± 1.2*
AdFlt-TRAIL + 2 Gy	11.8 ± 1.6*,**	11 ± 1.7*,**

* $P < 0.05$ in comparison with AdFlt-Luc control.
** $P < 0.05$ in comparison with radiation treatment alone.

In an attempt to improve the outcome of patients with prostate cancer, combined modality approaches are frequently considered. Combined therapy, most frequently radiosensitizing chemotherapy and radiation, has been shown to be particularly efficient and has become standard therapy for many tumor types. One of the most promising therapies that can be combined with ionizing radiation in the treatment of prostate cancer is antiangiogenic gene therapy. Angiogenesis is a critical requirement for local proliferation and metastasis in prostate cancer [49]. The tumor response to radiation is determined not only by tumor cell phenotype but also by microvascular sensitivity [50]. Inhibitors of tumor angiogenesis interrupt the angiogenic process to prevent new vessel formation. In this study, we used specifically targeted proapoptotic gene transfer to cause direct damage to the tumor endothelium and thus lead to extensive secondary tumor cell death. The application of such strategies as TRAIL expression in endothelial cells and tumor cells with conventional radiation treatments offers unique opportunities to develop more effective cancer therapies.

Our results suggest that specific TRAIL delivery employing the *FLT1* promoter can effectively inhibit tumor growth and demonstrate the advantage of combination radiotherapy and gene therapy for the treatment of prostate cancer. The *FLT1* gene is member of the VEGF/VEGF receptor family, which is extremely important for angiogenesis regulation. Neovascularization is an essential step in a number of different physiological processes. Thus, specific vascular-targeted gene therapy may be applied as a therapeutic intervention for angiogenesis regulation. For future studies of antiangiogenesis cancer treatment, specific gene therapy using recombinant AdFlt-TRAIL may help overcome the undesired neovascularization and decrease the risk of neoplastic growth and metastasis.

Materials and Methods

Adenoviral vectors, cell culture, and reagents

A replication-deficient recombinant adenoviral vector encoding the TRAIL gene under control of the human *FLT1* promoter element (AdFlt-TRAIL) was constructed using a method reported previously [51]. Briefly, to generate pShuttleFlt-TRAIL plasmid, the fragment including TRAIL cDNA and the SV40 late polyadenylation signal was removed from the pGT60hTRAIL plasmid (InvivoGen, San Diego, CA, USA), blunted, and cloned into the *FLT1* promoter element pShuttleFlt-Luc plasmid, which was digested and from which Luc cDNA was removed prior to cloning in the TRAIL cDNA and SV40 late polyadenylation signal fragment. The insert sequence was confirmed by restriction enzyme mapping and partial sequencing analysis. The resultant plasmid was linearized and cotransfected with pAdEasy-1 plasmid (Quantum Biotechnologies, Montreal, QC, Canada). Recombinant clones were confirmed by PCR analysis, linearized, and transected into 293 cells using the Superfect lipid-based transfection method (Qiagen, Chatsworth, CA, USA) to generate AdFlt-TRAIL recombi-

doi:10.1016/j.ymthe.2004.08.024

nant adenovirus, which was isolated from a single positive plaque and passed through three rounds of plaque purification and subsequently confirmed by PCR. AdFlt-Luc (encoding the firefly luciferase gene under the control of the human *FLT1* promoter element) and AdCMV-Luc (encoding the firefly luciferase gene under the control of the human CMV promoter element) were kindly provided by Dr. P. N. Reynolds (University of Adelaide, Adelaide, SA, Australia). All viruses were propagated in 293 cells, purified by ultracentrifugation in a cesium chloride gradient, and subjected to dialysis. Viral titer was measured by a standard 50% tissue culture infectious dose (TCID50) assay using 293 cells and by absorbance of the dissociated virus at A_{260} nm. Multiplicities of infection for subsequent experiments were expressed as TCID50 per cell.

For this study, cell lines, except human umbilical vein endothelial cells (HUVEC), were obtained from the American Type Culture Collection (Rockville, MD, USA). The HUVEC were obtained from Clonetics (San Diego, CA, USA) and were grown in EGM-2 growth medium (Clonetics). The normal human bronchial epithelial adenovirus 12–SV40 virus hybrid-transformed BEAS-2B cells were grown in BEGM growth medium (Clonetics). The human prostate adenocarcinoma PC3 and DU145 cells, transformed small vessel murine endothelial cells SVEC4-10 and 1P-1B, and human embryonic kidney HEK293 cells were grown in Dulbecco's modified Eagle's medium (DMEM) with 10% fetal bovine serum (FBS). All cells were maintained at 37°C in a humidified atmosphere with 5% CO_2.

Human recombinant VEGF protein was purchased from Pierce (Rockford, IL, USA). The full-length TRAIL protein of human origin was provided by Santa Cruz Biotechnology (Santa Cruz, CA, USA). Rat anti-mouse CD31 PECAM-1 antibody was obtained from BD Pharmingen (San Diego, CA, USA) and secondary donkey anti-rat antibody was purchased from Jackson ImmunoResearch Laboratories (West Grove, PA, USA).

Reporter gene assays

β-Gal assay. Cells were seeded in 24-well plates in triplicate at a density of 5×10^4 cells/well. The next day, the cells were infected with AdFlt-LacZ or AdCMV-LacZ (control) at an m.o.i. of 100 in DMEM with 2% FBS for 1 h and then maintained in complete medium. For staining, wells were washed with 1 mM $MgCl_2$ in PBS, and cells were fixed by 0.5% (v/v) glutaraldehyde at room temperature, then stained using X-gal reaction solution, and incubated at 37°C, until a color change was obtained, and the absorbance was measured at 420 nm using a V Max plate reader (Molecular Devices Corp., Sunnyvale, CA, USA). LacZ activities were normalized for differences in incubation times.

Luciferase assay. Cells were plated in 24-well plates in triplicate at a density of 5×10^4 cells/well. The next day, the cells were infected with AdFlt-Luc or AdCMV-Luc (control) at an m.o.i. of 50 in DMEM with 2% FBS for 1 h and then maintained in complete medium. Forty-eight hours after infection cells were harvested and treated with 100 μl of lysis buffer. A luciferase assay (Promega, Pittsburgh, PA, USA) and a FB12 luminometer (Zylux Corp., Oak Ridge, TN, USA) were used for the evaluation of luciferase activity of infected cells. Luciferase activity was normalized by the protein concentration in the cell lysate using the DC Protein Assay (Bio-Rad).

RNA preparation and RT-PCR. The levels of VEGF receptor *FLT1* messenger RNA were determined by RT-PCR. Total RNA was extracted using the RNeasy Mini Kit (Qiagen), following standard protocol, and quantified spectrophotometrically using an MBA 2000 spectrophotometer (Perkin–Elmer, Wellesley, MA, USA). cDNA was synthesized using random hexamer primers and an Omniscript RT kit (Qiagen). The first-strand cDNA was used as the template for PCR. For amplification of cDNA encoding *FLT1* the following primers were used: 5′-GAGGATTC-TGACGGTTTC-3′ (3199-FLT) and 5′-CCTGTCAGTATGGCATTG-3′ (FLT-3782). The human *GAPDH* cDNA was used as an internal standard for template loading of PCR by using primers 5′-TCCCATCACCATCTTCCA-3′ (GAPDH forward) and 5′-CATCACGCCACAGTTTCC-3′ (GAPDH reverse). PCR was performed under the following conditions: 30 cycles of 95°C for 45 s, 55°C for 45 s, and 72°C for 1 min). PCR products were analyzed by 1% agarose electrophoresis with ethidium bromide staining.

Cell proliferation assay. The dye in this colorimetric assay is crystal violet, which is a cationic triarylmethane dye that preferentially stains DNA and allows one to obtain quantitative information about the relative density of adherent cells. Upon solubilization, the amount of dye taken up by the monolayer can be quantitated by optical density. To determine cell growth after recombinant adenovirus infection, human prostate cancer cells were seeded in 96-well plates at 5×10^3 cells/well, incubated for 24 h with or without rhVEGF, and infected at different m.o.i. with AdFlt-TRAIL or AdFlt-Luc. At 72 h after incubation cell culture medium was removed and surviving cells were then fixed and stained with 2% (w/v) crystal violet (Sigma–Aldrich, St. Louis, MO, USA) in 70% ethanol for 3 h at room temperature. The plates were washed extensively and air-dried and optical density was measured at 570 nm using a V Max plate reader (Molecular Devices Corp.). Relative density of adherent cells was defined as OD570 of treated cells in comparison with untreated cells and the OD570 value of blank wells was subtracted.

Clonogenic survival assay. At 3 h after infection with an m.o.i. of 50 AdFlt-TRAIL or AdFlt-Luc, cells were trypsinized and diluted to the appropriate cell density into six-well culture plates, and after 24 h incubation at 37°C cells were either mock-irradiated or irradiated at 3 Gy dose using a ^{60}Co γ-irradiator (^{60}Co Picker Unit, Cleveland, OH, USA) and were then returned to the incubator and cultured for an additional 15 days. Cells were then fixed with 70% ethanol and stained with 2% (w/v) crystal violet (Sigma–Aldrich). Colonies comprising at least 50 cells were counted. The plating efficiencies were calculated as the number of colonies divided by the number of test cells plated for each data point. Plating efficiencies were referenced back to the mock-irradiated control plating efficiency to determine the surviving fraction for each dose.

Apoptosis assays

Annexin V staining and propidium iodide uptake of apoptotic cells. Annexin V and PI double staining (BioVision, Palo Alto, CA, USA) was used to determine apoptosis. Annexin V binds to cells that express phosphatidylserine on the outer layer of the cell membrane, and PI stains the cellular DNA of cells with a compromised cell membrane. This allows for the discrimination of live cells (unstained with either fluorochrome) from apoptotic cells (stained only with annexin V) and necrotic cells (stained with both annexin V and PI). Cells were collected and double stained with FITC-conjugated annexin V and PI for 15 min at room temperature. Annexin V and PI were added according to the manufacturer's recommendations (BioVision). Samples were immediately analyzed by flow cytometry. Annexin V and PI emissions were detected in the FL-1 (530/30 nm) and FL-2 (585/40 nm) channels, respectively. For each sample, data from approximately 1×10^4 cells were recorded in list mode on logarithmic scales. Analysis was performed with CellQuest software (Becton–Dickinson, San Jose, CA, USA) on cells characterized by forward/side scatter (FSC/SSC) parameters. Cell debris characterized by a low FSC/SSC was excluded from analysis. The percentages of apoptotic cells were calculated.

Caspase protease assay. Caspase-like activity was measured using Ac-DEVD-AFC as fluorometric substrates for caspase-3 (BioVision). Total adherent and floating cells were resuspended on ice in cell lysis buffer. The protein concentration in the samples was determined by the Biuret method using the BCA Protein Assay Kit (Pierce). Fifty micrograms of cell lysate was added (1:1, v/v) to 2× reaction buffer containing 10 mM DTT and AFC (7-amino-4-trifluoromethyl coumarin)-conjugated substrates (50 μM final concentration) and incubated at 37°C for 2 h. The optical density was measured in a VersaFluor fluorometer (Bio-Rad, Hercules, CA, USA) equipped with 400-nm excitation and 505-nm emission filters. The change in caspase-like activity was determined by comparing relative fluorescence of treated samples with the level of untreated controls.

In vivo tumor therapy studies

For *in vivo* experiments 8- to 10-week-old female nude mice (National Cancer Institute, Frederick Cancer Research and Development Center, Frederick, MD, USA) were subcutaneously inoculated with 5×10^6 DU145 tumor cells, which were mixed 1:1 with Matrigel (Becton–Dickinson). Treatment was started 22 days later at the time of established tumor growth (250–350 mm^3). Mice were randomly divided (10–12 mice/group)

into four groups receiving different treatments: (1) AdFlt-Luc (control), (2) AdFlt-Luc and ^{60}Co radiation treatment at 2 Gy, (3) AdFlt-TRAIL, and (4) AdFlt-TRAIL and 2 Gy radiation treatment. Animals were injected intratumorally with 1×10^9 $TCID_{50}$ recombinant adenoviruses. Radiation treatment was administered 24 h after adenoviral injection. Tumor volume ($0.5 \times$ length $\times$ width^2 in mm^3) was measured twice a week using calipers. Percentage change from baseline at 22 days was computed by comparing the baseline value to the tumor size on each day of measurement. Also, the times to death from tumor or treatment, to tumor regression, and to tumor recurrence were recorded.

In situ apoptosis detection by TUNEL staining

The formalin-fixed and paraffin-embedded 5-μm-thick sections of all tumor samples were studied by TUNEL staining by using the Apoptag Kit (Intergen, Purchase, NY, USA). The extent of apoptosis was evaluated by counting the positive brown-stained cells as well as the total number of cells at 10 arbitrarily selected fields in a blinded manner. The apoptotic index was calculated as the number of apoptotic cells per 200× microscope field.

Immunohistochemical analysis of tumors for CD31 expression

Sections from paraffin-embedded tumors (those used for TUNEL staining) were incubated overnight with rat anti-mouse CD31 polyclonal antibody. Then sections were incubated with donkey anti-rat antibody secondary antibody. Antigen–antibody complexes were visualized by incubation with 3,3′-diaminobenzidine substrate and counterstained with diluted Harris hematoxylin. Tumor vessels containing CD31-positive (brown) cells were quantified by microscopy in 100× fields (at least five random fields/tumor) and were calculated as relative vessel density.

Statistical analysis

All error terms are expressed as the standard deviation of the mean. Significance levels for comparison of differences between groups in the *in vitro* experiments were analyzed by the Student t test. The differences were considered significant when P value was <0.05. All reported P values are two-sided. In the animal model tumor therapy studies, the treatment groups were compared with respect to tumor size and percentage of original tumor size over time. To test for significant differences in tumor size between treatment groups, one-way analysis of variance (ANOVA) test was conducted. When the ANOVA indicated that a significant difference existed (P value <0.05), multiple comparison procedures were used to determine where the differences lay. Multiple drug effect analysis was performed using computer software [52]. To calculate combined AdFlt-TRAIL and ionizing radiation effects, the combination index isobologram method was used. Details of this methodology have been published previously [53]. Briefly, this method defines the expected additive effect of combined agents and then quantifies the degree of enhancement/reduction of effect by determining how much the combination effect differs from the expected additive effect using the combination index. The combination index equation takes into account both the potency and the shape of the dose–effect curves. In this analysis, synergy is defined as mean combination index values significantly less than 1.0, antagonism as mean combination index values significantly greater than 1.0, and additivity as mean combination index values not significantly different from 1.0.

ACKNOWLEDGMENT

The authors thank Sally B. Lagan for assistance in preparing the manuscript.

RECEIVED FOR PUBLICATION JUNE 8, 2004; ACCEPTED AUGUST 30, 2004.

REFERENCES

1. Jemal, A., *et al.* (2002). Cancer statistics. *CA J. Cancer Clin.* **52:** 23–47.
2. Schellhammer, P. F., and Lynch, D. F. (1997). Are monotherapy options reasonable for T3 prostate cancer? *Semin. Urol. Oncol.* **15:** 207–214.
3. Isaacs, W. B. (1995). Molecular genetics of prostate cancer. *Cancer Surv.* **25:** 357–379.
4. Steiner, M. S., Gingrich, J. R., and Chauhan, R. D. (2002). Prostate cancer gene therapy. *Surg. Oncol. Clin. North Am.* **11:** 607–620.
5. Folkman, J. (2003). Angiogenesis and apoptosis. *Semin. Cancer Biol.* **13:** 159–167.
6. Feng, D., *et al.* (2000). Ultrastructural localization of the vascular permeability factor/vascular endothelial growth factor (VPF/VEGF) receptor-2 (FLK-1, KDR) in normal mouse kidney and in the hyperpermeable vessels induced by VPF/VEGF-expressing tumors and adenoviral vectors. *J. Histochem. Cytochem.* **48:** 545–556.
7. Dvorak, H. F., *et al.* (1991). Distribution of vascular permeability factor (vascular endothelial growth factor) in tumors: concentration in tumor blood vessels. *J. Exp. Med.* **174:** 1275–1278.
8. Ferrer, F. A., *et al.* (1999). Expression of vascular endothelial growth factor receptors in human prostate cancer. *Urology* **54:** 567–572.
9. Fakhari, M., *et al.* (2002). Upregulation of vascular endothelial growth factor receptors is associated with advanced neuroblastoma. *J. Pediatr. Surg.* **37:** 582–587.
10. Soker, S., *et al.* (2001). Vascular endothelial growth factor-mediated autocrine stimulation of prostate tumor cells coincides with progression to a malignant phenotype. *Am. J. Pathol.* **159:** 651–659.
11. Sternberg, C. N. (2003). What's new in the treatment of advanced prostate cancer? *Eur. J. Cancer* **39:** 136–146.
12. Scappaticci, F. A., *et al.* (2001). Combination angiostatin and endostatin gene transfer induces synergistic antiangiogenic activity in vitro and antitumor efficacy in leukemia and solid tumors in mice. *Mol. Ther.* **3:** 186–196.
13. St George, J. A. (2003). Gene therapy progress and prospects: adenoviral vectors. *Gene Ther.* **10:** 1135–1141.
14. Nicklin, S. A., *et al.* (2003). Transductional and transcriptional targeting of cancer cells using genetically engineered viral vectors. *Cancer Lett.* **201:** 165–173.
15. Wiley, S. R., *et al.* (1995). Identification and characterization of a new member of the TNF family that induces apoptosis. *Immunity* **3:** 673–682.
16. Pan, G., *et al.* (1997). An antagonist decoy receptor and a death domain-containing receptor for TRAIL. *Science* **277:** 815–818.
17. Schneider, P., *et al.* (1997). TRAIL receptors 1 (DR4) and 2 (DR5) signal FADD-dependent apoptosis and activate NF-kappaB. *Immunity* **7:** 831–836.
18. Mabjeesh, N. J., Zhong, H., and Simons, J. W. (2002). Gene therapy of prostate cancer: current and future directions. *Endocr. Relat. Cancer* **9:** 115–139.
19. Collis, S. J., Khater, K., and DeWeese, T. L. (2003). Novel therapeutic strategies in prostate cancer management using gene therapy in combination with radiation therapy. *J. World Urol.* **21:** 275–289.
20. Nicklin, S. A., *et al.* (2001). Analysis of cell-specific promoters for viral gene therapy targeted at the vascular endothelium. *Hypertension* **38:** 65–70.
21. Reynolds, P. N., *et al.* (2001). Combined transductional and transcriptional targeting improves the specificity of transgene expression in vivo. *Nat. Biotechnol.* **19:** 838–842.
22. Abdollahi, A., *et al.* (2003). SU5416 and SU6668 attenuate the angiogenic effects of radiation-induced tumor cell growth factor production and amplify the direct anti-endothelial action of radiation in vitro. *Cancer Res.* **63:** 3755–3763.
23. Weidner, N., *et al.* (1993). Tumor angiogenesis correlates with metastasis in invasive prostate carcinoma. *Am. J. Pathol.* **143:** 401–409.
24. Bettencourt, M. C., *et al.* (1998). CD34 immunohistochemical assessment of angiogenesis as a prognostic marker for prostate cancer recurrence after radical prostatectomy. *J. Urol.* **160:** 459–465.
25. Balbay, M. D., *et al.* (1999). Highly metastatic human prostate cancer growing within the prostate of athymic mice overexpresses vascular endothelial growth factor. *Clin. Cancer Res.* **5:** 783–789.
26. Duque, J. L., *et al.* (1999). Plasma levels of vascular endothelial growth factor are increased in patients with metastatic prostate cancer. *Urology* **54:** 523–527.
27. von Marschall, Z., *et al.* (2000). De novo expression of vascular endothelial growth factor in human pancreatic cancer: evidence for an autocrine mitogenic loop. *Gastroenterology* **119:** 1358–1372.
28. Jackson, M. W., *et al.* (2002). A potential autocrine role for vascular endothelial growth factor in prostate cancer. *Cancer Res.* **62:** 854–859.
29. Denmeade, S. R., Lin, X. S., and Isaacs, J. T. (1996). Role of programmed (apoptotic) cell death during the progression and therapy for prostate cancer. *Prostate* **28:** 251–265.
30. Walczak, H., *et al.* (1999). Tumoricidal activity of tumor necrosis factor-related apoptosis-inducing ligand in vivo. *Nat. Med.* **5:** 157–163.
31. Ashkenazi, A., *et al.* (1999). Safety and antitumor activity of recombinant soluble Apo2 ligand. *J. Clin. Invest.* **104:** 155–162.
32. Lawrence, D., *et al.* (2001). Differential hepatocyte toxicity of recombinant Apo2L-TRAIL versions. *Nat. Med.* **7:** 383–385.
33. LeBlanc, H. N., and Ashkenazi, A. (2003). Apo2L-TRAIL and its death and decoy receptors. *Cell Death Differ.* **10:** 66–75.
34. Griffith, T. S., *et al.* (2000). Adenoviral-mediated transfer of the TNF-related apoptosis-inducing ligand/Apo-2 ligand gene induces tumor cell apoptosis. *J. Immunol.* **165:** 2886–2894.
35. Griffith, T. S., and Broghammer, E. L. (2001). Suppression of tumor growth following intralesional therapy with TRAIL recombinant adenovirus. *Mol. Ther.* **4:** 257–266.
36. Lee, J., Hampl, M., Albert, P., and Fine, H. A. (2002). Antitumor activity and prolonged expression from a TRAIL-expressing adenoviral vector. *Neoplasia* **4:** 312–323.
37. Huang, X., *et al.* (2002). Combined TRAIL and Bax gene therapy prolonged survival in mice with ovarian cancer xenograft. *Gene Ther.* **9:** 1379–1386.

doi:10.1016/j.ymthe.2004.08.024

38. Lin, T., *et al.* (2002). Targeted expression of green fluorescent protein/tumor necrosis factor-related apoptosis-inducing ligand fusion protein from human telomerase reverse transcriptase promoter elicits antitumor activity without toxic effect on primary human hepatocytes. *Cancer Res.* **62:** 3620–3625.
39. Lin, T., *et al.* (2002). Long-term tumor-free survival from treatment with the GFP–TRAIL fusion gene expressed from the hTERT promoter in breast cancer cells. *Oncogene* **21:** 8020–8028.
40. Armeanu, S., *et al.* (2003). Adenoviral gene transfer of tumor necrosis factor-related apoptosis-inducing ligand overcomes an impaired response of hepatoma cells but causes severe apoptosis in primary human hepatocytes. *Cancer Res.* **63:** 2369–2372.
41. Parker, C. C., and Dearnaley, D. P. (2003). Radical radiotherapy for prostate cancer. *Cancer Treat. Rev.* **29:** 161–169.
42. Teh, B. S., *et al.* (2002). Combining radiotherapy with gene therapy (from the bench to the bedside): a novel treatment strategy for prostate cancer. *Oncologist* **7:** 458–466.
43. Atkinson, G., and Hall, S. J. (1999). Prodrug activation gene therapy and external beam irradiation in the treatment of prostate cancer. *Urology* **54:** 1098–1104.
44. Stevens, C. W., Zeng, M., and Cerniglia, G. J. (1996). Ionizing radiation greatly improves gene transfer efficiency in mammalian cells. *Hum. Gene Ther.* **7:** 1727–1734.
45. Belka, C., *et al.* (2004). Apoptosis-modulating agents in combination with radiotherapy—current status and outlook. *Int. J. Radiat. Oncol. Biol. Phys.* **58:** 542–554.
46. Waxman, D. J., and Schwartz, P. S. (2003). Harnessing apoptosis for improved anticancer gene therapy. *Cancer Res.* **63:** 8563–8572.
47. Gliniak, B., and Le, T. (1999). Tumor necrosis factor-related apoptosis-inducing ligand's antitumor activity in vivo is enhanced by the chemotherapeutic agent CPT-11. *Cancer Res.* **59:** 6153–6158.
48. Chinnaiyan, A. M., *et al.* (2000). A combined effect of tumor necrosis factor-related apoptosis-inducing ligand and ionizing radiation in breast cancer therapy. *Proc. Natl. Acad. Sci. USA* **97:** 1754–1759.
49. Nicholson, B., and Theodorescu, D. (2004). Angiogenesis and prostate cancer tumor growth. *J. Cell. Biochem.* **91:** 125–150.
50. Garcia-Barros, M., *et al.* (2003). Tumor response to radiotherapy regulated by endothelial cell apoptosis. *Science* **300:** 1155–1159.
51. Kaliberov, S. A., *et al.* (2002). Adenovirus-mediated transfer of BAX driven by the vascular endothelial growth factor promoter induces apoptosis in lung cancer cells. *Mol. Ther.* **6:** 190–198.
52. Dressler, V., Muller, G., and Suhnel, J. (1999). CombiTool—a new computer program for analyzing combination experiments with biologically active agents. *Comput. Biomed. Res.* **32:** 145–160.
53. Chou, T. C., and Talalay, P. (1984). Quantitative analysis of dose–effect relationships: the combined effects of multiple drugs or enzyme inhibitors. *Adv. Enzymol. Regul.* **22:** 27–55.

Mol Ther 7:S315-S316, 2003

New Adenoviral Vectors for Molecular Chemotherapy of Prostate Cancer. *D.L. Della Manna, M. Yamamoto, V. Krasnykh, K.R. Zinn, J. Davydova, S. Chiz, and D.J. Buchsbaum.* Department of Radiation Oncology, Division of Human Gene Therapy, and Gene Therapy Center, University of Alabama at Birmingham, Birmingham, Alabama

Object. The goal of this project is to develop novel two gene adenovirus (Ad) vectors expressing somatostatin receptor subtype 2 (SSTr2) and cytosine deaminase (CD) under control of the cyclooxygenase-2 (cox2) promoter for radiolabeled peptide/molecular chemotherapy of prostate cancer. The tumor specific promoter cox2 was selected based on the fact that the liver is cox2 negative and is the predominant site of Ad vector localization after systemic administration, thus the Ad may infect normal liver cells but no transgene expression would occur. Two forms of the cox2 promoter were compared and contrasted to the cytelomegalovirus (CMV) promoter; a "long" form (cox2L) and a truncated "medium" form (cox2M). **Materials and Methods.** Ad were made using the AdEasy system and propagated in 911 cells. Somatostatin binding and internalization assays were performed by incubating infected cells with ^{99m}Tc-P2045, a peptide specific for SSTr2, and gamma camera imaging after the surface bound peptide was removed. CD conversion assays were performed with lysates from infected cells with the addition of ^{3}H-5-fluorocytosine (5-FC) at various time points, and separation on thin layer chromatography plates in butanol and water. Spots containing 5-FC and 5-fluorouracil (5-FU) were cut out, put into scintillation fluid, and counted in a beta counter. Cytotoxicity assays were performed using the MTS assay (Promega) as described in the manufacturer's protocol. **Results.** Six vectors expressing CD and SSTr2 were developed and evaluated using the prostate cancer cell lines DU145 and PC3: Adcox2LCDcox2LSSTr2, Adcox2LSSTr2cox2LCD, Adcox2LCDIRESSSTr2, Adcox2MCDcox2MSSTr2, Adcox2MSSTr2cox2MCD, and AdCMVCDCMVSSTr2. Based on CD conversion assays, cytotoxicity assays and SSTr2 binding assays, the vectors driven by cox2L proved to be superior to those driven by cox2M, however the cox2L vector constructed using IRES failed to bind ^{99m}Tc-P2045. Although AdCMVCDCMVSSTr2 infected cells converted more 5-FC to 5-FU than Adcox2LCDcox2LSSTr2 and Adcox2LSSTr2cox2LCD (7.53 *vs.* 2.95 and 2.51 pmol/min/mg, in DU145 cells; 2.46 *vs.* 1.21 and 0.87 pmol/min/mg in PC3 cells), higher cytotoxicity was demonstrated with the cox2L vectors after exposure to 5-FC in both cell lines tested (IC_{50} of 13.1 and 21.4 nM for Adcox2LCDcox2LSSTr2 and Adcox2LSSTr2cox2LCD with DU145 cells, and 24.5 and 30.4 nM, respectively with PC3 cells). **Conclusion.** The combination of the therapeutic genes CD and SSTr2 with the cox2L promoter should provide specificity for tumor uptake of radiolabeled peptides that bind to SSTr2 and selective 5-FC molecular chemotherapy, which are to be evaluated in metastatic prostate cancer models. *Supported by DOD grant DAMD17-02-1-0001.*

Annals of Nuclear Medicine Vol. 18, No. 4, 275–283, 2004

Gene expression imaging with radiolabeled peptides

Donald J. BUCHSBAUM,* Tandra R. CHAUDHURI,** Masato YAMAMOTO*** and Kurt R. ZINN****

*Department of Radiation Oncology, **Department of Radiology, ***Division of Human Gene Therapy, and ****Department of Medicine, University of Alabama at Birmingham

An approach to image radiolabeled peptide localization at tumor sites by inducing tumor cells to synthesize membrane expressed human somatostatin receptor subtype 2 (hSSTr2) with a high affinity for radiolabeled somatostatin analogues is described. The use of gene transfer technology to induce expression of high affinity membrane hSSTr2 can enhance the specificity and degree of radiolabeled peptide localization in tumors. Employing this strategy, induction of high levels of hSSTr2 expression with selective tumor uptake of radiolabeled peptides was achieved in both subcutaneous non-small cell lung cancer and intraperitoneal ovarian cancer mouse human tumor xenograft models. The features of this genetic transduction imaging approach are: (1) constitutive expression of a tumor-associated receptor is not required; (2) tumor cells are altered to express a new target receptor or increased quantities of a constitutive receptor at levels which may significantly increase tumor targeting of radiolabeled peptides compared to uptake in normal tissues; (3) gene transfer can be accomplished by local or regional injection of adenoviral vectors; (4) it is feasible to target adenovirus vectors to tumor cells by modifying adenoviral tropism (binding) or by the use of tumor-specific promoters such that the hSSTr2 will be specifically expressed in the desired tumor; and (5) this technique can be used to image expression of a second therapeutic gene.

Key words: somatostatin receptor, peptide imaging, gene expression imaging

INTRODUCTION

THE GROUP of somatostatin receptors includes gene products encoded by 5 separate somatostatin receptor genes.[1] Human somatostatin receptor subtype 2 (hSSTr2) is expressed on a number of human tumors including neuroendocrine, ovarian, renal, breast, prostate, lung, and meningiomas.[2–6] The receptors have varying tissue levels in the brain, gastrointestinal tract, pancreas, kidney, and spleen.[7–9] All 5 receptors show high affinity binding to natural somatostatin peptide (either somatostatin-14 or somatostatin-28). Octreotide, P829, and P2045 are synthetic somatostatin analogues that preferentially bind with high affinity to somatostatin receptor subtypes 2, 3, and 5.[7–12]

Received January 8, 2004, revision accepted January 8, 2004.

For reprint contact: Donald J. Buchsbaum, Ph.D., Department of Radiation Oncology, University of Alabama at Birmingham, 1530 3rd Avenue South, WTI 674, Birmingham, AL 35294–6832, USA.

E-mail: djb@uab.edu

Octreotide is an eight amino-acid peptide which has a high affinity for hSSTr2, which is the most prominent somatostatin receptor on human tumors, and is stable toward *in vivo* degradation relative to the endogenous 14 amino-acid somatostatin-14 peptide. Octreotide and other somatostatin analogues have been modified with bifunctional chelating agents, for complexing radiometals, and by changing the amino acid sequence in order to increase their hSSTr2 binding affinity and optimize their normal organ clearance. Somatostatin analogues have been labeled with ^{111}In and ^{99m}Tc for imaging applications.

Radiolabeled peptides (*e.g.* ^{111}In-DTPA-D-Phe^1-octreotide, Octreoscan® or ^{99m}Tc-P829, Neotect®) have been used to target hSSTr2 positive tumor cells for imaging in patients.[13–16] Despite the success of these investigations, improved targeting strategies are possible using a genetic approach, in which a gene transfer vector is injected to express hSSTr2 on the tumor cell surface which can be imaged after injection of a radiolabeled peptide (Fig. 1). This approach also offers the possibility for imaging gene transfer of a second therapeutic gene. Our focus has been the development of recombinant

adenoviral vectors that transfer the hSSTr2 gene alone or with a second therapeutic gene to tumor cells and use of radiolabeled peptides to image gene transfer.[17–23] A potential advantage of genetic transduction of hSSTr2 is that the level of expression may be greater than what are generally otherwise low tumor concentrations of this receptor.

In this genetic approach we are attempting to specifically increase the number of receptors on tumor cells that normally express a receptor, or to specifically induce expression on tumor cells that do not ordinarily express the receptor by the use of genetic transduction. It is our hypothesis that one can deliver a larger fraction of the administered dose of the radiolabeled peptide to the tumor cells through increased receptor expression at the tumor site. The potential advantages of the genetic transduction approach are: (1) constitutive expression of a tumor-associated receptor is not required; and (2) tumor cells are altered to express a target receptor at levels which may significantly improve tumor-to-normal tissue targeting of radiolabeled peptides. This method thus represents a new paradigm by which imaging of gene transfer can be achieved through radiolabeled peptide localization to tumors transduced *in situ* to express unique and novel receptors.

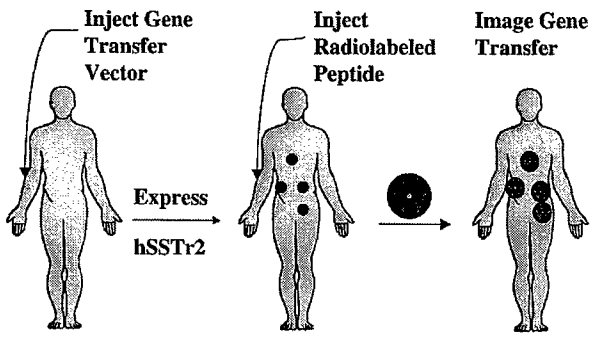

Fig. 1 Genetic radioisotope targeting strategy to image gene transfer.

GENETIC INDUCTION OF hSSTr2 *IN VITRO* AND *IN VIVO*

Imaging of human non-small cell lung and prostate cancer cells and tumor xenografts induced to express hSSTr2

An adenovirus encoding the gene for hSSTr2 under control of the cytomegalovirus promoter (AdCMVhSSTr2) was produced.[19] *In vitro* binding of ^{111}In-DTPA-D-Phe^1-octreotide to A-427 human non-small cell lung cancer cells infected with AdCMVhSSTr2 was demonstrated by imaging of cells in plates (Fig. 2).[24] Scatchard analysis of A-427 cells infected with 10 plaque forming units (pfu) AdCMVhSSTr2 and binding of ^{99m}Tc-P829 (Neotect) showed a B_{max} of 19,000 fmol/mg and the affinity of ^{99m}Tc-P829 to be 7 nM.[20]

Other studies showed the localization of ^{111}In-DTPA-D-Phe^1-octreotide to *s.c.* A-427 non-small cell lung tumors injected intratumorally (*i.t.*) with AdCMVhSSTr2.[24] The gamma camera region of interest analysis showed the tumor uptake of ^{111}In-DTPA-D-Phe^1-octreotide to be 2.8% ID/g 48 h after a single AdCMVhSSTr2 injection and 3.1% ID/g at 96 h (Fig. 3). Uptake of ^{111}In-DTPA-D-Phe^1-octreotide in control adenoviral-injected tumors with the thyrotropin-releasing hormone receptor gene (AdCMVTRHr) was <0.3% ID/g at both time points.

A novel ^{99m}Tc-labeled peptide (P2045) described by Diatide, Inc. binds with high affinity to hSSTr2.[11] We

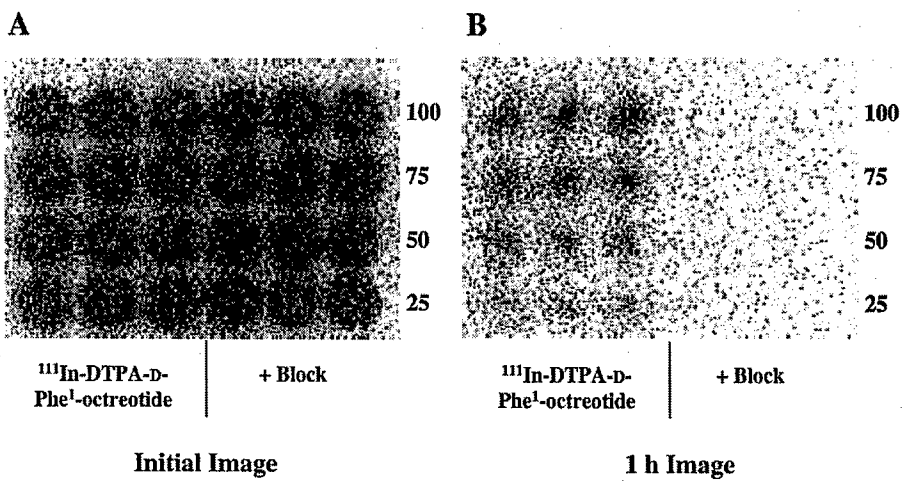

Fig. 2 Gamma camera imaging of AdCMVhSSTr2-infected A-427 non-small cell lung cancer cells mixed with uninfected cells (percentages of hSSTr2-positive cells indicated on the right) in a 24-well plate incubated with ^{111}In-DTPA-D-Phe^1-octreotide in the presence or absence of excess unlabeled octreotide as a blocking agent.[24] Reprinted with permission from the American Cancer Society.

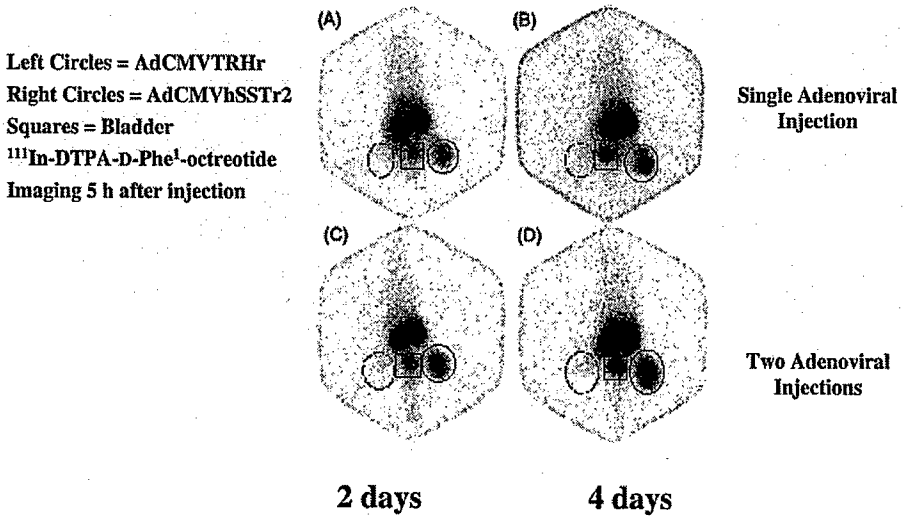

Fig. 3 Gamma camera images of mice after intratumoral AdCMVhSSTr2 injection into athymic nude mice bearing A-427 xenografts obtained at 2 or 4 days after *i.v.* injection of ^{111}In-DTPA-D-Phe^1-octreotide.[24] Reprinted with permission from the American Cancer Society.

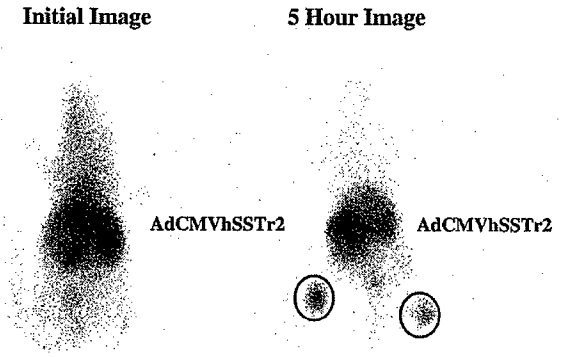

Fig. 4 Gamma camera imaging of ^{99m}Tc-P2045 in mice bearing DU145 *s.c.* tumor xenografts injected with AdCMVhSSTr2.

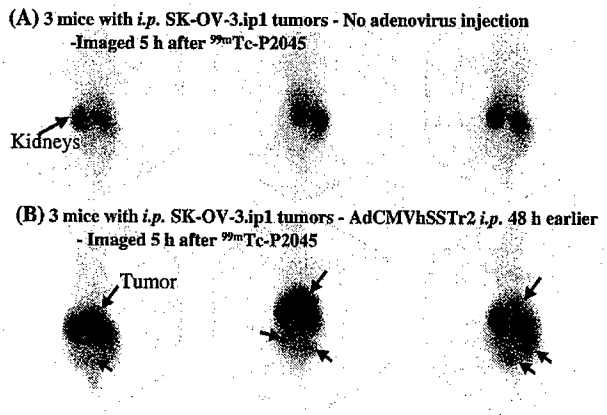

Fig. 5 Gamma camera imaging of AdCMVhSSTr2 gene transfer to *i.p.* SK-OV-3.ipl ovarian tumors after *i.v.* injection of ^{99m}Tc-P2045.[21] Reprinted with permission from Springer-Verlag.

evaluated P2045 in mice bearing *s.c.* A-427 tumors injected *i.t.* with AdCMVhSSTr2 or with a control adenovirus. ^{99m}Tc-P2045 was injected *i.v.* 2 or 4 days after AdCMVhSSTr2 injection and the animals were imaged using a gamma camera equipped with a pinhole collimator 3.5–4.5 h later. The images showed higher radioactive uptake in the tumors, compared with ^{99m}Tc-P829, for tumors injected with AdCMVhSSTr2 but background uptake in tumors injected with control adenovirus. No other tissue had greater uptake than the AdCMVhSSTr2-injected tumor[25]; ~85% ^{99m}Tc-P2045 was excreted by 4 h.

Gamma camera imaging was also used to detect hSSTr2 expression in DU145 prostate tumor xenografts infected with AdCMVhSSTr2 using ^{99m}Tc-P2045. Mice bearing *s.c.* DU145 tumors injected *i.t.* with AdCMVhSSTr2 showed uptake of *i.v.*-injected ^{99m}Tc-P2045 detected by gamma camera imaging (Fig. 4), while uptake was not observed when the tumors were infected with a control adenovirus (not shown). Uptake averaged 7.5 ± 1.0% for AdCMVhSSTr2 injected tumors. Of note, the tumor sizes for the mouse in Figure 4 were 144 and 167 mg for the left and right tumors, respectively. Independent confirmation of hSSTr2 expression was demonstrated by immunohistochemical analysis.

Imaging of human ovarian cancer xenografts induced to express hSSTr2

To evaluate the ability to induce receptor expression in ovarian cancer *in vivo*, AdCMVhSSTr2 was injected *i.p.* to induce hSSTr2 expression on SK-OV-3.ipl human ovarian tumors 5 days after tumor cell injection in the peritoneum in athymic nude mice. Two days later, tumor localization of ^{111}In-DTPA-D-Phe^1-octreotide at 4 h after *i.p.* injection was equal to 60.4% ID/g.[19] The uptake in

tumor decreased to 18.6% ID/g at 24 h after injection. The tumor localization was significantly lower (1.6% ID/g) when a control adenovirus encoding the gene for gastrin releasing peptide receptor (AdCMVGRPr) was injected. Imaging of hSSTr2 gene transfer to *i.p.* SK-OV-3.ipl tumors after injection of ^{99m}Tc-P2045 is shown in Figure 5.[21] Thus, these studies demonstrated that tumor uptake of ^{111}In-DTPA-D-Phe^1-octreotide and ^{99m}Tc-P2045 could be detected after infection of the ovarian tumors *in vivo* with AdCMVhSSTr2.

Tumor uptake of ^{99m}Tc-P2045 in nude mice bearing SK-OV-3.ipl tumors in the peritoneum at 48 h after *i.v.* injection averaged 2.2 ± 0.3% ID/g for mice injected *i.p.* with AdCMVhSSTr2 (1×10^9 pfu) as compared to 0.2 ± 0.002% ID/g in control mice not receiving adenoviral injection ($p < 0.05$) or in tumors from mice injected *i.p.* with an adenovirus encoding the green fluorescent protein (AdCMVGFP) which averaged 0.3 ± 0.2% ID/g.[26]

IMAGING OF THERAPEUTIC GENE EXPRESSION

The molecular suicide gene therapy approach involves insertion and expression of an enzyme in a target cell that converts a non-toxic prodrug to a toxic drug.[27,28] The two most widely studied systems are thymidine kinase (TK) and cytosine deaminase (CD). The enzyme CD is a non-mammalian enzyme which catalyzes the formation of uracil by the deamination of cytosine. When 5-fluorocytosine (5-FC) is the substrate, this enzyme will produce 5-fluorouracil (5-FU), a potent cancer chemotherapeutic and radiosensitizing agent.[29] The genes for bacterial and yeast CD have been cloned.[30–33] Because mammalian cells do not normally express the CD gene, 5-FC is nontoxic to these cells, even at high concentrations. 5-FC has been used as an antifungal drug because of its relative nontoxicity in humans. The CD gene has been used in gene therapy strategies to mediate intracellular conversion of 5-FC to 5-FU, and has been shown to be effective in animal tumor models.[34,35] This therapeutic strategy has the advantage of intracellular production of high concentrations of radiosensitizing drug as an alternative to systemic administration, therefore potentially limiting systemic toxicities.[36] Converted 5-FU passively diffuses across the cell membrane from CD-positive cells to nontransduced cells.[37,38] This bystander effect compensates for the inability of current vector systems to transduce all but a small fraction of cells in a given tumor.[28,39] The use of adenoviral vectors to encode CD and convert 5-FC to 5-FU to achieve cell killing has been reported by our group[40–43] and others.[35,38,44,45] We initially used an adenoviral vector encoding CD under control of the cytomegalovirus promoter (AdCMVCD) in combination with 5-FC and radiation treatment to demonstrate enhanced cytotoxicity against human colon, pancreatic, glioblastoma, and cholangiocarcinoma cells *in vitro* and *in vivo*.[40–42] More recently, we have used two gene vectors in which hSSTr2 has been used as an imaging gene and CD has been used as a therapeutic gene.

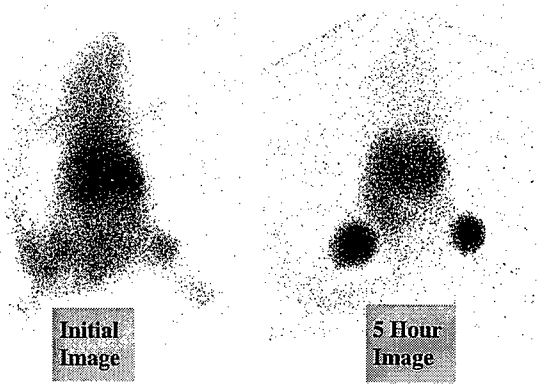

Fig. 6 Imaging of gene transfer in mice bearing A-427 *s.c.* tumors injected with AdCMVhSSTr2CD (*left*) or AdRGDCMVhSSTr2CD (*right*) followed 2 days later by *i.v.* injection of ^{99m}Tc-P2045.

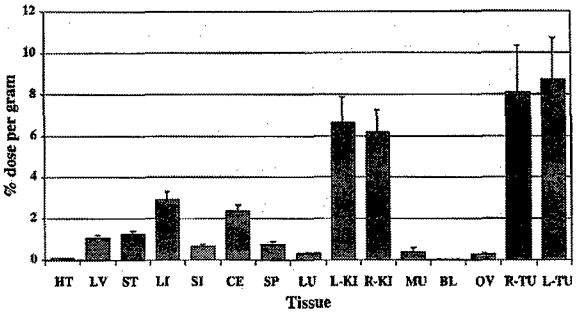

Fig. 7 Biodistribution of ^{99m}Tc-P2045 at 5 h after *i.v.* injection in nude mice bearing *s.c.* A-427 tumors injected with AdCMVhSSTr2CD (R-TU) or AdRGDCMVhSSTr2CD (L-TU). HT, heart; LV, liver; ST, stomach; LI, large intestine; SI, small intestine; CE, cecum; SP, spleen; LU, lungs; L-KI, left kidney; R-KI, right kidney; MU, leg muscle; BL, blood; OV, ovary; R-TU, right tumor; L-TU, left tumor.

Imaging of cytosine deaminase therapeutic gene transfer

Bicistronic adenoviral vectors encoding for hSSTr2 and the CD enzyme have been constructed and evaluated.[46] One rationale for the construction of these vectors is that hSSTr2 can be used as a target for non-invasive imaging to determine the expression of the therapeutic gene (CD) *in vivo*.[23] Second, hSSTr2 can be used for radiolabeled peptide therapy and the combination of this with CD mediated therapy through conversion of 5-FC to 5-FU may result in an additive or synergistic therapeutic effect. A-427 cells infected with bicistronic vectors AdCMVhSSTr2CD or AdRGDCMVhSSTr2CD, with the RGD peptide genetically engineered in the fiber knob to retarget adenovirus binding to integrins on the cell

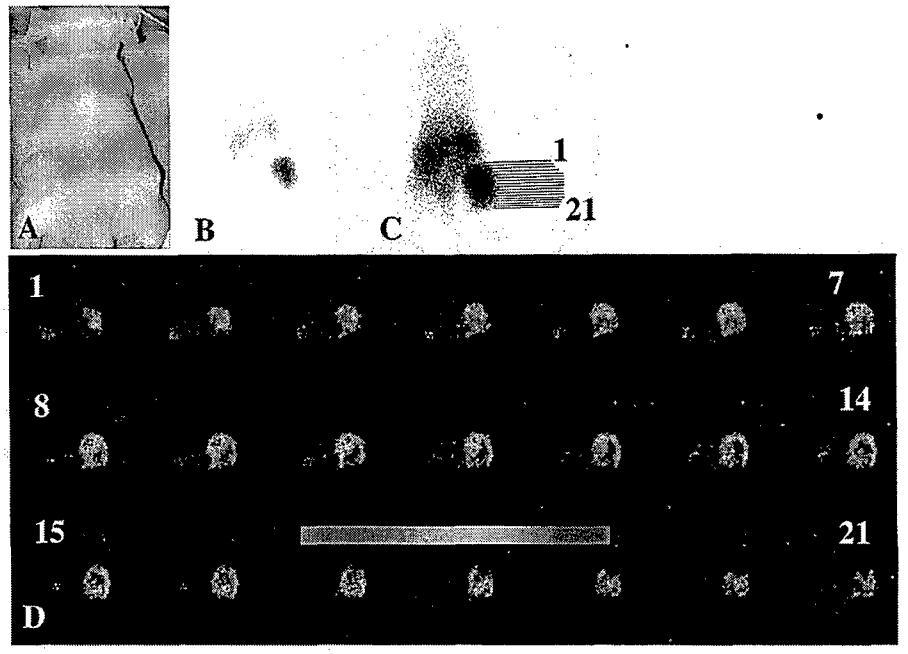

Fig. 8 SPECT imaging of adenovirus-mediated hSSTr2 expression in a tumor xenograft. (A) Photograph of representative mouse with two A-427 tumors. The right tumor was injected with 1×10^9 pfu AdhSSTr2GFP while the left tumor was injected with a control adenovirus vector. (B, C) planar gamma camera imaging at 5 h after *i.v.* ^{99m}Tc-P2045 injection, (D) Transverse slices (0.58 mm each) showing hSSTr2 expression within the tumor. The adenovirus-mediated hSSTr2 expression led to specific retention of ^{99m}Tc-P2045 in discrete areas of the tumor. Figure 8B shows the highest retention of the ^{99m}Tc-P2045 was in the right tumor.

surface, produced equivalent hSSTr2 expression as the single gene vector AdCMVhSSTr2.[47] In addition, the AdCMVhSSTr2CD and AdRGDCMVhSSTr2CD vectors produced similar CD enzyme activity levels as the single gene vector AdCMVCD.[47] Thus, both genes were active in the bicistronic vectors. We next investigated imaging of gene transfer in athymic nude mice bearing *s.c.* A-427 tumors injected with 1×10^9 pfu AdCMVhSSTr2 (left) or AdRGDCMVhSSTr2CD (right). After 2 days, ^{99m}Tc-P2045 was *i.v.* injected and imaging was conducted (Fig. 6). The corresponding biodistribution results obtained by counting of tissues in a gamma camera are shown in Figure 7.

SPECT imaging was applied to measure the distribution of adenovirus-mediated transgene expression within *s.c.* xenografts. Nude mice bearing two A-427 flank tumors were injected *i.t.* with bicistronic adenovirus vectors. The bicistronic Ad5 vector encoding hSSTr2 and green fluorescent protein (GFP) was *i.t.* injected (1×10^9 pfu) in the right A-427 tumor, while a control bicistronic vector was injected in the left tumor. Imaging studies were conducted after 2 days. A photograph of a representative mouse with two tumors is shown in Figure 8A. Planar gamma camera images are presented in Figures 8B and 8C at 5 h after *i.v.* injection of ^{99m}Tc-P2045 (55.5 MBq). The two planar images are identical, with the exception of scaling; Figure 8C shows the location of transverse slices (0.58 mm each) that are displayed in Figure 8D. The distribution of hSSTr2 expression within the tumor was non-uniform and tended to be concentrated at the periphery of the tumor (Fig. 8D). The SPECT imaging technique had sufficient sensitivity and spatial resolution to enable the 3-dimensional hSSTr2 expression to be measured. The A-SPECT system (Gamma Medica, Inc., North Ridge, CA) was used for this study, with a total of 64 individual projections collected (30 sec each) using a 1 mm pinhole collimator.

Imaging of thymidine kinase therapeutic gene transfer

Further studies were carried out using a bicistronic adenoviral vector encoding hSSTr2 and TK in the A-427 tumor model.[23] The tumors were injected *i.t.* with the bicistronic vector (AdCMVhSSTr2TK) and the animals imaged for hSSTr2 expression with ^{99m}Tc-P2045 and TK with ^{131}I-FIAU (Fig. 9). The biodistribution results showed the uptake of ^{99m}Tc-P2045 and ^{131}I-FIAU for AdCMVhSSTr2TK-injected tumors (n = 8) was 11.1% and 1.6% ID/g, respectively. AdCMVhSSTr2-injected tumors (n = 4) accumulated 10.2% ID/g of the ^{99m}Tc-P2045 and 0.3% of the ^{131}I-FIAU. AdCMVTK-injected tumors (n = 4) had 0.2% ID/g for the ^{99m}Tc-P2045 and 3.7% for ^{131}I-FIAU.

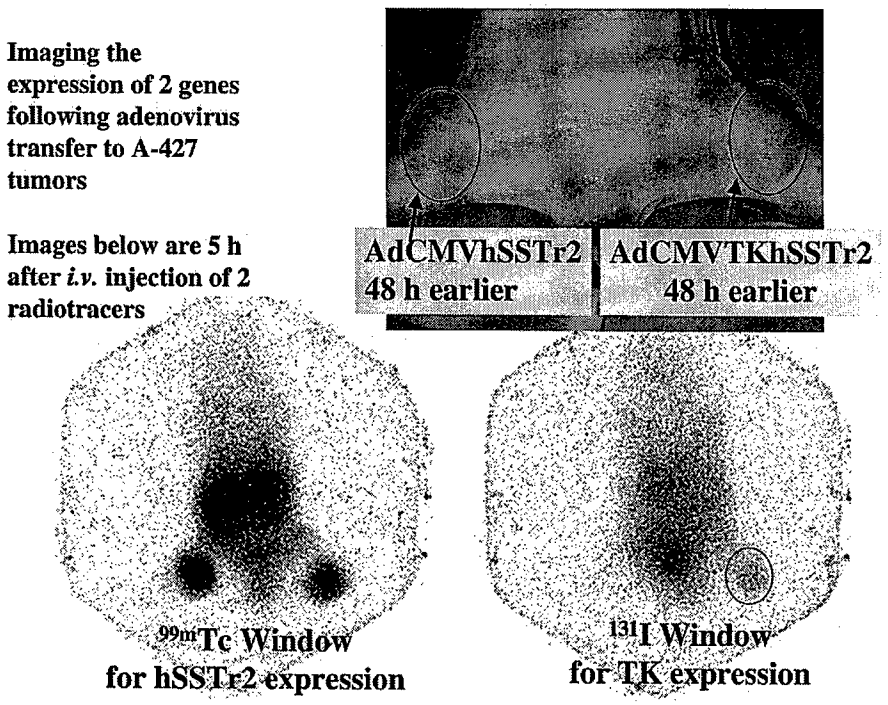

Fig. 9 Simultaneous imaging for hSSTr2 and TK expression in mice bearing *s.c.* A-427 tumors injected with AdCMVhSSTr2 or AdCMVTKhSSTr2. Photograph of the mouse shows tumor locations and adenoviral doses. The expression of hSSTr2 was identified by imaging tumor accumulation of ^{99m}Tc-P2045 (*bottom left*), while TK expression was depicted by imaging tumor accumulation of ^{131}I-FIAU (*bottom right*). The images were obtained 5 h after *i.v.* injection of the radiotracers.[23] Reprinted with permission from the Radiological Society of North America, Inc.

Table 1 Conversion of 5-FC to 5-FU in pmol/min/mg ± SD measured over a 1 h period after infection of DU145 cells with 100 pfu of each virus.

Vector	DU145
Uninfected	0.00
AdCMVCD	25.6 ± 1.3
AdCMVCDhSSTr2	7.5 ± 0.3
AdCox-2LCDhSSTr2	3.0 ± 0.2
AdCox-2LhSSTr2CD	2.5 ± 0.2

Table 2 Cytotoxicity of adenoviral infected DU145 human prostate cancer cells (10 pfu) exposed to 5-FC expressed as IC_{50} (nM).

Vector	DU145
Uninfected	202.6
AdCox-2LCDhSSTr2	13.1
AdCox-2LhSSTr2CD	21.4

Imaging of hSSTr2 gene transfer with adenoviral vectors controlled by the cyclooxygenase-2 promoter

The specificity of vectors for gene transfer may be improved by combining transductional targeting of adenovirus utilizing the tumor-specific promoter, cyclooxygenase-2 (Cox-2), to drive the transcription of the hSSTr2 and CD genes. The liver is the predominant site of adenovirus vector localization after systemic administration, and as a consequence is at risk when adenoviral vectors containing suicide genes such as CD ectopically localize to this site. Thus, a promoter with both tumor specificity and minimal transcriptional activity in hepatocytes would be ideal for cancer gene therapy.

Two new adenoviral vectors expressing CD and hSSTr2 were produced using the long (L) length Cox-2 promoter: AdCox-2LCDhSSTr2 and AdCox-2LhSSTr2CD. The new vectors expressing CD and hSSTr2 were tested to determine their conversion of 5-FC to 5-FU following infection of DU145 human prostate cancer cells (Table 1). The results indicate that AdCox-2LCDhSSTr2 and AdCox-2LhSSTr2CD produced a lower level of conversion of 5-FC to 5-FU in DU145 cells than AdCMVCD or AdCMVCDhSSTr2. These results support earlier observations that the CMV promoter is stronger than the Cox-2 promoter, although less specific.

In the next set of studies, we evaluated the cytotoxicity of the new vectors after infection of DU145 cells with 10 pfu/cell of virus. At 24 h after infection, the cells were seeded at 5,000 cells/well and exposed to varying concentrations of 5-FC. Cell viability was assessed by the MTS

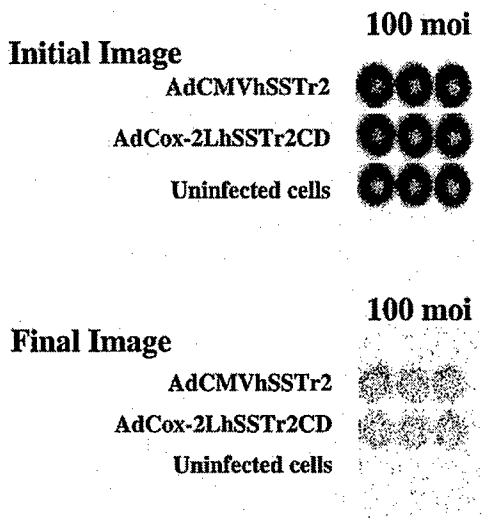

Fig. 10 Gamma camera imaging of hSSTr2 gene transfer to DU145 prostate cancer cells incubated with ^{99m}Tc-P2045 before (initial) and after (final) acid washing.

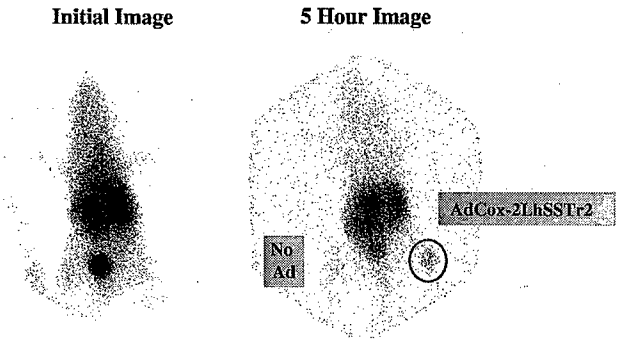

Fig. 11 Gamma camera imaging of ^{99m}Tc-P2045 administered *i.v.* in a nude mouse bearing DU145 *s.c.* tumors injected two days earlier with no adenovirus (Ad) or AdCox-2LhSSTr2.

assay (Celltiter 96 AQ, Promega). The IC_{50} values for these cell lines are shown in Table 2. The results indicate that AdCox-2LCDhSSTr2 and AdCox-2LhSSTr2CD produced cytotoxicity with a moderately low IC_{50} value.

In vitro binding of ^{99m}Tc-P2045 to DU145 cells infected with AdCMVhSSTr2 or AdCox-2LhSSTr2CD in plates detected by imaging with a gamma camera is shown in Figure 10. Gamma camera imaging of ^{99m}Tc-P2045 localization in a DU145 *s.c.* tumor injected with AdCox-2LhSSTr2 is shown in Figure 11. The combination of the therapeutic genes CD and hSSTr2 with the Cox-2L promoter should provide specificity for tumor uptake of radiolabeled peptides that bind to hSSTr2 and selective 5-FC molecular chemotherapy. However, the level of hSSTr2 expression from AdCox-2LhSSTr2CD was lower than with AdCMVhSSTr2CD infection. Thus, we are currently producing RGD modified Cox-2L CD and hSSTr2 two-gene vectors to achieve higher levels of hSSTr2 and CD expression.

CONCLUSIONS

These studies demonstrate that genetic induction of hSSTr2 results in tumor localization of radiolabeled peptides at a level sufficient for imaging. It should be emphasized that in this approach we are attempting to specifically increase the number of receptors on tumor cells that normally express a receptor, or to specifically induce expression on tumor cells that do not ordinarily express the receptor by the use of genetic transduction, with the result being increased targeting of the radiolabeled peptide to the tumor site. The potential advantages of the genetic transduction approach are: (1) constitutive expression of a tumor-associated receptor is not required; and (2) tumor cells are altered to express a target receptor at levels which may significantly improve tumor-to-normal tissue targeting of radiolabeled peptides. This method thus represents a new paradigm by which imaging of gene transfer can be achieved through radiolabeled peptide localization to tumors transduced *in situ* to express unique and novel receptors. For approaching disseminated disease, transductional targeting approaches can be used to alter the tropism of viral vectors to achieve tumor cell specific gene delivery. Selective tumor targeting may also be achieved by transcriptional approaches employing tumor-specific regulatory elements. Other approaches that are under active investigation in other laboratories include gene transfer of the type-2 dopamine receptor expressed on the tumor cell surface detected by PET using a radiolabeled antagonist or herpes simplex virus TK gene transfer detected by gamma camera or PET imaging with radiolabeled substrates trapped intracellularly after phosphorylation by the kinase.[48–50] Gene transfer of the sodium iodide symporter has also been used for imaging with radioiodine.[51] Additional studies are needed to confirm the feasibility of these approaches in humans.

ACKNOWLEDGMENTS

Mark Carpenter, Buck Rogers, David Curiel, and Victor Krasnykh are acknowledged for their contributions to the concepts and results presented. We thank J.-L. Vanderheyden (Mallinckrodt, Inc.) and Michael Azure (Diatide, Inc.) for the supply of somatostatin analogues, and Sally Lagan for manuscript preparation. Supported in part by DOE grant DE-FG05-93ER61654 and DOD grant DAMD 17-02-1-0001.

REFERENCES

1. Patel YC. Somatostatin and its receptor family. *Front Neuroendocrinol* 1999; 20: 157–198.
2. Reubi JC, Schaer JC, Waser B, Mengod G. Expression and localization of somatostatin receptor SSTR1, SSTR2, and SSTR3 messenger RNAs in primary human tumors using *in situ* hybridization. *Cancer Res* 1994; 54: 3455–3459.

3. Woltering EA, O'Dorisio MS, O'Dorisio TM. The role of radiolabeled somatostatin analogs in the management of cancer patients. In: *Principles and Practice of Oncology, PPO Updates*, DeVita Jr VT, Hellman S, Rosenberg SA, eds., Vol. 9. Philadelphia; Lippincott-Raven, 1995: 1–16.
4. Reubi JC, Waser B, Schaer JC, Markwalder R. Somatostatin receptors in human prostate and prostate cancer. *J Clin Endocrinol Metab* 1995; 80: 2806–2814.
5. Nilsson S, Reubi JC, Kalkner KM, Laissue JA, Horisberger U, Olerud C, et al. Metastatic hormone-refractory prostatic adenocarcinoma expresses somatostatin receptors and is visualized *in vivo* by [^{111}In]-labeled DTPA-D-[Phe^1]-octreotide scintigraphy. *Cancer Res* 1995; 55 (Suppl): 5805s–5810s.
6. Halmos G, Schally AV, Sun B, Davis R, Bostwick DG, Plonowski A. High expression of somatostatin receptors and messenger ribonucleic acid for its receptor subtypes in organ-confined and locally advanced human prostate cancers. *J Clin Endocrinol Metab* 2000; 85: 2564–2571.
7. Yamada Y, Post SR, Wang K, Tager HS, Bell GI, Seino S. Cloning and functional characterization of a family of human and mouse somatostatin receptors expressed in brain, gastrointestinal tract, and kidney. *Proc Natl Acad Sci USA* 1992; 89: 251–255.
8. Hoyer D, Bell GI, Berelowitz M, Epelbaum J, Feniuk W, Humphrey PP, et al. Classification and nomenclature of somatostatin receptors. *Trends Pharmacol Sci* 1995; 16: 86–88.
9. Feuerbach D, Fehlmann D, Nunn C, Siehler S, Langenegger D, Bouhelal R, et al. Cloning, expression and pharmacological characterisation of the mouse somatostatin sst(5) receptor. *Neuropharmacology* 2000; 39: 1451–1462.
10. Virgolini I, Leimer M, Handmaker H, Lastoria S, Bischof C, Muto P, et al. Somatostatin receptor subtype specificity and *in vivo* binding of a novel tumor tracer, ^{99m}Tc-P829. *Cancer Res* 1998; 58: 1850–1859.
11. Manchanda R, Azure M, Lister-James J, Bush L, Zinn K, Baggs R, et al. Tumor Regression in rat pancreatic (AR42J) tumor-bearing mice with Re-188 P2045—A somatostatin analog. *Clin Cancer Res* 1999; 5: 3769s.
12. Reubi JC, Schär JC, Waser B, Wenger S, Heppeler A, Schmitt JS, et al. Affinity profiles for human somatostatin receptor subtypes SST1-SST5 of somatostatin radiotracers selected for scintigraphic and radiotherapeutic use. *Eur J Nucl Med* 2000; 27: 273–282.
13. Virgolini I, Kurtaran A, Raderer M, Leimer M, Angelberger P, Havlik E, et al. Vasoactive intestinal peptide receptor scintigraphy. *J Nucl Med* 1995; 36: 1732–1739.
14. Lamberts SWJ, van der Lely A-J, de Herder WW, Hofland LJ. Octreotide. *N Engl J Med* 1996; 334: 246–254.
15. Blum JE, Handmaker H, Rinne NA. The utility of a somatostatin-type receptor binding peptide radiopharmaceutical (P829) in the evaluation of solitary pulmonary nodules. *Chest* 1999; 115: 224–232.
16. Traub T, Petkov V, Ofluoglu S, Pangerl T, Raderer M, Fueger BJ, et al. ^{111}In-DOTA-lanreotide scintigraphy in patients with tumors of the lung. *J Nucl Med* 2001; 42: 1309–1315.
17. Rogers BE, Garver RI Jr, Grizzle WE, Buchsbaum DJ. Genetic induction of antigens and receptors as targets for cancer radiotherapy. *Tumor Targeting* 1998; 3: 122–137.
18. Rogers BE, Douglas JT, Sosnowski BA, Ying W, Pierce G, Buchsbaum DJ, et al. Enhanced *in vivo* gene delivery to human ovarian cancer xenografts utilizing a tropism-modified adenovirus vector. *Tumor Targeting* 1998; 3: 25–31.
19. Rogers BE, McLean SF, Kirkman RL, Della Manna D, Bright SJ, Olsen CC, et al. *In vivo* localization of [^{111}In]-DTPA-D-Phe^1-octreotide to human ovarian tumor xenografts induced to express the somatostatin receptor subtype 2 using an adenoviral vector. *Clin Cancer Res* 1999; 5: 383–393.
20. Zinn KR, Buchsbaum DJ, Chaudhuri TR, Mountz JM, Grizzle WE, Rogers BE. Noninvasive monitoring of gene transfer using a reporter receptor imaged with a high-affinity peptide radiolabeled with ^{99m}Tc or ^{188}Re. *J Nucl Med* 2000; 41: 887–895.
21. Zinn KR, Chaudhuri TR. The type 2 human somatostatin receptor as a platform for reporter gene imaging. *Eur J Nucl Med* 2002; 29: 388–399.
22. Hemminki A, Zinn KR, Liu B, Chaudhuri TR, Desmond RA, Rogers BE, et al. *In vivo* molecular chemotherapy and noninvasive imaging with an infectivity-enhanced adenovirus. *J Natl Cancer Inst* 2002; 94: 741–749.
23. Zinn KR, Chaudhuri TR, Krasnykh VN, Buchsbaum DJ, Belousova N, Grizzle WE, et al. Gamma camera dual imaging with a somatostatin receptor and thymidine kinase after gene transfer with a bicistronic adenovirus. *Radiology* 2002; 223: 417–425.
24. Rogers BE, Zinn KR, Lin C-Y, Chaudhuri TR, Buchsbaum DJ. Targeted radiotherapy with [^{90}Y]-SMT 487 in mice bearing human nonsmall cell lung tumor xenografts induced to express human somatostatin receptor subtype 2 with an adenoviral vector. *Cancer* 2002; 94: 1298–1305.
25. Rogers BE, Zinn KR, Buchsbaum DJ. Gene transfer strategies for improving radiolabeled peptide imaging and therapy. *Q J Nucl Med* 2000; 44: 208–223.
26. Chaudhuri TR, Rogers BE, Buchsbaum DJ, Mountz JM, Zinn KR. A noninvasive reporter system to image adenoviral-mediated gene transfer to ovarian cancer xenografts. *Gynecol Oncol* 2001; 83: 432–438.
27. Freeman SM, Whartenby KA, Freeman JL, Abboud CN, Marrogi AJ. *In situ* use of suicide genes for cancer therapy. *Semin Oncol* 1996; 23: 31–45.
28. Morris JC. Enzyme/prodrug-based tumor vaccination: All politics (and immunity) are local. *J Natl Cancer Inst* 1999; 91: 1986–1989.
29. McGinn CJ, Shewach DS, Lawrence TS. Radiosensitizing nucleosides. *J Natl Cancer Inst* 1996; 88: 1193–1203.
30. Danielson S, Kilstrup M, Barilla K, Jochimsen B, Neuhard J. Characterization of the *Escherichia coli codBA* operon encoding cytosine permease and cytosine deaminase. *Mol Microbiol* 1992; 6: 1335–1344.
31. Austin EA, Huber BE. A first step in the development of gene therapy for colorectal carcinoma: Cloning, sequencing, and expression of *Escherichia coli* cytosine deaminase. *Mol Pharmacol* 1993; 43: 380–387.
32. Hamstra DA, Rice DJ, Pu A, Oyedijo D, Ross BD, Rehemtulla A. Combined radiation and enzyme/prodrug treatment for head and neck cancer in an orthotopic animal model. *Radiation Res* 1999; 152: 499–507.
33. Hamstra DA, Rice DJ, Fahmy S, Ross BD, Rehemtulla A.

Enzyme/prodrug therapy for head and neck cancer using a catalytically superior cytosine deaminase. *Hum Gene Ther* 1999; 10: 1993–2003.
34. Huber BE, Austin EA, Good SS, Knick VC, Tibbels S, Richards CA. *In vivo* antitumor activity of 5-fluorocytosine on human colorectal carcinoma cells genetically modified to express cytosine deaminase. *Cancer Res* 1993; 53: 4619–4626.
35. Hirschowitz EA, Ohwada A, Pascal WR, Russi TJ, Crystal RG. *In vivo* adenovirus-mediated gene transfer of the *Escherichia coli* cytosine deaminase gene to human colon carcinoma-derived tumors induces chemosensitivity to 5-fluorocytosine. *Hum Gene Ther* 1995; 6: 1055–1063.
36. Mullen C. Metabolic suicide genes in gene therapy. *Pharmacol Ther* 1994; 63: 199–207.
37. Huber BE, Austin EA, Richards CA, Davis ST, Good SS. Metabolism of 5-fluorocytosine to 5-fluorouracil in human colorectal tumor cells transduced with cytosine deaminase gene: Significant antitumor effects when only a small percentage of tumor cells express cytosine deaminase. *Proc Natl Acad Sci USA* 1994; 91: 8302–8306.
38. Dong Y, Wen P, Manome Y, Parr M, Hirshowitz A, Chen L, et al. *In vivo* replication-deficient adenovirus vector-mediated transduction of the cytosine deaminase gene sensitizes glioma cells to 5-fluorocytosine. *Hum Gene Ther* 1996; 7: 713–720.
39. DiMaio JM, Clary BM, Via DF, Coveney E, Pappas TN, Lyerly HK. Directed enzyme pro-drug gene therapy for pancreatic cancer *in vivo*. *Surgery* 1994; 116: 205–213.
40. Pederson LC, Buchsbaum DJ, Vickers SM, Kancharla SR, Mayo MS, Curiel DT, et al. Molecular chemotherapy combined with radiation therapy enhances killing of cholangiocarcinoma cells *in vitro* and *in vivo*. *Cancer Res* 1997; 57: 4325–4332.
41. Pederson LC, Vickers SM, Buchsbaum DJ, Kancharla SR, Mayo MS, Curiel DT, et al. Combining cytosine deaminase expression, 5-fluorocytosine exposure, and radiotherapy increases cytotoxicity to cholangiocarcinoma cells. *J Gastrointest Surg* 1998; 2: 283–291.
42. Stackhouse MA, Pederson LC, Grizzle WE, Curiel DT, Gebert J, Haack K, et al. Fractionated radiation therapy in combination with adenoviral delivery of the cytosine deaminase gene and 5-fluorocytosine enhances cytotoxic and antitumor effects in human colorectal and cholangiocarcinoma models. *Gene Ther* 2000; 7: 1019–1026.
43. Miller CR, Williams CR, Buchsbaum DJ, Gillespie GY. Intratumoral 5-fluorouracil produced by cytosine deaminase/5-fluorocytosine gene therapy is effective for experimental human glioblastomas. *Cancer Res* 2002; 62: 773–780.
44. Ohwada A, Hirschowitz EA, Crystal RG. Regional delivery of an adenovirus vector containing the *Escherichia coli* cytosine deaminase gene to provide local activation of 5-fluorocytosine to suppress the growth of colon carcinoma metastatic to liver. *Hum Gene Ther* 1996; 7: 1567–1576.
45. Hanna NN, Mauceri HJ, Wayne JD, Hallahan DE, Kufe DW, Weichselbaum RR. Virally directed cytosine deaminase/5-fluorocytosine gene therapy enhances radiation response in human cancer xenografts. *Cancer Res* 1997; 57: 4205–4209.
46. Chaudhuri TR, Krasnykh VN, Belousova N, Zinn KR, Buchsbaum DJ, Mountz JM, et al. An Ad-based strategy for imaging, radiotherapy, and enhanced tumor killing. *Mol Ther* 2001; 3: S25.
47. Buchsbaum DJ. Imaging and therapy of tumors induced to express somatostatin receptor by gene transfer using radiolabeled peptides and single chain antibody constructs. *Semin Nucl Med* 2004; 34: 32–46.
48. Liang Q, Gotts J, Satyamurthy N, Barrio J, Phelps ME, Gambhir SS, et al. Noninvasive, repetitive, quantitative measurement of gene expression from a bicistronic message by positron emission tomography, following gene transfer with adenovirus. *Mol Ther* 2002; 6: 73–82.
49. Tjuvajev JG, Doubrovin M, Akhurst T, Cai S, Balatoni J, Alauddin MM, et al. Comparison of radiolabeled nucleoside probes (FIAU, FHBG, and FHPG) for PET imaging of HSV1-*tk* gene expression. *J Nucl Med* 2002; 43: 1072–1083.
50. Blasberg RG. Molecular imaging and cancer. *Mol Cancer Ther* 2003; 2: 335–343.
51. Chung J-K. Sodium iodide symporter: Its role in nuclear medicine. *J Nucl Med* 2002; 43: 1188–1200.

Radiotargeted Gene Therapy

Donald J. Buchsbaum, PhD[1]; Tandra R. Chaudhuri, PhD[2]; and Kurt R. Zinn, DVM, PhD[3]

[1]Department of Radiation Oncology, University of Alabama at Birmingham, Birmingham, Alabama; [2]Department of Radiology, University of Alabama at Birmingham, Birmingham, Alabama; and [3]Department of Medicine, University of Alabama at Birmingham, Birmingham, Alabama

The radiotargeted gene therapy approach to localizing radionuclides at tumor sites involves inducing tumor cells to synthesize a membrane-expressed receptor with a high affinity for injected radiolabeled ligands. A second strategy involves transduction of the sodium iodide symporter (NIS) and free radionuclide therapy. Using the first strategy, induction of high levels of human somatostatin receptor subtype 2 expression and selective tumor uptake, imaging, or growth inhibition with radiolabeled somatostatin analogues has been achieved in human tumor xenograft models. Therapy studies have been performed on several tumor xenograft models with various radionuclides using the NIS radiotargeted gene therapy approach. The use of gene transfer technology to induce expression of high affinity membrane receptors or transporters can enhance the specificity and extent of radioligand or radionuclide localization in tumors, and the use of radionuclides with appropriate emissions can deliver radiation-absorbed cytotoxic doses across several cell diameters to compensate for limited transduction efficiency. Clinical studies are needed to determine the most promising of these new therapeutic approaches.

Key Words: human somatostatin receptor subtype 2; sodium iodide symporter; gene therapy; radiopharmaceuticals; radiolabeled peptides

J Nucl Med 2004; 45:000–000

Radiolabeled somatostatin analogues (e.g., ^{111}In-pentetreotide [OctreoScan; Mallinckrodt Inc.] or ^{99m}Tc-depreotide [Neotect; Diatide Inc.]) have been used to target human somatostatin receptor subtype 2 (hSSTr2)–positive tumor cells for imaging of patients (*1,2*). The peptides have been labeled with various radionuclides for therapeutic applications, which have been performed on preclinical animal models (*3–5*) and on cancer patients (*6,7*). Despite the success of these investigations, improved targeting strategies are needed to produce an even greater effect in the treatment of cancer. One approach is to use gene transfer methods to upregulate tumor-associated receptor expression, followed by systemic administration of radiolabeled peptide. We have developed replication-defective adenoviral (Ad) recombinant vectors that transfer the hSSTr2-encoding gene to tumors, enhancing uptake of radiolabeled somatostatin peptide analogues to tumor cells. The use of these vectors to produce preferential tumor localization of radiolabeled somatostatin analogues in animal xenograft models has been described (*8–11*). A potential advantage of genetic transduction of hSSTr2 is that the level of expression may be greater than what are the generally otherwise low tumor concentrations of such receptors.

A second approach to radiotargeted gene therapy is the transduction of tumors with transporters such as the sodium iodide symporter (NIS) gene, which is responsible for the active uptake and concentration of iodide, pertechnetate, perrhenate, and astatide (*12–14*). Both approaches for radiotargeted gene therapy may be enhanced by codelivery of a second therapeutic gene such as herpes virus thymidine kinase (TK) or cytosine deaminase (CD) to accomplish molecular prodrug therapy (*11,15*). That therapeutic approach involves insertion and expression of an enzyme in a target cell that converts a nontoxic prodrug to a toxic drug. Two of the most widely studied systems are TK and CD. Transduction of tumor cells with the TK gene phosphorylates nucleoside prodrugs such as ganciclovir (GCV), resulting in inhibition of DNA synthesis and cell death. CD is a nonmammalian enzyme that catalyzes the formation of uracil by the deamination of cytosine. When 5-fluorocytosine (5-FC) is the substrate, CD will produce 5-fluorouracil, a cancer chemotherapeutic and radiosensitizing agent. The CD gene has been used successfully in gene therapy studies in animal tumor models. Results reported by our group and other investigators involving combination of radiation therapy with molecular prodrug therapy have shown that CD-based prodrug therapy sensitizes tumor cells to external-beam radiation both in vitro and in vivo (*16*). Studies involving combination of radiolabeled peptide therapy with molecular prodrug therapy are described in this article.

Linking tumor transduction of the hSSTr2 or the NIS to induced binding of radiolabeled ligands or radionuclides might enhance the therapeutic effect, since cells near bound ligand or internalized radionuclide may be killed from exposure to the local radiation field. When used with radionuclide therapy, uniform systemic incorporation of the genetic construct into tumor cells is not necessary, because of this crossfire effect. There are 2 potential advantages to the

Received May 7, 2004; revision accepted Aug. 13, 2004.
For correspondence or reprints contact: Donald J. Buchsbaum, PhD, Department of Radiation Oncology, University of Alabama at Birmingham, 1530 3rd Ave. S., WTI 674, Birmingham, AL 35294-6832.
E-mail: djb@uab.edu

genetic transduction approach: Constitutive expression of a tumor-associated receptor or transporter is not required, and tumor cells are altered to express a new target receptor or transporter at levels that increase tumor targeting of radiolabeled ligands or free radionuclides and increase therapeutic efficacy.

The target of many therapy studies with radiolabeled peptides has been hSSTr2, which is expressed on several human tumors including neuroendocrine, ovary, kidney, breast, prostate, lung, and meningioma tumors (*17*). The somatostatin receptor group includes gene products encoded by 5 separate somatostatin receptor genes. Somatostatin receptor subtype 2 is the most prominent somatostatin receptor on human tumors. The receptors are expressed at varying levels in the brain, gastrointestinal tract, pancreas, kidney, and spleen. All 5 receptors show high-affinity binding to natural somatostatin peptide (either somatostatin-14 or somatostatin-28). Octreotide, P829, and P2045 are synthetic somatostatin analogues that preferentially bind with high affinity to somatostatin receptor subtypes 2, 3, and 5 of human, mouse, or rat origin (*18–20*). Somatostatin and its analogues effectively inhibit the proliferation of various types of cancer cells as a result of binding to hSSTr2 (*21*).

Octreotide is an 8-amino-acid peptide that has a high affinity for hSSTr2 and is stable toward in vivo degradation relative to the endogenous 14-amino-acid somatostatin-14 peptide. Octreotide and other somatostatin analogues have been conjugated with bifunctional chelating agents, for complexing radiometals, and by changing the amino acid sequence to increase their hSSTr2 binding affinity and optimize their normal organ clearance. Somatostatin analogues have been labeled with several radionuclides, including ^{111}In, ^{90}Y, ^{64}Cu, ^{177}Lu, and ^{188}Re, for therapeutic applications in preclinical models (*3–5,22*) or clinical trials (*23–25*). ^{90}Y-1,4,7,10-tetraazacyclododecane-*N,N′,N″,N‴*-tetraacetic acid (DOTA)-D-Phe^1-Tyr^3-octreotide (SMT 487) was administered to patients with malignant tumors (carcinoids, breast cancer, medullary thyroid cancer, meningioma) in a phase I trial (*23*). Complete and partial responses were obtained in 25% of patients, and 55% showed stable disease lasting at least 3 mo. Thus, several radiolabeled somatostatin analogues have shown potential as radiotherapeutic agents in animal tumor models and in humans.

STUDIES COMBINING RADIOTHERAPY AND MOLECULAR PRODRUG THERAPY

Study Descriptions

A replication-incompetent Ad vector encoding the gene for hSSTr2 (subtype a) under control of the cytomegalovirus promoter (AdCMVhSSTr2) was produced (*8*). In vitro binding of ^{125}I-somatostatin, ^{99m}Tc-P829 (^{99m}Tc-depreotide), and ^{111}In-diethylenetriaminepentaacetic acid (DTPA)-D-Phe^1-octreotide (^{111}In-pentetreotide) to cells or cell membrane preparations of human ovarian and non–small cell lung cancer cells infected with AdCMVhSSTr2 was shown by imaging of cells in plates (*26*) or counting of cell membrane preparations (*8*). To evaluate the ability to induce receptor expression in an animal model, AdCMVhSSTr2 was injected intraperitoneally into athymic nude mice bearing SK-OV-3.ip1 human ovarian tumors in the peritoneum. γ-Camera imaging was used to detect hSSTr2 expression in subcutaneous A-427 non–small cell lung tumors injected with AdCMVhSSTr2 using ^{188}Re-P829 somatostatin analog (*9*).

^{99m}Tc-P2045 binds with high affinity to hSSTr2 and has favorable in vivo biodistribution (*19*). ^{99m}Tc-P2045 tumor uptake was evaluated in mice bearing SK-OV-3.ip1 tumors in the peritoneum injected intraperitoneally with AdCMVhSSTr2 (1×10^9 plaque-forming units [pfu]). In another study, ^{99m}Tc-P2045 was injected intravenously 2 or 4 d after AdCMVhSSTr2 intratumoral injection in mice bearing subcutaneous A-427 tumors, and the animals were imaged using a γ-camera 3.5–4.5 h later.

Tumor localization of ^{64}Cu-triethylenetetramine (TETA)-octreotide was studied in mice bearing intraperitoneal SK-OV-3.ip1 human ovarian tumors induced to express hSSTr2 with AdCMVhSSTr2. ^{64}Cu is a potentially therapeutic radionuclide that can be imaged by PET. In a therapy study, a single administration of 51.8 or 74 MBq of ^{64}Cu-TETA-octreotide 2 d after AdCMVhSSTr2 injection was used in mice bearing intraperitoneal SK-OV-3.ip1 tumors. Also, 51.8 MBq of ^{64}Cu-TETA-octreotide was administered 2 d after AdCMVhSSTr2 injection, followed by a second dose of AdCMVhSSTr2 11 d later and administration of 25.9 MBq of ^{64}Cu-TETA-octreotide 2 d afterward.

Another somatostatin analog that has been used for therapy is ^{90}Y-SMT 487 (*4,23*). Nude mice bearing subcutaneous A-427 tumors were administered 1×10^9 pfu of AdCMVhSSTr2 intratumorally (day 0). Mice received an intravenous injection of either 14.8 or 18.5 MBq of ^{90}Y-SMT 487 on days 2 and 4. The mice received an additional intratumoral injection of AdCMVhSSTr2 on day 7, followed by 2 more 14.8- or 18.5-MBq doses of ^{90}Y-SMT 487 on days 9 and 11. Control tumor-bearing mice either did not receive treatment or received four 18.5-MBq doses of ^{90}Y-SMT 487 on days 2, 4, 9, and 11 without AdCMVhSSTr2 injections (*27*).

Ad vectors were produced expressing hSSTr2 with a second therapeutic gene (TK or CD). This offers the potential for combination therapy using radiolabeled somatostatin analogues and prodrugs such as GCV or 5-FC. Localization and imaging studies were performed using a bicistronic nonreplicative Ad vector encoding hSSTr2 and TK in a non–small cell lung cancer xenograft model (*11*). The A-427 tumors were injected intratumorally with the bicistronic vector (AdCMVhSSTr2TK), and the animals were imaged for hSSTr2 expression with ^{99m}Tc-P2045 and TK with ^{131}I-fialuridine (FIAU).

Bicistronic Ad vectors encoding for hSSTr2 and the TK enzyme were constructed and evaluated (*11*). The rationale for the construction of these vectors is 2-fold. First, hSSTR2 can be used for noninvasive imaging to determine expression of the therapeutic gene (TK) in vivo (*11*). Second, hSSTR2 can be used for therapy, and the combination of this with TK-mediated prodrug therapy may have an additive or synergistic therapeutic effect. The AdCMVhSSTr2TK was injected intratumorally into A-427 tumors at 2×10^8 pfu on days 20 and 27. The ^{90}Y-SMT 487 was administered intravenously on days 22, 24, 29, and 31 at 18.5 MBq per injection. The GCV was administered intraperitoneally at 50 mg/kg daily for 14 d beginning on day 22. Controls included administration of unlabeled SMT 487 alone, GCV alone, or ^{90}Y-SMT 487 alone.

Bicistronic Ad vectors encoding for hSSTr2 and the CD enzyme were constructed and tested. Ad vectors expressing CD and hSSTr2 (AdCox-2LCDhSSTr2 and AdCox-2LhSSTr2CD) were produced using the long (L) length Cox-2 promoter. hSSTr2 has been used as a target for noninvasive imaging to determine expression of the therapeutic gene (CD) in vivo (*11*). Also, hSSTr2 can be used for radioligand therapy, and the combination of this with CD-mediated molecular prodrug therapy may result in radiosensitization. The A-SPECT system (γ-Medica, Inc.) was used for SPECT, with a total of 64 individual projections collected (30 s each) using a 1-mm pinhole collimator. Therapy studies were performed with AdCMVhSSTr2CD injected intratumorally into A-427 tumors at 1×10^9 pfu on days 20 and 27. ^{90}Y-SMT 487 was administered intravenously on days 22, 24, 29, and 31 at 18.5 MBq per injection. The 5-FC was administered intraperitoneally at 400 mg/kg twice a day for 5 d beginning on day 21, followed by another 5 d cycle beginning on day 28.

Study Results

Induction of hSSTr2 In Vivo and Localization/Imaging of Radiolabeled Somatostatin Analogues. Tumor localization of ^{111}In-DTPA-D-Phe^1-octreotide in mice bearing intraperitoneal SK-OV-3.ip1 tumors injected intraperitoneally with AdCMVhSSTr2 2 d earlier at 4 h after intraperitoneal injection was 60.4 percentage injected dose per gram (%ID/g), which decreased to 18.6 %ID/g at 24 h after injection (*8*). Thus, these studies demonstrated that tumor uptake of ^{111}In-DTPA-D-Phe^1-octreotide could be achieved after transduction of the ovarian tumor in vivo with AdCMVhSSTr2.

Another study investigated the localization of ^{111}In-DTPA-D-Phe^1-octreotide to subcutaneous A-427 non–small cell lung tumors injected intratumorally with AdCMVhSSTr2 (*27*). γ-Camera imaging showed the tumor uptake of ^{111}In-DTPA-D-Phe^1-octreotide to be 2.8 %ID/g at 48 h after injection and 3.1 %ID/g at 96 h. Uptake of ^{111}In-DTPA-D-Phe^1-octreotide in control Ad-injected tumors with the thyrotropin-releasing hormone receptor gene (AdCMVTRHr) was <0.3 %ID/g at both time points.

^{188}Re is a potentially therapeutic radionuclide that can be imaged with a γ-camera. ^{188}Re-P829 bound with high affinity (6–7 nmol/L) to membrane preparations from A-427 cells infected with AdCMVhSSTr2 (*9*). Mice bearing subcutaneous A-427 tumors injected intratumorally with AdCMVSSTr2 showed uptake of intravenously injected ^{188}Re-P829 detected by γ-camera imaging, whereas uptake was not observed when the tumors were infected with a control Ad. This was confirmed by counting the tumors in a γ-counter, which showed 2.9 %ID/g of ^{188}Re-P829 in the AdCMVhSSTr2-injected tumors, compared with <0.4 %ID/g in the tumors infected with the control Ad. hSSTr2 expression was independently confirmed by immunohistochemical analysis.

Uptake of ^{99m}Tc-P2045 in intraperitoneal SK-OV-3.ip1 tumors in the peritoneum of mice injected intraperitoneally with AdCMVhSSTr2 at 48 h after intravenous injection averaged 2.2 ± 0.3 %ID/g, compared with 0.2 ± 0.002 %ID/g in control mice not receiving Ad injection ($P < 0.05$) or with 0.3 ± 0.2 %ID/g in mice injected intraperitoneally with an Ad encoding the green fluorescent protein (AdCMVGFP) (*28*). Images of mice bearing subcutaneous A-427 tumors injected with ^{99m}Tc-P2045 showed uptake in the tumors injected with AdCMVhSSTr2 but background uptake in tumors injected with control Ad. The tumor uptake results in the mice 4 d after AdCMVhSSTr2 injection and 4 h after ^{99m}Tc-P2045 injection were 7.8 %ID/g. No other tissue had greater uptake than the AdCMVhSSTr2-injected tumor (*26*). In another study, mice bearing subcutaneous MCF-7 breast tumor xenografts were injected intratumorally with AdCMVhSSTr2GFP. hSSTr2 gene expression was detected with ^{99m}Tc-P2045 via γ-camera imaging, and GFP was detected by fluorescent stereomicroscopic imaging (Fig. 1). AQ: D F1

Therapy Studies with the Single-Gene Vector AdCMVhSSTr2. Untreated animals bearing intraperitoneal SK-OV-3.ip1 tumors had a median survival of 34 d, whereas the median survivals were 36 d after AdCMVhSSTr2 injection and a single 51.8 MBq dose of ^{64}Cu-TETA-octreotide and 14 d after AdCMVhSSTr2 injection and a single 74 MBq dose. The mice that received 2 doses of ^{64}Cu-TETA-octreotide (51.8 MBq plus 25.9 MBq) had a median survival of 62 d. Thus, the combination of AdCMVhSSTr2 gene transfer and ^{64}Cu-TETA-octreotide significantly lengthened survival of the mice. These results establish the key feasibilities of inducing hSSTr2 expression in ovarian tumors and therapy with a radiolabeled somatostatin analog.

Mice bearing subcutaneous A-427 tumors that received 2 intratumoral injections of AdCMVhSSTr2 and four 14.8- or 18.5-MBq doses of ^{90}Y-SMT 487 had significantly longer median tumor-quadrupling times (40 and 44 d, respectively) than did the mice receiving no treatment and the mice receiving four 18.5-MBq doses of ^{90}Y-SMT 487 but no virus (16 and 25 d, respectively). The difference in time to tumor quadrupling between the groups that received AdCMVhSSTr2 plus ^{90}Y-SMT 487 and the control groups was statistically significant.

Enhancement of Tumor Killing by Radiosensitization Through Molecular Prodrug Therapy. Subcutaneous A-427 tumors injected with AdCMVhSSTr2 or AdCMVhSSTr2TK

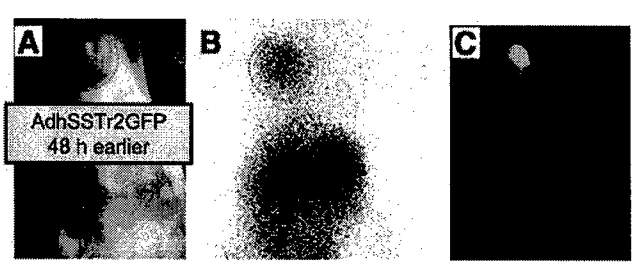

COLOR

FIGURE 1. Dual reporter genes detected by γ-camera imaging and fluorescent imaging. (A) Representative mouse bearing a MCF-7 human breast tumor xenograft was dosed with AdCMVhSSTr2GFP (1×10^9 pfu) and, after 48 h, received intravenous injection of ^{99m}Tc-P2045. (B and C) Dual-modality imaging after 5 h included γ-camera imaging (B) and fluorescent stereomicroscopic imaging (C).

COLOR

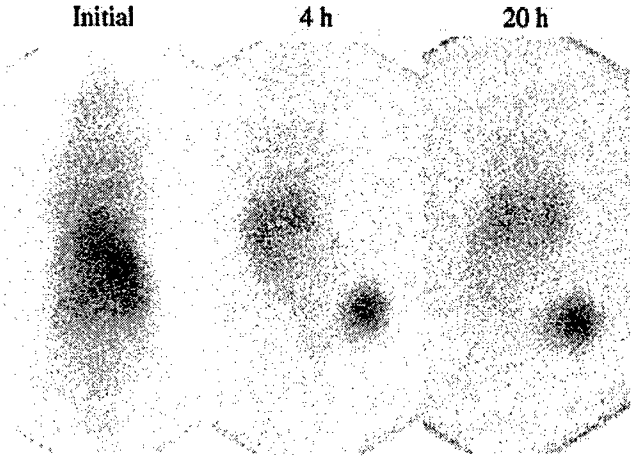

FIGURE 2. Imaging of accumulation of ^{188}Re-P2045 in A-427 tumor previously injected with AdCMVhSSTr2TK. ^{188}Re-P2045 was injected intravenously 2 d after intratumoral injection of Ad vector. Images were collected initially and after 4 and 20 h.

could be seen by imaging with ^{99m}Tc-P2045, and tumors injected with AdCMVhSSTr2TK or AdCMVTK could be seen by imaging with ^{131}I-FIAU. Tumors injected with AdCMVTK did not accumulate ^{99m}Tc-P2045 (*11*). Uptake of ^{99m}Tc-P2045 and ^{131}I-FIAU for AdCMVhSSTr2TK-injected tumors was 11.1 and 1.6 %ID/g, respectively. AdCMVhSSTr2-injected tumors accumulated 10.2 %ID/g of the ^{99m}Tc-P2045 and 0.3% of the ^{131}I-FIAU. AdCMVTK-injected tumors had 0.2 %ID/g for the ^{99m}Tc-P2045 and 3.7% for ^{131}I-FIAU. A separate group of mice bearing a single subcutaneous A-427 tumor (on the right side) was injected intratumorally with AdCMVhSSTr2TK. After 2 d, ^{188}Re-P2045 was injected intravenously (11.1 MBq) and the mice were imaged. Images from a representative mouse are presented in Figure 2 and demonstrate accumulation of ^{188}Re-P2045 in the tumor. F2

Mice bearing intraperitoneal SK-OV-3.ip1 tumors injected with 1×10^9 pfu of AdCMVhSSTr2 5 d after tumor cell inoculation, followed by intraperitoneal injection of ^{64}Cu-TETA-octreotide 2 d later, had tumor uptake of 25.1 %ID/g at 4 h after ^{64}Cu-TETA-octreotide administration—a value that was significantly greater than that when the control Ad (AdCMVLacZ) was given (1.6 %ID/g). However, the tumor uptake of ^{64}Cu-TETA-octreotide after AdCMVhSSTr2 administration decreased to 7.2 %ID/g at 18 h after injection.

Therapy Studies with the Bicistronic Vector AdCMVhSSTr2TK. The AdCMVhSSTr2TK bicistronic vector induced a level of hSSTr2 expression in A427 cells equivalent to that induced by the single-gene AdCMVhSSTr2 virus, as shown in Figure 3. Transfected cells were killed after exposure to the prodrug GCV (Fig. 4). Having demonstrated that this bicistronic vector was functionally active, we initiated therapy studies. Table 1 contains the efficacy summary for these studies. The GCV treatment group had the only 2 tumors that regressed. Significant differences were found with respect to tumor-doubling time overall ($P < 0.001$), with multiple comparisons showing that ^{90}Y-SMT 487 (14.8 MBq × 4) alone or in combination with GCV had the greatest tumor growth suppression over all treatment groups, with no other significant differences. However, the combination of ^{90}Y-SMT 487 and GCV resulted in severe toxicity as demonstrated by a dramatic loss of animal weight. Liver toxicity has been reported with Ad-mediated delivery of the TK gene and GCV prodrug administration. The toxicity issue was addressed by reducing the dose of ^{90}Y-SMT 487 from 18.5 MBq per injection to 14.8 MBq per injection. The results show that tumor inhibition was achieved with ^{90}Y-SMT 487 alone and with ^{90}Y-SMT 487 in combination with GCV (Table 1). However, the combination treatment did not improve the results achieved with ^{90}Y-SMT 487 alone. Toxicity was greatly reduced using 14.8 MBq of ^{90}Y-SMT 487 instead of the 18.5-MBq dose. In view of the toxicity obtained with the AQ: E F3 F4 T1 AQ: F

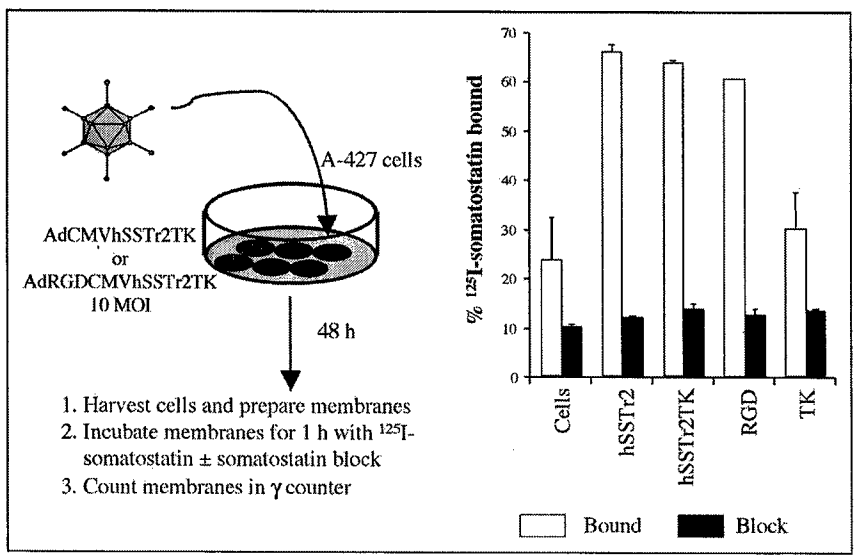

FIGURE 3. Evaluation of AdhSSTr2TK bicistronic vectors for expression of hSSTr2 in infected A-427 cells by ^{125}I-somatostatin binding.

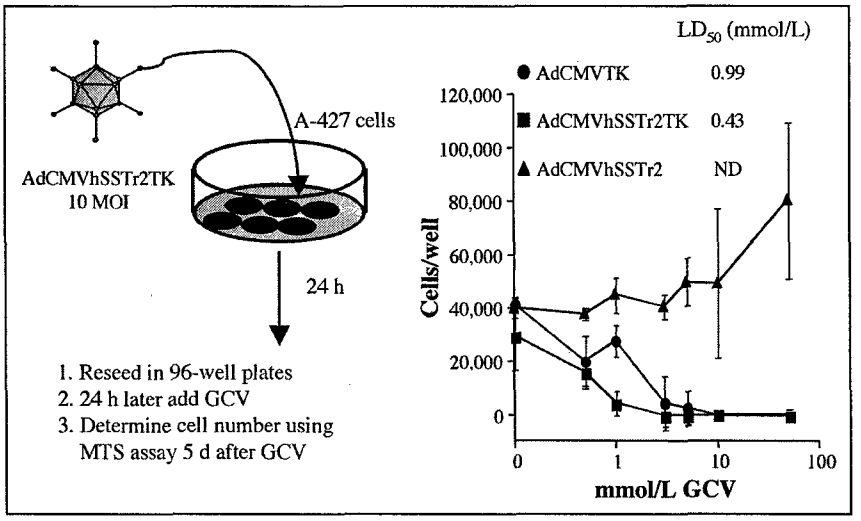

FIGURE 4. Evaluation of AdhSSTr2TK bicistronic vectors for TK activity in infected A-427 cells exposed to GCV.

AdCMVhSSTr2TK vector and radiolabeled peptide, we chose to next investigate the CD/hSSTr2 2 gene vector.

Therapy Studies with the Bicistronic Vector AdCMVhSSTr2CD. A-427 cells infected with bicistronic vector AdCMVhSSTr2CD or AdCMVhSSTr2CDRGD, with the RGD peptide genetically engineered in the fiber knob to retarget Ad binding to integrins on the cell surface, had hSSTr2 expression equivalent to that of the single-gene vector AdCMVhSSTr2 (*29*). In addition, the AdCMVhSSTr2CD and AdCMVhSSTr2CDRGD vectors produced CD enzyme activity levels similar to those of the single-gene vector AdCMVCD (*29*). Thus, both genes were active in the bicistronic vectors. We next investigated imaging of gene transfer in athymic nude mice bearing subcutaneous A-427 tumors injected with 1×10^9 pfu of AdCMVhSSTr2 or AdCMVhSSTr2CDRGD. After 2 d, ^{99m}Tc-P2045 was intravenously injected and γ-camera imaging demonstrated localization in the tumors (Fig. 5) (*30*). SPECT was used to measure the distribution of Ad-mediated transgene expression within subcutaneous xenografts. Nude mice bearing 2 A-427 flank tumors were injected intratumorally with AdCVhSSTr2GFP (1×10^9 pfu) in the right A-427 tumor, and a control bicistronic vector was injected in the left tumor. Imaging studies were conducted after 2 d (Fig. 6). The SPECT technique had sufficient sensitivity and spatial resolution to enable the 3-dimensional hSSTr2 expression to be measured.

Tumor inhibition results in mice with subcutaneous A-427 tumors injected intratumorally with AdCMVhSSTr2 showed that ^{90}Y-SMT 487 and ^{90}Y-SMT 487 in combination with 5-FC slowed tumor growth (*29*). The combination treatment inhibited tumor growth more than did the ^{90}Y-SMT 487 treatment alone, and the levels of toxicity (weight loss) were modest (*29*). The next therapy study consisted of radiotargeted gene therapy in combination with external-beam radiation therapy. Tumor inhibition results were encouraging, as they showed that the combination of ^{90}Y-SMT 487, 5-FC, and ^{60}Co resulted in tumor regressions (Fig. 7; Table 1). All combination therapies had at least 2 complete regressions, with most being recurrence free. However, the intense triple-therapy regimen was not well tolerated and produced significant weight loss.

Use of a Tumor-Specific Promoter to Drive Gene Expression. The specificity of vectors for gene transfer may be improved by combining transductional targeting of Ad using a tumor-specific promoter to drive the transcription of the hSSTr2 and CD genes (*30*). The liver is the predominant site of Ad vector localization after systemic administration

TABLE 1
Tumor Doubling Times and Complete Regressions in AdCMVhSSTr2TK Experiments

Treatment	*n*	Tumor doubling time		Complete regressions	
		Mean	Median	Total	No relapse
^{90}Y-SMT 487 (500 μCi × 4) + GCV	10	8	6	0	0
SMT 487	20	8	7	0	0
GCV (50 mg/kg)	20	14	7	2	2
^{90}Y-SMT 487 (18.5 MBq × 4)	10	18	12	0	0
^{90}Y-SMT 487 (14.8 MBq × 4) + GCV	10	25	11	0	0
^{90}Y-SMT 487 (14.8 MBq × 4)	10	39	38	0	0

COLOR

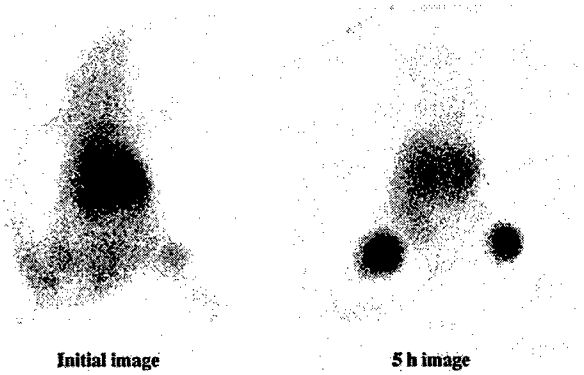

FIGURE 5. γ-Camera imaging of gene transfer in mice bearing A-427 subcutaneous tumors injected with AdCMVhSSTr2CD (left) or AdRGDCMVhSSTr2CD (right), followed 2 d later by intravenous injection of ^{99m}Tc-P2045.

and consequently is at risk when Ad vectors containing suicide genes such as TK or CD localize to this site. Thus, a promoter with both tumor specificity and minimal transcriptional activity in hepatocytes would be ideal for cancer gene therapy. Both AdCox-2LCDhSSTr2 and AdCox-2LhSSTr2CD produced cytotoxicity after infection of DU145 human prostate cancer cells in vitro in the presence of 5-FC, with a moderately low value for inhibitory concentration of 50%. Binding of ^{99m}Tc-P2045 to DU145 cells infected with AdCMVhSSTr2 or AdCox-2LhSSTr2CD was detected in plates by imaging with a γ-camera (*30*). ^{99m}Tc-P2045 localization in DU145 subcutaneous tumors injected with AdCox-2LhSSTr2 was demonstrated by γ-camera imaging (*30*). Another promising approach would be to use a radiation-inducible promoter. Takahashi et al. (*31*) reported that radionuclides can activate early growth response gene 1 (Egr-1) transcription in vitro and arrest the growth of tumor cells transfected with a pEgr-TK plasmid.

Gene Transfer of the NIS. Iodide transport into the thyroid gland is mediated by a specific sodium-dependent iodide transporter. This NIS is the plasma membrane glycoprotein responsible for active uptake and concentration of iodide in the thyroid gland, salivary glands, and gastric mucosa (*14*). The ability of the thyroid gland to accumulate iodide has provided an effective means for imaging and treatment of hyperthyroidism and both primary and metastatic thyroid carcinoma (*32*).

In 1996, both rat and human NIS complementary DNA was cloned and characterized (*33,34*). Gene transfer of the NIS gene has been performed with a variety of vectors, cell lines, and tumor xenografts, with successful localization and imaging of tumor xenografts demonstrated after systemic injection of ^{131}I, ^{123}I, ^{124}I, ^{125}I, and ^{99m}Tc (*13,14,35,36*). This approach may also be useful for detection of gene transfer of coexpressed therapeutic genes delivered during gene therapy (*15,37*). In this regard, Barton et al. (*15*) imaged CD/TK gene expression in dog prostate using the NIS gene and ^{99m}Tc.

Therapy studies have been performed on several tumor xenograft models using this radiotargeted gene therapy approach (*14,35,38*). The results with ^{131}I were not always encouraging, because of the rapid cellular efflux of this radionuclide that resulted from a lack of organification in transfected tumors (*36,38,39*). To deal with this problem, the therapeutic potential of other NIS-transported therapeutic radionuclides with a shorter physical half-life or superior decay proprieties, including ^{188}Re and ^{211}At, has been reported (*12,14*).

DISCUSSION

These studies demonstrate that genetic induction of hSSTr2 results in tumor localization of radiolabeled somatostatin analogues at a level sufficient to produce therapeutic effects and that therapeutic efficacy is enhanced by combination with molecular prodrug therapy wherein a second therapeutic gene, TK or CD, is codelivered with the hSSTR2 gene. Efforts continue to optimize this novel approach to cancer gene therapy by the use of radiation-inducible tumor-specific promoters. Another radiotargeted gene therapy approach has been to transfect tumor cells with the noradrenaline transporter to actively accumulate ^{131}I-metaiodobenzylguanidine (*40*). This approach has been tested on cells and spheroids but not on animal models. Gene transfer of the NIS has been used successfully for imaging and therapy in preclinical animal models.

The ability to localize radiolabeled ligands or radionuclides within the target tumor provides a new, specific approach to killing cancer cells. The radiotargeted gene

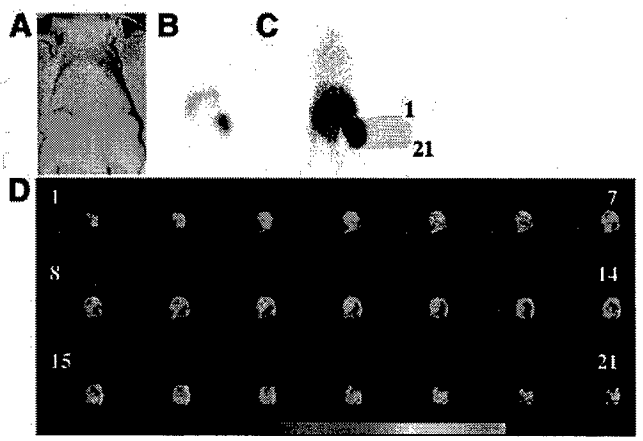

COLOR

FIGURE 6. SPECT of adenovirus-mediated hSSTr2 expression in tumor xenograft. (A) Photograph of representative mouse with 2 A-427 tumors. Right tumor was injected with 1 × 10^9 pfu of AdCMVhSSTr2GFP, and left tumor was injected with control Ad vector. (B and C) Planar γ-camera images obtained 5 h after intravenous ^{99m}Tc-P2045 injection (55.5 MBq) show that highest retention of ^{99m}Tc-P2045 was in right tumor. These 2 images are identical, with the exception of scaling. (D) Transverse γ-camera images (0.58-mm slices at location of planar slice shown in C) show hSSTr2 expression within tumor. Adenovirus-mediated hSSTr2 expression led to specific retention of ^{99m}Tc-P2045 in nonuniform, discrete tumor areas tending to be concentrated at periphery. (Reprinted with permission from (*X*).)

AQ: J
AQ: K
AQ: L

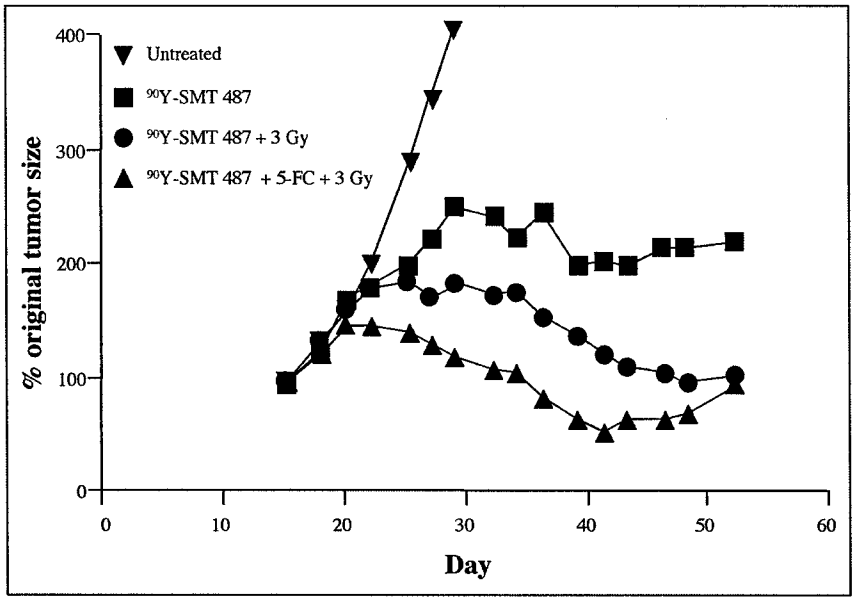

FIGURE . 7. Therapy results with AdCMVhSSTr2CD, ^{90}Y-SMT 487, 5-FC, and ^{60}Co in athymic nude mice bearing subcutaneous A-427 xenografts. AdCMVhSSTr2CD (1×10^9 pfu) was injected into A-427 tumors on days 18, 25, 32, and 39. ^{90}Y-SMT 487 (18.5 MBq per injection) was administered intravenously on days 20, 22, 27, 29, 34, 36, 41, and 43. 5-FC (400 mg/kg twice a day) was administered intraperitoneally for 5 d beginning on day 19 followed by 3 more 5-d cycles beginning on days 26, 33, and 40. ^{60}Co external-beam radiation was given as a single 3-Gy dose on days 21, 28, 35, and 42. (Reprinted with permission from (*X*).)

therapy approach has several advantages. Constitutive expression of a tumor-associated receptor or transporter is not required. Tumor cells are altered to express a new target receptor (hSSTr2) or a transporter (NIS) or to express an existing receptor at higher levels to significantly improve uptake of radiolabeled ligands or radionuclides, compared with uptake in normal tissues. Gene transfer can be effected by intratumoral or regional injection of gene vectors. Another advantage is the feasibility of targeting viral vectors to receptors overexpressed on tumor cells by modifying tropism (binding) or by using tumor-specific promoters such that the virus will specifically be targeted to the desired tumor or the gene product selectively expressed in the tumor. Finally, it is possible to enhance the therapeutic effect by coexpressing the receptor or transporter gene and a second therapeutic gene such as TK or CD for molecular prodrug therapy. However, vector delivery and gene expression are currently limited to locoregional administration.

In conclusion, radiotargeted gene therapy has potential for the treatment of cancer, especially when used in combination with other therapeutic modalities. Clinical studies are needed to determine the most promising of these new therapeutic approaches.

ACKNOWLEDGMENTS

Masato Yamamoto, David Curiel, Mark Carpenter, and Buck Rogers are acknowledged for their contributions to the concepts and results presented. The research of the authors is supported in part by Department of Energy grant DE-FG05-93ER61654, Department of Defense grant DAMD17-02-1-0001, and National Institutes of Health contract N01-CO-97110 and grant CA80104.

AQ: H

REFERENCES

1. Lamberts SWJ, van der Lely A-J, de Herder WW, et al. Octreotide. *N Engl J Med.* 1996;334:246–254.
2. Blum JE, Handmaker H, Rinne NA. The utility of a somatostatin-type receptor binding peptide radiopharmaceutical (P829) in the evaluation of solitary pulmonary nodules. *Chest.* 1999;115:224–232.
3. Zamora PO, Gulhke S, Bender H, et al. Experimental radiotherapy of receptor-positive human prostate adenocarcinoma with ^{188}Re-RC-160, a directly-radiolabeled somatostatin analogue. *Int J Cancer.* 1996;65:214–220.
4. Stolz B, Weckbecker G, Smith-Jones PM, et al. The somatostatin receptor-targeted radiotherapeutic [^{90}Y-DOTA-DPhe^1, Tyr^3]octreotide (^{90}Y-SMT 487) eradicates experimental rat pancreatic CA 20948 tumours. *Eur J Nucl Med.* 1998;25:668–674.
5. Lewis JS, Lewis MR, Cutler PD, et al. Radiotherapy and dosimetry of ^{64}Cu-TETA-Tyr^3-octreotate in a somatostatin receptor-positive, tumor-bearing rat model. *Clin Cancer Res.* 1999;5:3608–3616.
6. de Jong M, Krenning E. New advances in peptide receptor radionuclide therapy. *J Nucl Med.* 2002;43:617–620.
7. de Jong M, Valkema R, Jamar F, et al. Somatostatin receptor-targeted radionuclide therapy of tumors: preclinical and clinical findings. *Semin Nucl Med.* 2002;32:133–140.
8. Rogers BE, McLean SF, Kirkman RL, et al. *In vivo* localization of [^{111}In]-DTPA-D-Phe^1-octreotide to human ovarian tumor xenografts induced to express the somatostatin receptor subtype 2 using an adenoviral vector. *Clin Cancer Res.* 1999;5:383–393.
9. Zinn KR, Buchsbaum DJ, Chaudhuri TR, et al. Noninvasive monitoring of gene transfer using a reporter receptor imaged with a high-affinity peptide radiolabeled with ^{99m}Tc or ^{188}Re. *J Nucl Med.* 2000;41:887–895.
10. Chaudhuri TR, Mountz JM, Rogers BE, et al. Light-based imaging of green fluorescent protein-positive ovarian cancer xenografts during therapy. *Gynecol Oncol.* 2001;82:581–589.
11. Zinn KR, Chaudhuri TR, Krasnykh VN, et al. Gamma camera dual imaging with a somatostatin receptor and thymidine kinase after gene transfer with a bicistronic adenovirus. *Radiology.* 2002;223:417–425.
12. Carlin S, Mairs RJ, Welsh P, et al. Sodium-iodide symporter (NIS)-mediated accumulation of [^{211}At]astatide in NIS-transfected human cancer cells. *Nucl Med Biol.* 2002;29:729–739.
13. Chung J-K. Sodium iodide symporter: its role in nuclear medicine. *J Nucl Med.* 2002;43:1188–1200.
14. Dadachova E, Carrasco N. The Na^+/I^- symporter (NIS): imaging and therapeutic applications. *Semin Nucl Med.* 2004;34:23–31.
15. Barton KN, Tyson D, Stricker H, et al. GENIS: gene expression of sodium iodide symporter for noninvasive imaging of gene therapy vectors and quantification of gene expression *in vivo*. *Mol Ther.* 2003;8:508–518.
16. Stackhouse MA, Pederson LC, Grizzle WE, et al. Fractionated radiation therapy in combination with adenoviral delivery of the cytosine deaminase gene and 5-fluorocytosine enhances cytotoxic and antitumor effects in human colorectal and cholangiocarcinoma models. *Gene Ther.* 2000;7:1019–1026.
17. Woltering EA, O'Dorisio MS, O'Dorisio TM. The role of radiolabeled somatostatin analogs in the management of cancer patients. In: DeVita VT Jr, Hellman

S, Rosenberg SA, eds. *Principles and Practice of Oncology: PPO Updates.* Vol. 9. 4th ed. Philadelphia, PA: Lippincott-Raven; 1995:1–16.

18. Virgolini I, Leimer M, Handmaker H, et al. Somatostatin receptor subtype specificity and *in vivo* binding of a novel tumor tracer, ^{99m}Tc-P829. *Cancer Res.* 1998;58:1850–1859.
19. Manchanda R, Azure M, Lister-James J, et al. Tumor regression in rat pancreatic (AR42J) tumor-bearing mice with Re-188 P2045: a somatostatin analog [abstract]. *Clin Cancer Res.* 1999;5:3769s.
20. Reubi JC, Schar JC, Waser B, et al. Affinity profiles for human somatostatin receptor subtypes SST1-SST5 of somatostatin radiotracers selected for scintigraphic and radiotherapeutic use. *Eur J Nucl Med.* 2000;27:273–282.
21. Buscail L, Saint-Laurent N, Chastre E, et al. Loss of sst2 somatostatin receptor gene expression in human pancreatic and colorectal cancer. *Cancer Res.* 1996; 56:1823–1827.
22. de Jong M, Breeman WAP, Bernard BF, et al. [^{177}Lu-DOTA^0,Tyr^3] octreotate for somatostatin receptor-targeted radionuclide therapy. *Int J Cancer.* 2001;92:628–633.
23. Paganelli G, Zoboli S, Cremonesi M, et al. Receptor-mediated radionuclide therapy with ^{90}Y-DOTA-D-Phe^1-Tyr^3-octreotide: preliminary report in cancer patients. *Cancer Biother Radiopharm.* 1999;14:477–483.
24. Kwekkeboom DJ, Bakker WH, Kooij PPM, et al. [^{177}Lu-DOTA^0,Tyr^3]octreotate: comparison with [^{111}In-DTPA^0]octreotide in patients. *Eur J Nucl Med.* 2001;28: 1319–1325.
25. de Jong M, Kwekkeboom D, Valkema R, et al. Radiolabelled peptides for tumour therapy: current status and future directions—plenary lecture at the EANM 2002. *Eur J Nucl Med Mol Imaging.* 2003;30:463–469.
26. Rogers BE, Zinn KR, Buchsbaum DJ. Gene transfer strategies for improving radiolabeled peptide imaging and therapy. *Q J Nucl Med.* 2000;44:208–223.
27. Rogers BE, Zinn KR, Lin C-Y, et al. Targeted radiotherapy with [^{90}Y]-SMT 487 in mice bearing human nonsmall cell lung tumor xenografts induced to express human somatostatin receptor subtype 2 with an adenoviral vector. *Cancer.* 2002;94:1298–1305.
28. Chaudhuri TR, Rogers BE, Buchsbaum DJ, et al. A noninvasive reporter system to image adenoviral-mediated gene transfer to ovarian cancer xenografts. *Gynecol Oncol.* 2001;83:432–438.
29. Buchsbaum DJ. Imaging and therapy of tumors induced to express somatostatin receptor by gene transfer using radiolabeled peptides and single chain antibody constructs. *Semin Nucl Med.* 2004;34:32–46.
30. Buchsbaum DJ, Chaudhuri TR, Yamamoto M, et al. Gene expression imaging with radiolabeled peptides. *Ann Nucl Med.* 2004. In press.
31. Takahashi T, Namiki Y, Ohno T. Induction of the suicide HSV-TK gene by activation of the Egr-1 promoter with radioisotopes. *Hum Gene Ther.* 1997;8: 827–833.
32. Mazzaferri EL, Kloos RT. Clinical review 128: current approaches to primary therapy for papillary and follicular thyroid cancer. *J Clin Endocrinol Metab.* 2001;86:1447–1463.
33. Dai G, Levy O, Carrasco N. Cloning and characterization of the thyroid iodide transporter. *Nature.* 1996;379:458–460.
34. Smanik PA, Liu Q, Furminger TL, et al. Cloning of the human sodium iodide symporter. *Biochem Biophys Res Commun.* 1996;226:339–345.
35. Cho J-Y, Shen DHY, Yang W, et al. *In vivo* imaging and radioiodine therapy following sodium iodide symporter gene transfer in animal model of intracerebral gliomas. *Gene Ther.* 2002;9:1139–1145.
36. Dingli D, Peng K-W, Harvey ME, et al. Image-guided radiovirotherapy for multiple myeloma using a recombinant measles virus expressing the thyroidal sodium iodide symporter. *Blood.* 2004;103:1641–1646.
37. Niu G, Gaut AW, Ponto LLB, et al. Multimodality noninvasive imaging of gene transfer using the human sodium iodide symporter. *J Nucl Med.* 2004;45:445–449.
38. Spitzweg C, Dietz AB, O'Connor MK, et al. *In vivo* sodium iodide symporter gene therapy of prostate cancer. *Gene Ther.* 2001;8:1524–1531.
39. Haberkorn U, Kinscherf R, Kissel M, et al. Enhanced iodide transport after transfer of the human sodium iodide symporter gene is associated with lack of retention and low absorbed dose. *Gene Ther.* 2003;10:774–780.
40. Boyd M, Mairs RJ, Cunningham SH, et al. A gene therapy/targeted radiotherapy strategy for radiation cell kill by [^{131}I]-meta-iodobenzylguanidine. *J Gene Med.* 2001;3:165–172.

Imaging and Therapy of Tumors Induced to Express Somatostatin Receptor by Gene Transfer Using Radiolabeled Peptides and Single Chain Antibody Constructs

Donald J. Buchsbaum

The fields of radioimmunodetection and radioimmunotherapy began with an initial paradigm that a targeting molecule (eg, antibody) carrying a radioisotope had the potential of selectively imaging and delivering a therapeutic dose of radiation to tumor sites. A second paradigm was developed in which injection of the targeting molecule was separated from injection of a short-lived radioisotope-labeled ligand (so-called "pretargeting strategy"). This strategy has improved radioisotope delivery to tumors in animal models, enhanced radioimmune imaging in man, and therapeutic trials are in an early phase. We proposed a third paradigm to achieve radioisotopic localization at tumor sites by inducing tumor cells to synthesize a membrane expressed receptor with a high affinity for infused radiolabeled ligands. The use of gene transfer technology to induce expression of high affinity membrane receptors can enhance the specificity of radioligand localization, while the use of radioisotopes with the ability to deliver radiation damage across several cell diameters will compensate for less than perfect transduction efficiency. This approach was termed "Genetic Radioisotope Targeting Strategy." Using this strategy, induction of high levels of gastrin releasing peptide receptor or human somatostatin receptor subtype 2 expression and selective tumor uptake of radiolabeled peptides was achieved. The advantages of the genetic transduction approach are (1) constitutive expression of a tumor-associated antigen/receptor is not required; (2) tumor cells are altered to express a new target receptor or increased quantities of an existing receptor at levels that may significantly improve tumor targeting of radiolabeled ligands compared with normal tissues; (3) gene transfer can be achieved by intratumoral or regional injection of gene vectors; (4) it is feasible to target adenovirus vectors to receptors overexpressed on tumor cells by modifying adenoviral tropism (binding) so that the virus will be targeted specifically to the desired tumor; and (5) it is possible to coexpress the receptor gene and a therapeutic gene, such as cytosine deaminase, for molecular prodrug therapy to produce an enhanced therapeutic effect.

THE USE of radiolabeled monoclonal antibodies (mAb) to "target" radioactivity to tumor sites is a promising strategy, as shown in a number of animal models and in human trials.[1-7] Radioimmunotherapy (RIT) is typically administered systemically. However, it also has been delivered intraperitoneally (IP) or intralesionally. Favorable results have been observed in the treatment of lymphomas, in tumors confined within the peritoneal cavity (ovarian), and in malignant gliomas through direct intratumoral injection.[8-20] Another strategy has used radiolabeled peptides (eg, Octreoscan, Mallinckrodt, Hazelwood, MO, or Neotect, Berlex Laboratories, Inc, Wayne, NJ) to target human somatostatin receptor subtype 2 (hSSTr2) positive tumor cells for imaging in patients.[21-24] The peptides can be labeled with radioisotopes for therapeutic applications, which have been performed in preclinical animal models and in patients with cancer.[25-32] Despite the success of these investigations, improved delivery systems and/or targeting strategies are needed for RIT to have an even greater effect in the treatment of cancer.

LIMITATIONS OF CURRENT TARGETED RADIODETECTION AND RADIOTHERAPY STRATEGIES

The success of radioimmunodetection (RID) and RIT has been limited by the low percentage uptake of injected radioactivity in tumors due to low target antigen expression and slow penetration of the large (160 kDa) intact mAb, the normal tissue uptake of the radiolabeled mAb, the bone marrow toxicity due to the long blood circulation time of the radiolabeled mAb in blood, radioresistance of the tumor, and the development of human anti-mouse antibody responses.[2,33] Strategies to overcome these limitations have included the use of

From the Department of Radiation Oncology, University of Alabama at Birmingham, Birmingham, AL.

Address reprint requests to Donald J. Buchsbaum, PhD, Department of Radiation Oncology, University of Alabama at Birmingham, 1530 3rd Ave. South, WTI 674, Birmingham, AL 35294-6832.

This work was supported by DOE grant DE-FG05 93ER61654.

0001-2998/04/3401-0005$30.00/0

doi:10.1053/j.semnuclmed.2003.09.005

mAb fragments, single chain antibodies (scFv) and minibodies or diabodies,[34-37] radiolabeled peptides,[21,22,25,27,38] locoregional administration of the radiolabeled ligand,[39-41] the use of cleavable chelating agents,[42,43] biological response modifiers such as interferon or gene transfer methods to upregulate tumor-associated antigen/receptor expression,[44-51] irradiation of the tumor to increase vascular permeability,[2] the use of radiosensitizing agents,[52-54] and antiangiogenic therapy.[55-57]

Strategies to Overcome Targeted Radiotherapy Limitations

There are several strategies designed to overcome the limitations of RID and RIT. Several desirable features can be envisioned for optimum receptor-ligand systems for tumor detection and therapy. Expression of an endogenous receptor exclusively on malignant cells within the normal tissue parenchyma would provide a certain degree of specificity and safety. If cross-reactivity of the radioligand with corresponding human receptors is known, it would be most desirable if the human receptor-positive cells were expendable or were isolated from the treatment area. Thus, nontumor localization of radioligand would not have significant deleterious clinical sequelae. Our group showed that an adenoviral (Ad) vector encoding the gene for carcinoembryonic antigen (CEA) could infect human glioma cells and induce the expression of CEA in vitro and in vivo, as evidenced by an increase in the binding and localization of a radiolabeled anti-CEA antibody when compared with uninfected cells.[48] Another desirable feature of candidate ligand-receptor systems would be the potential for a high affinity ligand-receptor interaction. Our recent focus has been on the development of recombinant vectors that transfer receptor-encoding genes with high binding affinities to radiolabeled peptides to tumor cells. Receptors that we investigated for targeting with radiolabeled peptides include hSSTr2 and the gastrin releasing peptide receptor (GRPr). Our group has published on the use of Ad vectors encoding the genes for hSSTr2,[58-61] GRPr,[49,50] and epidermal growth factor receptor[62,63] in the genetic radioisotope targeting approach. A potential advantage of genetic transduction of a receptor is that the level of expression may be higher than what are generally otherwise low tumor concentrations of such receptors.[38]

Radiolabeled Peptides Targeting Somatostatin Receptors in Cancer Detection and Therapy

We identified one lead system that seemed to offer the desired features for use in the proposed context. The target of most imaging and therapy studies with radiolabeled peptides has been the hSSTr2, which is expressed on a number of human tumors, including neuroendocrine, ovarian, renal, breast, lung, and meningiomas.[64-68] The somatostatin receptor group includes gene products encoded by 5 separate somatostatin receptor genes.[69] The subtype 2 exists in 2 forms due to alternate splicing of hSSTr2 messenger ribonucleic acid, which produces 2 products. The subtype 2A receptor (herein referenced as hSSTr2) is slightly longer (369 amino acids), while the shorter subtype 2B differs only in regard to a truncation on the C-terminal tail (356 amino acids). The receptors have varying tissue levels in the brain, gastrointestinal tract, pancreas, kidney, and spleen.[70-72] It is for this reason that it might be helpful to produce ligands reactive with a mutated form of hSSTr2 to achieve more selective binding to transfected tumors without inducing toxicity to normal tissues that naturally express hSSTr2. All 5 receptors show high affinity binding to natural somatostatin peptide, either somatostatin-14 or somatostatin-28. Octreotide, P829, and P2045 are synthetic somatostatin analogues that preferentially bind with high affinity to somatostatin receptor subtypes 2, 3, and 5 of human, mouse, or rat origin.[70-74] Somatostatin and its analogues effectively inhibit the proliferation of various types of cancer cells as a result of binding to hSSTr2.[75-77]

Octreotide is an 8 amino-acid peptide that has a high affinity for hSSTr2 and is stable towards in vivo degradation relative to the endogenous 14 amino-acid somatostatin-14 peptide. Octreotide and other somatostatin analogues have been modified with bifunctional chelating agents, for complexing radioactive metals, and by changing the amino acid sequence to increase their hSSTr2 binding affinity and optimize their normal organ clearance. Somatostatin analogues have been labeled with ^{111}In, ^{90}Y, ^{64}Cu, and ^{188}Re for therapeutic applications. Smith-Jones and coworkers showed that a single 0.48 mCi IP injection of a ^{90}Y-labeled somatostatin analogue in nude mice bearing subcutaneous (s.c.) AR42J rat pancreatic tumors resulted in a significant reduction in tumor

growth.[78] Stolz and colleagues showed that a single dose of ^{90}Y-DOTA-D-Phe^{1}-Tyr^{3}-octreotide (^{90}Y-SMT 487) led to reductions of 60% and 50% of the initial tumor volume in nude mice bearing AR42J and NCI-H69 human small cell lung cancer tumors, respectively.[79] Complete remissions were observed in rats bearing (s.c.) CA20948 rat pancreatic tumors when a single 2.0 mCi dose of ^{90}Y-DOTA-Tyr^{3}-octreotide was administered.[27] The ^{90}Y-DOTA-lanreotide that binds to hSSTr produced a therapeutic response in a patient with metastatic gastrinoma.[80] The ^{90}Y-SMT 487 was administered to 20 patients with malignant tumors (17 carcinoids, 1 breast cancer, 1 medullary thyroid cancer, 1 meningioma) in a phase I trial.[81] Complete and partial responses were obtained in 25% of patients along with 55% showing stable disease lasting at least 3 months. The ^{90}Y-SMT 487 has been tested in patients with neuroendocrine tumors.[27,81,82]

Zamora and coworkers labeled the somatostatin analogue RC-160 with ^{188}Re and administered 7 doses of 0.2 mCi over a 14-day period intralesionally to nude mice bearing PC-3 human prostate cancer tumors.[25] They reported that animals receiving ^{188}Re-RC-160 had 60% survival compared with no survivors when control animals were injected with saline. Anderson and colleagues showed tumor growth inhibition of s.c. CA20948 tumors in Lewis rats using either single or multiple intravenous (IV) doses of ^{64}Cu-TETA-octreotide.[26] Thus, several radiolabeled somatostatin analogues have shown potential as radiotherapeutic agents in animal tumor models and in humans. However, in most of the published studies, there has been limited tumor uptake and retention of the radiolabeled peptides (peak uptake $<10\%$ injected dose [ID]/g), presumably due to the rapid clearance from the blood. This has resulted in the use of rather high quantities of radionuclides in preclinical studies with multiple administrations. Moreover, large radionuclide doses (0.4 to 1 Ci) have been administered to patients.[83-87]

Tumor Killing is Enhanced by Increasing Radiosensitivity Through Molecular Prodrug Therapy

The molecular prodrug gene therapy approach involves insertion and expression of an enzyme in a target cell that converts a nontoxic prodrug to a toxic drug.[88,89] The enzyme cytosine deaminase (CD) is a nonmammalian enzyme that normally catalyzes the formation of uracil by the deamination of cytosine. When 5-fluorocytosine (5-FC) is the substrate, this enzyme will produce 5-fluorouracil (5-FU), a potent cancer chemotherapeutic and radiosensitizing agent.[90] The genes for bacterial and yeast CD have been cloned.[91-94] Because mammalian cells do not normally express the CD gene, 5-FC is nontoxic to these cells, even at high concentrations. The 5-FC has been used as an antifungal drug because of its relative nontoxicity in humans. The CD gene has been used in gene therapy strategies to mediate intracellular conversion of 5-FC to 5-FU, and has been effective in animal tumor models.[95,96] This therapeutic strategy has the advantage of intracellular production of high concentrations of radiosensitizing drug as an alternative to systemic administration, therefore potentially limiting systemic toxicities.[97] Direct injection of 5-FU itself into a solid tumor would not be effective because it would be washed out immediately. Converted 5-FU passively diffuses across the cell membrane from CD-positive cells to nontransduced cells.[98,99] This bystander effect compensates for the inability of current vector systems to transduce all but a small fraction of cells in a given tumor.[89,100]

Recent studies by our group and others involving combination of radiation therapy with molecular prodrug therapy have shown that CD-based prodrug therapy sensitizes tumor cells to radiation in vitro and in vivo.[101-103] Human colon and head and neck cancer cells that were stably transduced to express the CD gene were radiosensitized by the addition of 5-FC in vitro and in vivo.[93,94,104,105] The use of Ad vectors to encode CD and convert 5-FC to 5-FU to achieve cell killing has been reported by our group[102,103,106,107] and others.[96,99,101,108] We initially used an Ad vector encoding CD under the control of the cytomegalovirus promoter (AdCMVCD) in combination with 5-FC and radiation treatment to show enhanced cytotoxicity against human colon, pancreatic, glioblastoma, and cholangiocarcinoma cells in vitro and in vivo.[101-103,109] Recent results in a lung cancer animal model are described later. The results of a CD/5-FC molecular prodrug therapy phase I trial in patients with breast cancer have been published.[110] There was evidence of reduction of tumor volume in 4 of 12 patients.

Phage Display Technology: In Vitro Generation of Recombinant Antibodies

Within the last decade, a novel approach has facilitated the in vitro production of recombinant antibodies directed against a variety of targets. The key technology in this approach is the surface expression of antigen-binding fragments of mAb on filamentous bacteriophage (Phage Display).[111] Recombinant antibodies can be expressed in *Escherichia coli* as a single polypeptide consisting of 2 antigen binding domains, V_H and V_L, joined by a flexible peptide linker (termed scFv – single chain antibody variable fragment). The further development of recombinant antibody technology has led to creation of libraries of antibody genes obtained from immunized or nonimmunized donors. These antibody genes are expressed as scFvs on the surface of bacteriophage. This phage display approach allows selection of clones with highly specific antigen binding out of a vast number of primary clones in the library. Using this principle, extremely large antibody gene libraries can be screened.

Recombinant antibodies also can be isolated from hybridoma cell lines. The genetic information for the recombinant antibody V_H and V_L structural domains is amplified from hybridoma cells using the polymerase chain reaction with antibody gene-specific primers. The necessity of creating phage display libraries when recombinant mAb are generated from hybridomas is dictated by their sequence heterogeneity.[112]

Tumor Targeting With Radiolabeled Minibodies and Diabodies

The engineering of antibodies can be used to produce recombinant fragments with properties optimized for in vivo applications. Intact, murine mAb are immunogenic in humans and display poor pharmacokinetics for RID. ScFvs (constructed from hybridoma cells or isolated via phage display, as described previously) are themselves poor reagents for targeting radionuclides to tumors due to their small size and that they only contain a single binding site. Nonetheless, scFvs provide an excellent building block for intermediate size engineered fragments, such as minibodies, in which the scFv have been fused to the human IgG1 hinge and CH3 regions to provide a dimerization domain[113] and diabodies, where scFv self-assemble into noncovalent dimers containing 2 functional antigen binding sites.[114] These fragments show antigen binding comparable to intact bivalent antibodies, and may show improved tumor penetration and faster normal tissue clearance. They include the scFv (27 kDa), diabody (a noncovalent dimer of scFv, 55 kDa), and the minibody (a dimer of scFv-hinge-CH3, 80 kDa).

Biodistribution and tumor targeting studies of radioiodinated or radiometal-labeled anti-CEA minibodies and diabodies in athymic mice bearing s.c. LS174T human colon cancer xenografts showed that these fragments localize to CEA-positive tumors with fast clearance from blood and normal tissues (β half-life 3 to 5 hours) after IV injection.[113,115,116] Maximum uptake levels of 10% to 15% ID/g for radioiodinated diabody at 1 to 2 hours after injection, or 20% to 25% ID/g for minibody at 6 to 12 hours after injection occurred following IV administration to mice. The blood pharmacokinetics of ^{111}In- and ^{64}Cu-labeled minibodies was similar, and high uptake in LS174T tumors occurred. However, radiometal-chelate conjugated minibody showed uptake in the liver, and the anti-CEA diabody localized in the kidneys. Nevertheless, the rapid blood clearance of both of these antibody fragments resulted in high tumor-to-normal tissue ratios for other tissues. Results in the CEA system have been confirmed in other tumor-associated antigen systems, including TAG-72, Her2/neu, placental alkaline phosphatase, and fibronectin ED-B domain.[117] Furthermore, antibody fragments, such as diabodies or scFv, show improved tumor penetration.[34,118] Anti-CEA minibodies labeled with ^{64}Cu have been used for imaging by micro-positron emission tomography (PET),[117] and potentially provide a vehicle for the delivery of therapeutic radionuclides either as a single agent or in genetic radioisotope and molecular prodrug therapy approaches as described herein.

COMBINATION OF GENE THERAPY AND TARGETED RADIOTHERAPY ADDRESSES THE KEY SHORTCOMINGS IN GENE THERAPY (LESS THAN COMPLETE TRANSDUCTION) AND TARGETED RADIOTHERAPY (INADEQUATE DELIVERY/LOCALIZATION OF RADIOLIGANDS)

The ability of recombinant Ad vectors to accomplish efficient gene transfer to tumor cells in vivo has led to the use of this vector approach in several,

clinical cancer gene therapy trials.[119] A number of gene therapy approaches use direct in situ transduction of tumor for the purpose of achieving an anticancer effect. In these various strategies, the limited transduction frequency achievable with currently available vectors mitigates against efficacy. Thus, strategies to amplify the biologic effects of genetic transduction events would potentially allow the enhanced therapeutic effect of these gene therapy methods. By linking tumor transduction to the induced binding of radiolabeled ligands, it is possible that this effect may be achieved because cells in proximity to bound ligand may be killed as a result of exposure to the local radiation field. It should be understood that with this approach, we are attempting to increase specifically the number of receptors on tumor cells that normally express a receptor or to induce specifically expression on tumor cells that do not ordinarily express the receptor by genetic transduction, with the result being increased targeting of the radiolabeled ligand to the tumor site. It is our hypothesis that one can deliver a larger fraction of the administered dose of the radiolabeled ligand to the tumor cells selectively through increased receptor expression at the tumor site.

When used with radiation therapy, uniform systemic incorporation of the genetic construct into tumor cells is not necessary. It should be emphasized that the advantage of the proposed strategy is that transduction of 20% to 40% of tumor cells may be all that is necessary for radiolabeled ligands to produce tumor responses, given the ability of β-emitters to deliver radiation across several cell diameters in primary tumor sites and metastases. Current strategies only transduce 5% to 10% of the tumor cells. The chief stumbling block in the use of radiolabeled peptides has been the low dose of radiation that can be delivered to the tumor due to rapid catabolism. The use of high affinity radiolabeled minibodies and diabodies will likely increase the delivered radiation dose to tumor due to better tumor uptake and retention. There should be enhanced cell killing as a result of gene transfer being combined with radiation therapy.

We have developed an approach to increase expression of targetable cell surface receptors in tumor cells using a gene transfer strategy. Using this strategy, we have accomplished induction of high levels of receptors for radioligand targeting, as described later. The advantages of the genetic transduction approach are (1) constitutive expression of a tumor-associated receptor is not required, and (2) tumor cells are altered to express a new target receptor at levels that may significantly improve tumor to normal tissue targeting of radiolabeled ligands. This method thus represents a new paradigm by which augmented therapeutic efficacy can be achieved through enhanced radiolabeled ligand localization to tumors transduced in situ to express unique and novel receptors. The use of modern molecular biology techniques to increase the expression of tumor-associated receptors for radiolabeled ligands is a novel approach to the treatment of cancer. The importance of this approach lies in that although each modality alone has limitations, the combination of gene transfer and radioligand therapy would be synergistic in effect.

INDUCTION OF RECEPTOR IN VITRO

We produced an Ad encoding the gene for hSSTr2 under the control of the cytomegalovirus promoter (AdCMVhSSTr2), and showed in vitro binding of ^{125}I-somatostatin and ^{111}In-DTPA-D-Phe^1-octreotide to cell membrane preparations of SK-OV-3.ip1 human ovarian cancer cells and A-427 human nonsmall cell lung cancer cells infected with AdCMVhSSTr2.[60] The cells were infected with various amounts of AdCMVhSSTr2, and binding assays on membrane preparations from these cells showed high expression of hSSTr2 (Fig 1).[120] In addition, reverse transcriptase polymerase chain reaction analysis showed the presence of hSSTr2 messenger ribonucleic acid in A-427 and SK-OV-3.ip1 cells infected with AdCMVhSSTr2. Scatchard analysis of A-427 cells infected with 10 plaque forming units (pfu) AdCMVhSSTr2 and binding of ^{99m}Tc-P829 (Neotect) showed a B_{max} of 19,000 fmol/mg and the affinity of ^{99m}Tc-P829 to be 7 nM.

INDUCTION OF RECEPTORS IN VIVO

To evaluate the ability to induce receptor expression in vivo, AdCMVhSSTr2 was injected IP to induce hSSTr2 expression on SK-OV-3.ip1 tumors 5 days after tumor cell injection in the peritoneum in nude mice. Two days later, tumor localization of ^{111}In-DTPA-D-Phe^1-octreotide 4 hours after IP injection was equal to 60.4% ID/g of the radiolabeled peptide.[60] However, the uptake in tumor decreased to 18.6% ID/g at 24 hours after

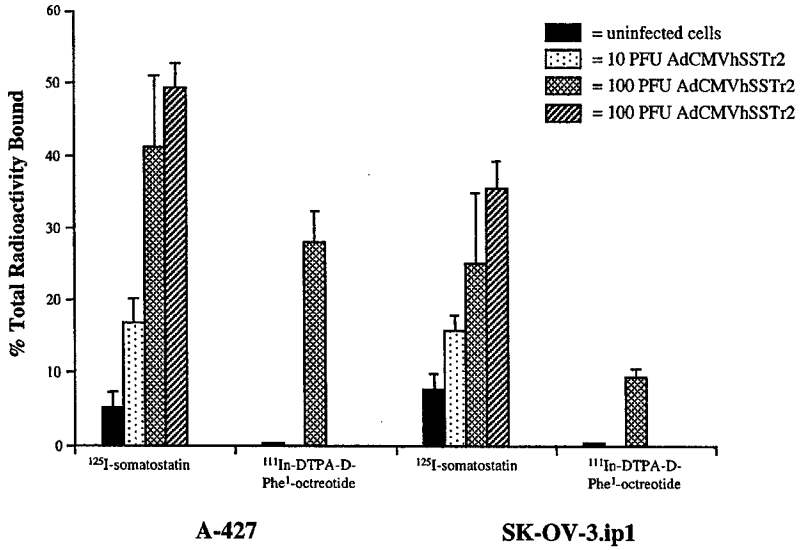

Fig 1. Binding of ^{125}I-Tyr^1-somatostatin and ^{111}In-DTPA-D-Phe^1-octreotide to A-427 and SK-OV-3.ip1 membrane preparations.

injection (Fig 2). The tumor localization was significantly lower (1.6% ID/g) when a control Ad (AdCMVGRPr) was injected. These studies also showed that the tumor uptake of ^{111}In-DTPA-D-Phe^1-octreotide was similar 1, 2, or 4 days after AdCMVhSSTr2 injection and that 2 injections of AdCMVhSSTr2 did not improve the tumor localization of ^{111}In-DTPA-D-Phe^1-octreotide. Thus, these studies showed that tumor uptake of ^{111}In-DTPA-D-Phe^1-octreotide could be achieved after infection of the ovarian tumor in vivo with AdCMVhSSTr2.

Other studies have investigated the localization of ^{111}In-DTPA-D-Phe^1-octreotide to s.c. A-427 nonsmall cell lung tumors injected intratumorally (i.t.) with AdCMVhSSTr2.[121] The gamma camera region of interest analysis showed the tumor uptake of ^{111}In-DTPA-D-Phe^1-octreotide to be 2.8% ID/g 48 hours after a single intratumoral AdCMVhSSTr2 injection and 3.1% ID/g at 96 hours. Uptake of ^{111}In-DTPA-D-Phe^1-octreotide in control Ad-injected tumors was <0.3% ID/g at both times.

Gamma camera imaging was used to detect hSSTr2 expression in s.c. A-427 tumors infected with AdCMVhSSTr2 using a ^{99m}Tc- or ^{188}Re-

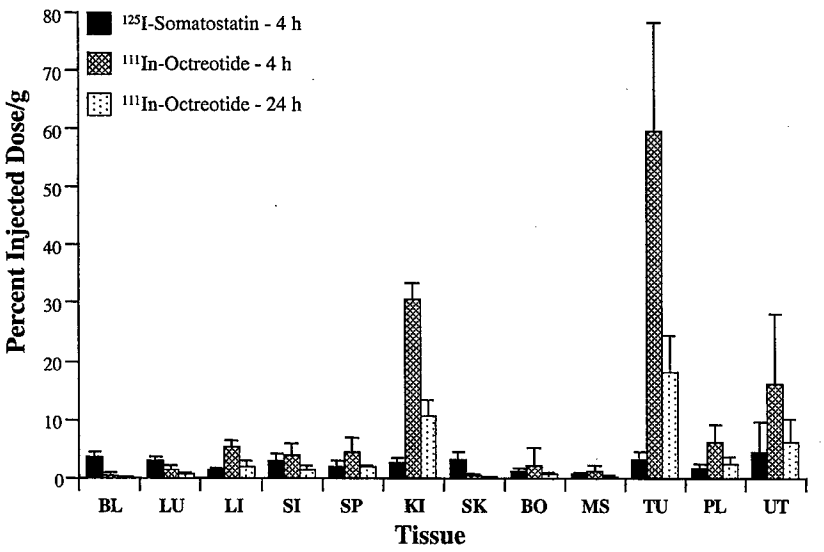

Fig 2. Biodistribution of ^{125}I-somatostatin and ^{111}In-DTPA-D-Phe^1-octreotide in mice bearing intraperitoneal (IP) SK-OV-3.ip1 tumors injected with AdCMVhSSTr2. BL, blood; LU, lung; LI, liver; SI, small intestine; SP, spleen; KI, kidney; SK, skin; BO, bone; MS, muscle; TU, tumor; PL, peritoneal lining; UT, uterus. Reprinted with permission from the American Association for Cancer Research, Inc.

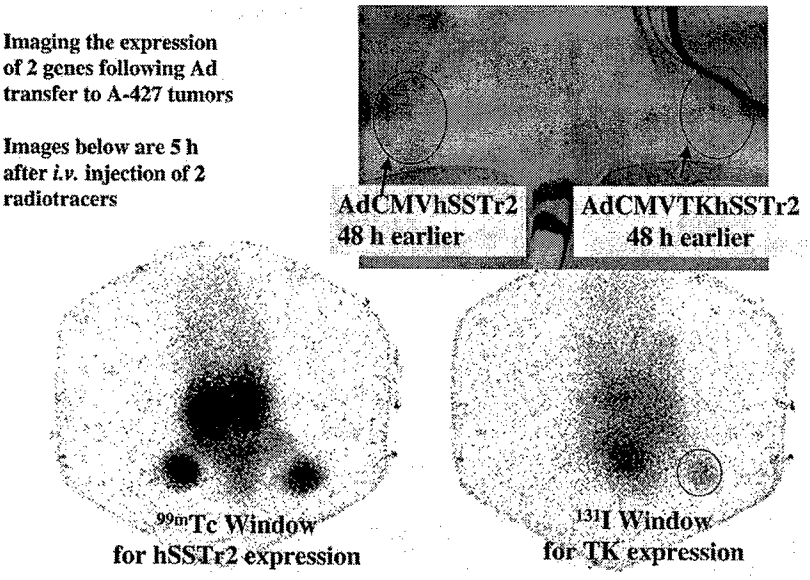

Fig 3. In vivo simultaneous imaging for human somatostatin receptor subtype 2 (hSSTr2) and thymidine kinase (TK) expression. Photograph of the mouse shows tumor locations and adenoviral (Ad) doses. The expression of hSSTr2 was depicted with imaging tumor accumulation of ^{99m}Tc-labeled P2045 (bottom left), while TK expression was depicted with imaging tumor accumulation of ^{131}I-labeled FIAU (bottom right). The images were obtained 5 hours after intravenous (IV) injection of the radiotracers. Reprinted with permission from the Radiological Society of North America, Inc.

labeled somatostatin analogue.[122] The somatostatin analogue, P829, was radiolabeled with ^{99m}Tc at high specific activity and was shown to bind with high affinity to hSSTr2-positive tumors by external scintigraphic imaging. The ^{99m}Tc-P829 and ^{188}Re-P829 bound with high affinity (6 to 7 nM) to membrane preparations from A-427 cells infected with AdCMVhSSTr2, and were internalized similarly by AdCMVhSSTr2-infected A-427 cells.[122] Mice bearing s.c. A-427 tumors injected i.t. with AdCMVhSSTr2 showed uptake of IV-injected ^{99m}Tc-P829 and ^{188}Re-P829 detected by gamma camera imaging, while uptake was not observed when the tumors were infected with a control Ad. This result was confirmed by counting the tumors in a gamma counter, which showed 3.8% and 2.9% ID/g of ^{99m}Tc-P829 and ^{188}Re-P829 in the AdCMVhSSTr2 injected tumors, respectively, compared with <0.4% ID/g in the tumors infected with the control Ad. Independent confirmation of hSSTr2 expression was shown by immunohistochemical analysis.

A novel ^{99m}Tc-labeled peptide (P2045) recently described by Diatide, Inc.[123] binds with high affinity to hSSTr2 and has favorable in vivo biodistribution. This peptide was evaluated in mice bearing SK-OV-3.ip1 tumors in the peritoneum. Tumor uptake of ^{99m}Tc-P2045 at 48 hours after IV injection averaged 2.2 ± 0.3% ID/g for mice injected IP with AdCMVhSSTr2 (1×10^9 pfu), as compared with 0.18 ± 0.002% ID/g in control mice not receiving Ad injection ($P < 0.05$) or in tumors from mice injected IP with an Ad encoding the green fluorescent protein, which averaged 0.26 ± 0.17% ID/g.[124] We also evaluated P2045 in mice bearing s.c. A-427 tumors injected i.t. with AdCMVhSSTr2 or with a control Ad. The ^{99m}Tc-P2045 was injected IV 2 or 4 days after AdCMVhSSTr2 injection, and the animals were imaged using a gamma camera equipped with a pinhole collimator 3.5 to 4.5 hours later. The images showed similar uptake of ^{99m}Tc-P2045 in the tumors injected with AdCMVhSSTr2, but background uptake in tumors injected with control Ad. The biodistribution results in the mice 4 days after AdCMVhSSTr2 injection and 4 hours after ^{99m}Tc-P2045 injection showed 7.8% ID/g in the positive tumor. No other tissue had higher uptake than the AdCMVhSSTr2-injected tumor.[120]

Further studies were reported using a bicistronic Ad vector encoding hSSTr2 and thymidine kinase (TK) in the same mouse tumor model.[125] The tumors were injected i.t. with the bicistronic vector (AdCMVhSSTr2TK), and the animals were imaged for hSSTr2 expression with ^{99m}Tc-P2045 and TK with ^{131}I-FIAU (Fig 3). The biodistribution results showed the uptake of ^{99m}Tc-labeled P2045 and ^{131}I-labeled FIAU for AdCMVhSSTr2TK-injected tumors (n = 8) was 11.1% and 1.6% ID/g, respectively. AdCMVhSSTr2-injected tumors (n = 4) accumulated 10.2% ID/g of the ^{99m}Tc-labeled P2045 and 0.3% of the ^{131}I-labeled FIAU. AdCMVTK-injected tumors (n = 4) had 0.2% ID/g for

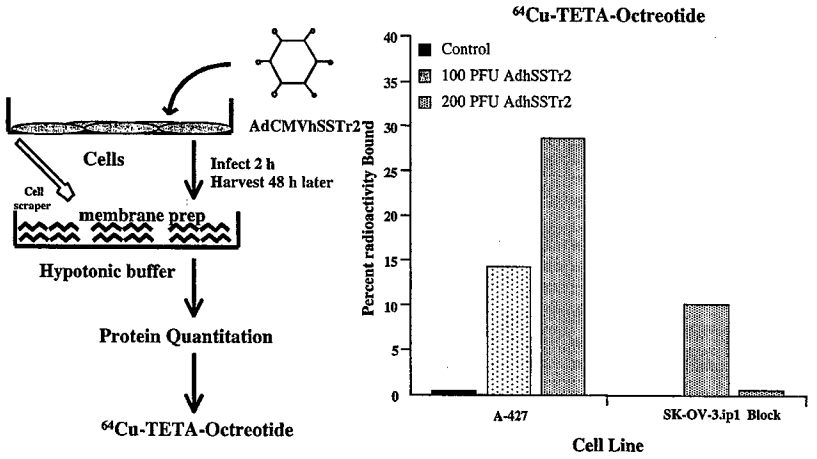

Fig 4. Induction of human somatostatin receptor subtype 2 (hSSTr2) and ^{64}Cu-TETA-octreotide binding in vitro.

the ^{99m}Tc-labeled P2045 and 3.7% for ^{131}I-labeled FIAU.

It was shown that ^{64}Cu-TETA-octreotide bound to cell membrane preparations of A-427 and SK-OV-3.ip1 cells infected with AdCMVhSSTr2 (Fig 4). Tumor localization and pharmacokinetics of ^{64}Cu-TETA-octreotide was investigated in mice bearing IP SK-OV-3.ip1 human ovarian tumors induced to express hSSTr2 with AdCMVhSSTr2. Mice bearing IP SK-OV-3.ip1 tumors infected with 1×10^9 pfu AdCMVhSSTr2 5 days after tumor cell inoculation followed by IP injection of ^{64}Cu-TETA-octreotide 2 days later had median tumor uptake of 25.1%ID/g at 4 hours after ^{64}Cu-TETA-octreotide administration (Fig 5). The uptake at 4 hours was significantly higher than when the control Ad (AdCMVLacZ) was given (1.6% ID/g). The tumor uptake of ^{64}Cu-TETA-octreotide decreased to 7.2% ID/g at 18 hours after injection.

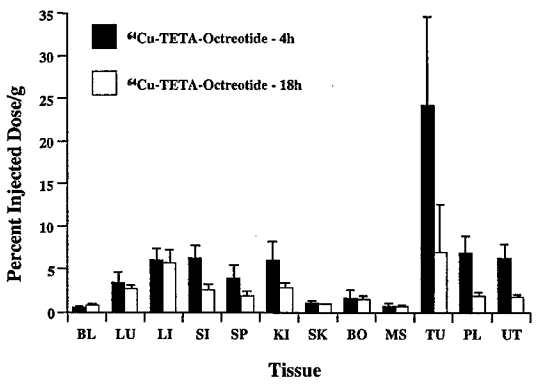

Fig 5. Biodistribution of ^{64}Cu-TETA-octreotide in mice bearing intraperitoneal (IP) SK-OV-03.ip1 tumors injected with AdCMVhSSTr2.

THERAPY STUDIES WITH THE SINGLE GENE VECTOR AdCMVhSSTr2

In a therapy study, we evaluated a single administration of 1.4 or 2.0 mCi of ^{64}Cu-TETA-octreotide 2 days after AdCMVhSSTr2 injection in mice bearing IP SK-OV-3.ip1 tumors. Also, mice received 2 doses of ^{64}Cu-TETA-octreotide. In this group of animals, 1.4 mCi of ^{64}Cu-TETA-octreotide was administered 2 days after AdCMVhSSTr2, followed by an additional dose of AdCMVhSSTr2 13 days after the first, and administration of 700 μCi of ^{64}Cu-TETA-octreotide 2 days later. Untreated animals had a median survival of 34 days, while median survival following a single 1.4 mCi dose was 36 days, and a single 2.0 mCi dose was 14 days. The mice that received 2 doses of ^{64}Cu-TETA-octreotide (1.4 plus 0.7 mCi) had a median survival of 62 days (Fig 6). Overall, the combination of gene therapy and ^{64}Cu-TETA-octreotide resulted in significantly ($P < 0.05$) longer survival of the mice. These results establish

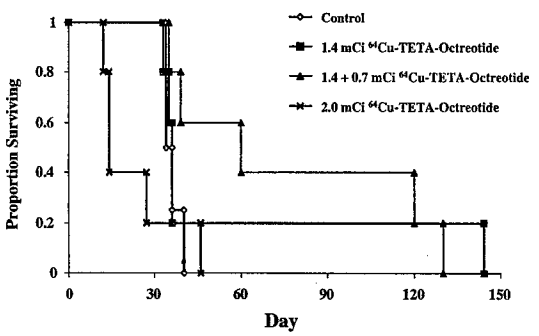

Fig 6. Survival of nude mice bearing intraperitoneal (IP) SK-OV-3.ip1 tumors treated with ^{64}Cu-TETA-octreotide.

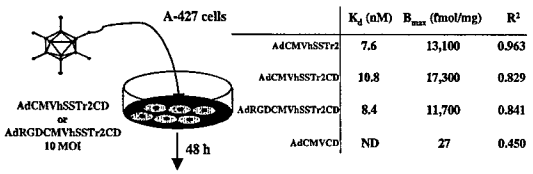

	K_d (nM)	B_{max} (fmol/mg)	R^2
AdCMVhSSTr2	7.6	13,100	0.963
AdCMVhSSTr2CD	10.8	17,300	0.829
AdRGDCMVhSSTr2CD	8.4	11,700	0.841
AdCMVCD	ND	27	0.450

Fig 7. Evaluation of AdSSTr2CD bicistronic vectors for expression of human somatostatin receptor subtype 2 (hSSTr2).

the key feasibilities of inducing hSSTr2 expression in ovarian tumors and achieving therapy with a radiolabeled somatostatin analogue. Our hypothesis is that a radiolabeled ligand with a longer retention time would deliver a higher radiation absorbed dose and result in higher therapeutic efficacy.

Another somatostatin analogue that is being used for therapy is ^{90}Y-SMT 487.[27,81] Nude mice were inoculated s.c. with 2×10^6 A-427 cells. Twenty-four days later the mice were administered 1×10^9 pfu AdCMVhSSTr2 i.t. (day 0), and the first measurement of the tumor size (surface area equal to length x width) was made with vernier calipers. Mice received an IV injection of either 400 or 500 μCi ^{90}Y-SMT 487 on days 2 and 4. The mice then received an additional i.t. injection of AdCMVhSSTr2 on day 7, followed by 2 more 400 or 500 μCi doses of ^{90}Y-SMT 487 on days 9 and 11. Control tumor-bearing mice either did not receive treatment or received 4, 500 μCi doses of ^{90}Y-SMT 487 on days 2, 4, 9, and 11 without AdCMVhSSTr2 injections.[121] Mice that received 2 i.t. injections of AdCMVhSSTr2 and 4 doses of 400 or 500 μCi ^{90}Y-SMT 487 had median tumor quadrupling times of 40 and 44 days, respectively. The log-rank test revealed a statistically significant difference in time to tumor, quadrupling between the AdCMVhSSTr2 + ^{90}Y-SMT 487 treatment groups and the control groups ($P < 0.02$). The median tumor quadrupling times of the no treatment group and the no virus + 4 doses of 500 μCi ^{90}Y-SMT 487 group were 16 and 25 days, respectively.

THERAPY WITH THE BICISTRONIC VECTOR AdCMVhSSTr2CD

We have constructed and evaluated bicistronic Ad vectors encoding for hSSTr2 and the CD enzyme.[126] The rationale for the construction of these vectors is 2-fold. First, hSSTr2 can be used for noninvasive imaging to determine the expression of the therapeutic gene (CD) in vivo.[125] Second, hSSTr2 can be used for therapy as discussed previously, and the combination of this with CD mediated therapy through conversion of 5-FC to 5-FU may result in an additive or synergistic therapeutic effect. The A-427 cells infected with bicistronic vectors AdCMVhSSTr2CD or AdCMVhSSTr2CDRGD with the arginine–glycine–aspartic acid (RGD) peptide genetically engineered in the fiber knob to retarget Ad binding to integrins on the cell surface had equivalent hSSTr2 expression as the single gene vector AdCMVhSSTr2 (Fig 7). In addition, the AdCMVhSSTr2CD and AdCMVhSSTr2CDRGD vectors produced similar CD enzyme activity levels as the single gene vector AdCMVCD (Fig 8). Thus, both genes

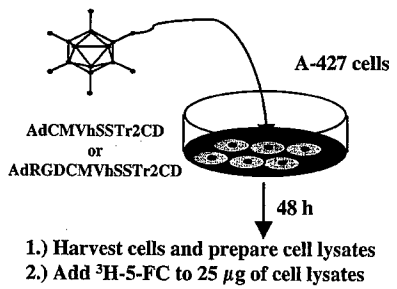

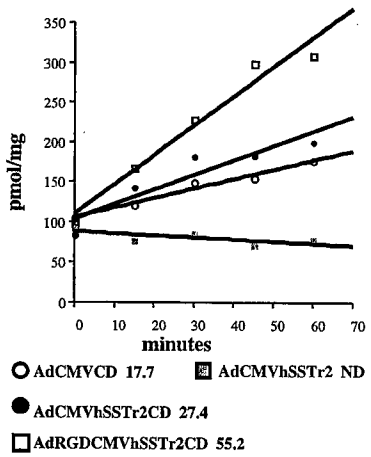

Fig 8. Evaluation of AdSSTr2CD bicistronic vectors for cytosine deaminase (CD) activity.

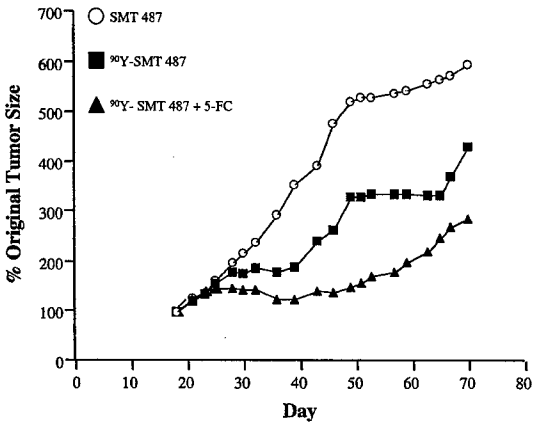

Fig 9. Therapy results with AdCMVSSTr2CD, 5-FC, and ^{90}Y-SMT 487 in athymic nude mice bearing subcutaneous (s.c.) A-427 xenografts.

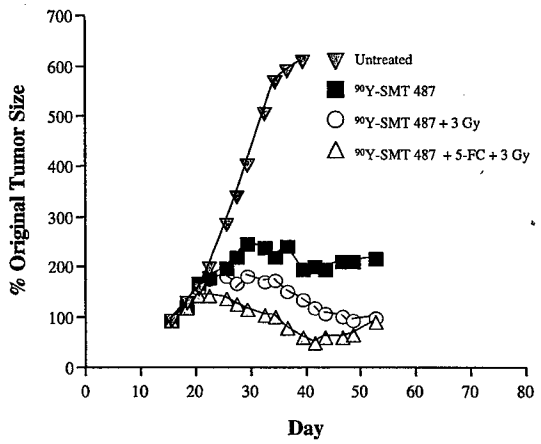

Fig 11. Therapy results with AdCMVSSTr2CD, 5-FC, ^{60}Co, and ^{90}Y-SMT 487 in athymic nude mice bearing subcutaneous (s.c.) A-427 xenografts.

were active in the bicistronic vectors. Therefore, therapy studies were initiated with AdCMVhSSTr2CD and ^{90}Y-SMT 487 in combination with 5-FC.

The AdCMVhSSTr2CD was injected i.t. into A-427 tumors at 1×10^9 pfu on days 20 and 27. The ^{90}Y-SMT 487 was administered IV on days 22, 24, 29, and 31 at 500 μCi per injection. The 5-FC was administered IP at 400 mg/kg twice a day for 5 days beginning on day 21, followed by another 5-day cycle beginning on day 28. Tumor inhibition results showed that ^{90}Y-SMT 487 and ^{90}Y-SMT 487 in combination with 5-FC inhibited tumor growth (Fig 9). Importantly, the combination treatment had a higher tumor growth inhibition than the ^{90}Y-SMT 487 treatment alone. In addition, the levels of toxicity (weight loss) were modest (Fig 10).

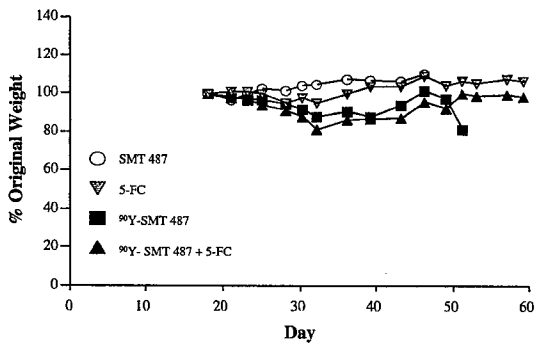

Fig 10. Toxicity with AdCMVSSTr2CD, 5-FC, and ^{90}Y-SMT 487 in athymic nude mice bearing subcutaneous (s.c.) A-427 xenografts.

The next therapy study consisted of intratumoral injections of AdCMVhSSTr2CD into A-427 tumors at 1×10^9 pfu on days 18, 25, 32, and 39. The ^{90}Y-SMT 487 was administered IV on days 20, 22, 27, 29, 34, 36, 41, and 43 at 500 μCi per injection. The 5-FC was administered IP at 400 mg/kg twice a day for 5 days beginning on day 19, followed by 3 more 5-day cycles beginning on days 26, 33, and 40. The ^{60}Co was given as a single 3 Gy dose on days 21, 28, 35, and 42. Tumor inhibition results were extremely encouraging because they show that the combination of ^{90}Y-SMT 487 + 5-FC + 3 Gy resulted in tumor regressions (Fig 11 and Table 1). All combination therapies had at least 2 complete regressions with most being recurrence-free. The triple therapy groups had the highest mean tumor growth suppression of all treatment groups, but these differences were not statistically significant ($P = 0.116$). The problem, however, was that the intense therapeutic regimen was not well tolerated (Table 2). A summary of the weight change data is shown in Table 2. From before and after weight (paired t-test) comparisons, the controls had a significant weight gain ($P < 0.001$), while ^{90}Y-SMT 487 (400 μCi x8) and ^{90}Y-SMT 487 (500 μCi x4) + 5-FC + 3 Gy had no significant weight changes ($P = 0.065$ and 0.216, respectively), and all other treatments groups had significant mean weight losses (all $P \leq 0.01$). We plan to investigate lower doses of 5-FC and ^{90}Y-SMT 487 in future studies.

Table 1. Tumor Doubling Times and Complete Regressions in AdCMVhSSTr2CD Experiments

Treatment	no.	Tumor Doubling Time (mean/median)	Complete Regressions	
			Total (n)	No Relapse (n)
Untreated controls	15	16/10	1	1
^{90}Y-SMT 487 (500 μCi × 8)	8	19/9	0	0
^{90}Y-SMT 487 (400 μCi × 8)	8	25/12	0	0
^{90}Y-SMT 487 (500 μCi × 8) + 3 Gy	8	29/25	3	2
^{90}Y-SMT 487 (400 μCi × 8) + 3 Gy	8	32/19	2	1
^{90}Y-SMT 487 (500 μCi × 4) + 5-FC + 3 Gy	8	47/19	3	3
^{90}Y-SMT 487 (400 μCi × 8) + 5-FC + 3 Gy	8	53/32	3	3

CONCLUSION

These studies show that genetic induction of hSSTr2 results in tumor localization of radiolabeled peptides at a level sufficient to produce therapeutic effects. Efforts continue to optimize this novel approach to cancer gene therapy by molecular chemotherapy and radiation therapy.

Table 2. Animal Weight Changes in AdCMVhSSTr2CD Experiments

Treatment	no.	Percent Change	Percentage with >20% loss
Untreated controls	15	117	0
^{90}Y-SMT 487 (500 μCi × 8)	8	78	63
^{90}Y-SMT 487 (400 μCi × 8)	8	85	38
^{90}Y-SMT 487 (500 μCi × 8) + 3 Gy	8	84	38
^{90}Y-SMT 487 (400 μCi × 8) + 3 Gy	8	78	50
^{90}Y-SMT 487 (500 μCi × 4) + 5-FC + 3 Gy	8	91	50
^{90}Y-SMT 487 (400 μCi × 8) + 5-FC + 3 Gy	8	79	50

The development of new ligands (eg, minibody and diabodies) against hSSTr2 and mutant forms of hSSTr2 offer the potential for higher and more specific tumor uptake and, thus, improved sensitivity of detection and higher therapeutic efficacy. Other approaches that are under active investigation include gene transfer of the type-2 dopamine receptor expressed on the tumor cell surface detected by PET using a radiolabeled antagonist, or herpes simples virus TK gene transfer detected by gamma camera or PET imaging with radiolabeled substrates trapped intracellularly after phosphorylation by the kinase.[127-129] Gene transfer of the sodium iodide symporter has also been used for imaging and therapy. Clinical studies are needed to determine the most promising approach.

ACKNOWLEDGMENTS

Anna Wu, Alex Pereboev, Kurt Zinn, Tandra Chaudhuri, Mark Carpenter, and Buck Rogers are acknowledged for their contributions to the concepts and results presented.

REFERENCES

1. Buchsbaum DJ, Langmuir VK, Wessels BW: Experimental radioimmunotherapy. Med Phys 20:551-567, 1993

2. Buchsbaum DJ: Experimental radioimmunotherapy and methods to increase therapeutic efficacy. in Goldenberg DM (ed): Cancer Therapy with Radiolabeled Antibodies. Boca Raton, FL, CRC Press, 1995, pp 115-140

3. Knox SJ: Overview of studies on experimental radioimmunotherapy. Cancer Res 55:5832s-5836s, 1995 (suppl)

4. Imam SK: Status of radioimmunotherapy in the new millennium. Cancer Biother Radiopharm 16:237-256, 2001

5. Goldenberg DM: Targeted therapy of cancer with radiolabeled antibodies. J Nucl Med 43:693-713, 2002

6. Dillman RO: Radiolabeled anti-CD20 monoclonal antibodies for the treatment of B-cell lymphoma. J Clin Oncol 20:3545-3557, 2002

7. Juweid ME: Radioimmunotherapy of B-cell non-Hodgkin's lymphoma: From clinical trials to clinical practice. J Nucl Med 43:1507-1529, 2002

8. Vose JM, Wahl RL, Saleh M, et al: Multicenter phase II study of iodine-131 tositumomab for chemotherapy-relapsed/refractory low-grade and transformed low-grade B-cell non-Hodgkin's lymphomas. J Clin Oncol 18:1316-1323, 2000

9. Press OW, Eary JF, Gooley T, et al: A phase I/II trial of iodine-131-tositumomab (anti-CD20), etoposide, cyclophosphamide, and autologous stem cell transplantation for relapsed B-cell lymphomas. Blood 96:2934-2942, 2000

10. Kaminski MS, Zelenetz AD, Press OW, et al: Pivotal study of iodine I 131 tositumomab for chemotherapy-refractory low-grade or transformed low-grade B-cell non-Hodgkin's lymphomas. J Clin Oncol 19:3918-3928, 2001

11. Wiseman GA, Gordon LI, Multani PS, et al: Ibritumomab tiuxetan radioimmunotherapy for patients with relapsed or refractory non-Hodgkin lymphoma and mild thrombocytopenia: A phase II multicenter trial. Blood 99:4336-4342, 2002

12. Witzig TE, Gordon LI, Cabanillas F, et al: Randomized controlled trial of yttrium-90-labeled ibritumomab tiuxetan radioimmunotherapy versus rituximab immunotherapy for patients with relapsed or refractory low-grade, follicular, or transformed B-cell non-Hodgkin's lymphoma. J Clin Oncol 20:2453-2463, 2002

13. van Zanten-Przybysz I, Molthoff CF, Roos JC, et al: Radioimmunotherapy with intravenously administered ^{131}I-labeled chimeric monoclonal antibody MOv18 in patients with ovarian cancer. J Nucl Med 41:1168-1176, 2000

14. Meredith RF, Alvarez RD, Partridge EE, et al: Intraperitoneal radioimmunochemotherapy of ovarian cancer: A phase I study. Cancer Biother Radiopharm 16:305-315, 2001

15. Alvarez RD, Huh WK, Khazaeli MB, et al: A phase I study of combined modality ^{90}Yttrium-CC49 intraperitoneal radioimmunotherapy for ovarian cancer. Clin Cancer Res 8:2806-2811, 2002

16. Hopkins K, Papanastassiou V, Kemshead JT: The treatment of patients with recurrent malignant gliomas with intratumoral radioimmunoconjugates. Recent Results Cancer Res 141:141-159, 1996

17. Cokgor I, Akabani G, Kuan C-T, et al: Phase I trial results of iodine-131-labeled antitenascin monoclonal antibody 81C6 treatment of patients with newly diagnosed malignant gliomas. J Clin Oncol 18:3862-3872, 2000

18. Menda Y, Kahn D: Somatostatin receptor imaging of non-small cell lung cancer with ^{99m}Tc depreotide. Semin Nucl Med 32:92-96, 2002

19. Warner RRP, O'Dorisio TM: Radiolabeled peptides in diagnosis and tumor imaging: Clinical overview. Semin Nucl Med 32:79-83, 2002

20. Machac J, Krynyckyi B, Kim C: Peptide and antibody imaging in lung cancer. Semin Nucl Med 32:276-292, 2002

21. Virgolini I, Kurtaran A, Raderer M, et al: Vasoactive intestinal peptide receptor scintigraphy. J Nucl Med 36:1732-1739, 1995

22. Lamberts SWJ, van der Lely AJ, de Herder WW, et al: Octreotide. N Engl J Med 334:246-254, 1996

23. Blum JE, Handmaker H, Rinne NA: The utility of a somatostatin-type receptor binding peptide radiopharmaceutical (P829) in the evaluation of solitary pulmonary nodules. Chest 115:224-232, 1999

24. Traub T, Petkov V, Ofluoglu S, et al: ^{111}In-DOTA-lanreotide scintigraphy in patients with tumors of the lung. J Nucl Med 42:1309-1315, 2001

25. Zamora PO, Gulhke S, Bender H, et al: Experimental radiotherapy of receptor-positive human prostate adenocarcinoma with ^{188}Re-RC-160, a directly-radiolabeled somatostatin analogue. Int J Cancer 65:214-220, 1996

26. Anderson CJ, Jones LA, Bass LA, et al: Radiotherapy, toxicity and dosimetry of copper-64-TETA-octreotide in tumor-bearing rats. J Nucl Med 39:1944-1951, 1998

27. Stolz B, Weckbecker G, Smith-Jones PM: The somatostatin receptor-targeted radiotherapeutic [^{90}Y-DOTA-DPhe^1, Tyr^3]octreotide (^{90}Y-SMT 487) eradicates experimental rat pancreatic CA 20948 tumours. Eur J Nucl Med 25:668-674, 1998

28. de Jong M, Breeman WAP, Bernard BF, et al: Tumor response after [^{90}Y-DOTA^0, Tyr^3]octreotide radionuclide therapy in a transplantable rat tumor model is dependent on tumor size. J Nucl Med 42:1841-1846, 2001

29. Bugaj JE, Erion JL, Johnson MA, et al: Radiotherapeutic efficacy of ^{153}Sm-CMDTPA-Tyr^3-octreotate in tumor-bearing rats. Nucl Med Biol 28:327-334, 2001

30. Chinol M, Paganelli G, Zoboli S, et al: ^{90}Y-DOTATOC treatment of patients with SSTr2 positive tumors: Preliminary results of phase I-II study. J Nucl Med 40:18P, 1999

31. de Jong M, Krenning E: New advances in peptide receptor radionuclide therapy. J Nucl Med 43:617-620, 2002

32. de Jong M, Valkema R, Jamar F, et al: Somatostatin receptor-targeted radionuclide therapy of tumors: Preclinical and clinical findings. Semin Nucl Med 32:133-140, 2002

33. Khazaeli MB, Conry RM, LoBuglio AF: Human immune response to monoclonal antibodies. J Immunother 15:42-52, 1994

34. Yokota T, Milenic DE, Whitlow M, et al: Rapid tumor penetration of a single-chain Fv and comparison with other immunoglobulin forms. Cancer Res 52:3402-3408, 1992

35. Vogel C-A, Bischof-Delaloye A, Mach JP, et al: Direct comparison of a radioiodinated intact chimeric anti-CEA MAb with its F(ab')$_2$ fragment in nude mice bearing different human colon cancer xenografts. Br J Cancer 68:684-690, 1993

36. Tai M-S, McCartney JE, Adams GP, et al: Targeting c-erbB-2 expressing tumors using single-chain Fv monomers and dimers. Cancer Res 55:5983s-5989s, 1995 (suppl)

37. Moffatt FL Jr, Pinsky CM, Hammershaimb L, et al: Clinical utility of external immunoscintigraphy with the IMMU-4 technetium-99m Fab' antibody fragment in patients undergoing surgery for carcinoma of the colon and rectum: Results of a pivotal, phase III trial. J Clin Oncol 14:2295-2305, 1996

38. Fischman AJ, Babich JW, Strauss HW: A ticket to ride: Peptide radiopharmaceuticals. J Nucl Med 34:2253-2263, 1993

39. Rowlinson G, Snook D, Busza A, et al: Antibody-guided localization of intraperitoneal tumors following intraperitoneal or intravenous antibody administration. Cancer Res 47:6528-6531, 1987

40. Zalutsky MR, Moseley RP, Benjamin JC, et al: Monoclonal antibody and F(ab')$_2$ fragment delivery to tumor in patients with glioma: Comparison of intracarotid and intravenous administration. Cancer Res 50:4105-4110, 1990

41. Quadri SM, Malik AB, Chu HB, et al: Intraperitoneal indium-111- and yttrium-90-labeled human IgM (AC6C3–2B12) in nude mice bearing peritoneal carcinomatosis. J Nucl Med 37:1545-1551, 1996

42. Kinuya S, Jeong JM, Garmestani K, et al: Effect of metabolism on retention of indium-111-labeled monoclonal antibody in liver and blood. J Nucl Med 35:1851-1857, 1994

43. Arano Y, Wakisaka K, Mukai T, et al: Stability of a metabolizable ester bond in radioimmunoconjugates. Nucl Med Biol 23:129-136, 1996

44. Rosenblum MG, Lamki LM, Murray JL, et al: Interferon-induced changes in pharmacokinetics and tumor uptake of ^{111}In-labeled antimelanoma antibody 96.5 in melanoma patients. J Natl Cancer Inst 80:160-165, 1988

45. Kuhn JA, Wong JYC, Beatty BG: γ-Interferon enhancement of a multiple treatment regimen for radioimmunotherapy. Antibody Immunoconj Radiopharm 4:837-845, 1991

46. Greiner JW, Ullmann CD, Nieroda C, et al: Improved radioimmunotherapeutic efficacy of an anticarcinoma monoclonal antibody (^{131}I-CC49) when given in combination with γ-interferon. Cancer Res 53:600-608, 1993

47. Roselli M, Guadagni F, Buonomo O, et al: Systemic administration of recombinant interferon alfa in carcinoma patients upregulates the expression of the carcinoma-associated antigens tumor-associated glycoprotein-72 and carcinoembryonic antigen. J Clin Oncol 14:2031-2042, 1996

48. Raben D, Buchsbaum DJ, Khazaeli MB, et al: Enhancement of radiolabeled antibody binding and tumor localization through adenoviral transduction of the human carcinoembryonic antigen gene. Gene Ther 3:567-580, 1996

49. Rogers BE, Rosenfeld ME, Khazaeli MB, et al: Localization of iodine-125-mIP-Des-Met^{14}-bombesin (7-13)NH_2 in ovarian carcinoma induced to express the gastrin releasing peptide receptor by adenoviral vector-mediated gene transfer. J Nucl Med 38:1221-1229, 1997

50. Rosenfeld ME, Rogers BE, Khazaeli MB, et al: Adenoviral mediated delivery of gastrin releasing peptide receptor results in specific tumor localization of a bombesin analogue in vivo. Clin Cancer Res 3:1187-1194, 1997

51. Rogers BE, Curiel DT, Mayo MS, et al: Tumor localization of a radiolabeled bombesin analogue in mice bearing human ovarian tumors induced to express the gastrin releasing peptide receptor by an adenoviral vector. Cancer 80:2419-2424, 1997

52. Clarke K, Lee FT, Brechbiel MW, et al: Therapeutic efficacy of anti-Lewis^y humanized 3S193 radioimmunotherapy in a breast cancer model: Enhanced activity when combined with taxol chemotherapy. Clin Cancer Res 6:3621-3628, 2000

53. O'Donnell RT, DeNardo SJ, Miers LA, et al: Combined modality radioimmunotherapy for human prostate cancer xenografts with taxanes and ^{90}yttrium-DOTA-peptide-ChL6. Prostate 50:27-37, 2002

54. Welt S, Ritter G, Williams C Jr, et al: Preliminary report of a phase I study of combination chemotherapy and humanized A33 antibody immunotherapy in patients with advanced colorectal cancer. Clin Cancer Res 9:1347-1353, 2003

55. Kinuya S, Kawashima A, Yokoyama K, et al: Cooperative effect of radioimmunotherapy and antiangiogenic therapy with thalidomide in human cancer xenografts. J Nucl Med 43:1084-1089, 2002

56. Pedley RB, El-Emir E, Flynn AA, et al: Synergy between vascular targeting agents and antibody-directed therapy. Int J Radiat Oncol Biol Phys 54:1524-1531, 2002

57. Burke PA, DeNardo SJ, Miers LA, et al: Cilengitide targeting of $\alpha_v\beta_3$ integrin receptor synergizes with radioimmunotherapy to increase efficacy and apoptosis in breast cancer xenografts. Cancer Res 62:4263-4272, 2002

58. Rogers BE, Garver RI Jr, Grizzle WE, et al: Genetic induction of antigens and receptors as targets for cancer radiotherapy. Tumor Targeting 3:122-137, 1998

59. Rogers BE, Douglas JT, Sosnowski BA, et al: Enhanced in vivo gene delivery to human ovarian cancer xenografts utilizing a tropism-modified adenovirus vector. Tumor Targeting 3:25-31, 1998

60. Rogers BE, McLean SF, Kirkman RL, et al: In vivo localization of [^{111}In]-DTPA-D-Phe^1-octreotide to human ovarian tumor xenografts induced to express the somatostatin receptor subtype 2 using an adenoviral vector. Clin Cancer Res 5:383-393, 1999

61. Zinn KR, Chaudhuri TR: The type 2 human somatostatin receptor as a platform for reporter gene imaging. Eur J Nucl Med 29:388-399, 2002

62. Rogers BE, Anderson CJ, Mayo MS, et al: Localization of Cu-64-TETA-octreotide to human ovarian cancer xenografts induced to express SSTr2 with an adenoviral vector. J Nucl Med 39:63P, 1998

63. Bonner, JA, Buchsbaum, DJ, Russo, SM, et al: A gene therapy-based approach for increasing tumor cell expression of epidermal growth factor receptor (EGFr). Semin Radiat Oncol (in press)

64. Reubi JC, Schaer JC, Waser B, et al: Expression and localization of somatostatin receptor SSTR1, SSTR2, and SSTR3 messenger RNAs in primary human tumors using in situ hybridization. Cancer Res 54:3455-3459, 1994

65. Woltering EA, O'Dorisio MS, O'Dorisio TM: The role of radiolabeled somatostatin analogs in the management of cancer patients. in DeVita VT Jr, Hellman S, Rosenberg SA (eds): Principles and Practice of Oncology, PPO Updates, vol 9 (ed 4). Philadelphia, PA, Lippincott-Raven, 1995, pp 1-16

66. Reubi JC, Waser B, Schaer JC, et al: Somatostatin receptors in human prostate and prostate cancer. J Clin Endocrinol Metab 80:2806-2814, 1995

67. Nilsson S, Reubi JC, Kalkner KM, et al: Metastatic hormone-refractory prostatic adenocarcinoma expresses somatostatin receptors and is visualized in vivo by [^{111}In]-labeled DTPA-D-[Phe^1]-octreotide scintigraphy. Cancer Res 55:5805s-5810s, 1995 (suppl)

68. Halmos G, Schally AV, Sun B, et al: High expression of somatostatin receptors and messenger ribonucleic acid for its receptor subtypes in organ-confined and locally advanced human prostate cancers. J Clin Endocrinol Metab 85:2564-2571, 2000

69. Patel YC: Somatostatin and its receptor family. Front Neuroendocrinol 20:157-198, 1999

70. Yamada Y, Post SR, Wang K, et al: Cloning and functional characterization of a family of human and mouse somatostatin receptors expressed in brain, gastrointestinal tract, and kidney. Proc Natl Acad Sci U S A 89:251-255, 1992

71. Hoyer D, Bell GI, Berelowitz M, et al: Classification and nomenclature of somatostatin receptors. Trends Pharmacol Sci 16:86-88, 1995

72. Feuerbach D, Fehlmann D, Nunn C, et al: Cloning, expression and pharmacological characterisation of the mouse somatostatin sst(5) receptor. Neuropharmacology 39:1451-1462, 2000

73. Virgolini I, Leimer M, Handmaker H, et al: Somatostatin receptor subtype specificity and in vivo binding of a novel tumor tracer, ^{99m}Tc-P829. Cancer Res 58:1850-1859, 1998

74. Reubi JC, Schar JC, Waser B, et al: Affinity profiles for human somatostatin receptor subtypes SST1-SST5 of somatostatin radiotracers selected for scintigraphic and radiotherapeutic use. Eur J Nucl Med 27:273-282, 2000

75. Schally AV: Oncological applications of somatostatin analogues. Cancer Res 48:6977-6985, 1988

76. Bruns C, Weckbecker G, Raulf F, et al: Molecular pharmacology of somatostatin-receptor subtypes. Ann N Y Acad Sci 733:138-146, 1994

77. Buscail L, Saint-Laurent N, Chastre E, et al: Loss of sst2 somatostatin receptor gene expression in human pancreatic and colorectal cancer. Cancer Res 56:1823-1827, 1996

78. Smith-Jones PM, Stolz B, Albert R, et al: Synthesis, radiolabelling, and evaluation of DTPA/octreotide conjugates for radiotherapy. J Labelled Comp Radiopharm 37:499-501, 1995

79. Stolz B, Smith-Jones P, Weckbecker G, et al: Radiotherapy with yttrium-90 labeled DOTA-Tyr^3-octreotide in tumor bearing rodents. J Nucl Med 38:18P, 1997

80. Leimer M, Kurtaran A, Smith-Jones P, et al: Response to treatment with yttrium 90-DOTA-lanreotide of a patient with metastatic gastrinoma. J Nucl Med 39:2090-2094, 1998

81. Paganelli G, Zoboli S, Cremonesi M, et al: Receptor-mediated radionuclide therapy with ^{90}Y-DOTA-D-Phe^{1}-Tyr^{3}-Octreotide: Preliminary report in cancer patients. Cancer Biother Radiopharm 14:477-483, 1999

82. Mathieu I, Jamar F, Walrand S, et al: Biodistribution of Y-86-DOTA-Tyr^{3}-octreotide (SMT487) and renal protective effect of amino acid infusion: A phase I study. Eur J Nucl Med 25:837, 1998

83. Smith MC, Liu J, Chen T, et al: OctreoTher™: Ongoing early clinical development of a somatostatin-receptor-targeted radionuclide antineoplastic therapy. Digestion 62:69-72, 2000 (suppl 1)

84. Valkema R, Kvols L, Jamar F, et al: Phase I study of therapy with ^{90}Y-SMT487 (octreother) in patients with somatostatin receptor (SS-R) positive tumors. J Nucl Med 5:33P, 2002

85. Valkema R, Pauwels S, Kvols L, et al: Peptide receptor radionuclide therapy (PRRT) with ^{90}Y-DOTA^{0}, Tyr^{3}-octreotide (Y-Oc) and ^{111}In-DTPA^{0}-octreotide (In-Oc): Comparison of tumor response and toxicity. J Nucl Med 5:34P, 2002

86. Buscombe JR, Caplin ME, Bouvier C, et al: Treating somatostatin receptor positive tumours with ^{90}Y-lanreotide. J Nucl Med 5:34P, 2002

87. Kwekkeboom DJ, Kam BL, Bakker WH, et al: Treatment with ^{177}Lu-DOTA-Tyr3-octreotate in patients with somatostatin receptor positive tumors. J Nucl Med 5:34P, 2002

88. Freeman SM, Whartenby KA, Freeman JL, et al: In situ use of suicide genes for cancer therapy. Semin Oncol 23:31-45, 1996

89. Morris JC: Enzyme/prodrug-based tumor vaccination: All politics (and immunity) are local. J Natl Cancer Inst 91:1986-1989, 1999

90. McGinn CJ, Shewach DS, Lawrence TS: Radiosensitizing nucleosides. J Natl Cancer Inst 88:1193-1203, 1996

91. Danielson S, Kilstrup M, Barilla K, et al: Characterization of the *Escherichia coli codBA* operon encoding cytosine permease and cytosine deaminase. Mol Microbiol 6:1335-1344, 1992

92. Austin EA, Huber BE: A first step in the development of gene therapy for colorectal carcinoma: Cloning, sequencing, and expression of *escherichia coli* cytosine deaminase. Mol Pharmacol 43:380-387, 1993

93. Hamstra DA, Rice DJ, Pu A, et al: Combined radiation and enzyme/prodrug treatment for head and neck cancer in an orthotopic animal model. Radiation Res 152:499-507, 1999

94. Hamstra DA, Rice DJ, Fahmy S, et al: Enzyme/prodrug therapy for head and neck cancer using a catalytically superior cytosine deaminase. Hum Gene Ther 10:1993-2003, 1999

95. Huber BE, Austin EA, Good SS, et al: In vivo antitumor activity of 5-fluorocytosine on human colorectal carcinoma cells genetically modified to express cytosine deaminase. Cancer Res 53:4619-4626, 1993

96. Hirschowitz EA, Ohwada A, Pascal WR, et al: In vivo adenovirus-mediated gene transfer of the *Escherichia coli* cytosine deaminase gene to human colon carcinoma-derived tumors induces chemosensitivity to 5-fluorocytosine. Human Gene Ther 6:1055-1063, 1995

97. Mullen C: Metabolic suicide genes in gene therapy. Pharmacol Ther 63:199-207, 1994

98. Huber BE, Austin EA, Richards CA, et al: Metabolism of 5-fluorocytosine to 5-fluorouracil in human colorectal tumor cells transduced with cytosine deaminase gene: Significant antitumor effects when only a small percentage of tumor cells express cytosine deaminase. Proc Natl Acad Sci U S A 91:8302-8306, 1994

99. Dong Y, Wen P, Manome Y, et al: In vivo replication-deficient adenovirus vector-mediated transduction of the cytosine deaminase gene sensitizes glioma cells to 5-fluorocytosine. Human Gene Ther 7:713-720, 1996

100. DiMaio JM, Clary BM, Via DF, et al: Directed enzyme pro-drug gene therapy for pancreatic cancer in vivo. Surgery 116:205-213, 1994

101. Hanna NN, Mauceri HJ, Wayne JD, et al: Virally directed cytosine deaminase/5-fluorocytosine gene therapy enhances radiation response in human cancer xenografts. Cancer Res 57:4205-4209, 1997

102. Pederson LC, Buchsbaum DJ, Vickers SM, et al: Molecular chemotherapy combined with radiation therapy enhances killing of cholangiocarcinoma cells in vitro and in vivo. Cancer Res 57:4325-4332, 1997

103. Stackhouse MA, Pederson LC, Grizzle WE, et al: Fractionated radiation therapy in combination with adenoviral delivery of the cytosine deaminase gene and 5-fluorocytosine enhances cytotoxic and antitumor effects in human colorectal and cholangiocarcinoma models. Gene Ther 7:1019-1026, 2000

104. Khil MS, Kim JH, Mullen CA, et al: Radiosensitization by 5-fluorocytosine of human colorectal carcinoma cells in culture transduced with cytosine deaminease gene. Clin Cancer Res 2:53-57, 1996

105. Gabel M, Kim JH, Kolozsvary A, et al: Selective in vivo radiosensitization by 5-fluorocytosine of human colorectal carcinoma cells transduced with the *E. coli* cytosine deaminase (CD) gene. Int J Radiat Oncol Biol Phys 41:883-887, 1998

106. Pederson LC, Vickers SM, Buchsbaum DJ, et al: Combining cytosine deaminase expression, 5-fluorocytosine exposure, and radiotherapy increases cytotoxicity to cholangiocarcinoma cells. J Gastrointest Surg 2:283-291, 1998

107. Pederson LC, Stackhouse, MA, Vickers, SM, et al: Redirection of cytosine deaminase gene transfer via basic fibroblast growth factor receptor enhances pancreatic carcinoma and cholangiocarcinoma cytotoxicity mediated by conversion of 5-fluorocytosine to 5-fluorouracil. Ann Surg (submitted)

108. Ohwada A, Hirschowitz EA, Crystal RG: Regional delivery of an adenovirus vector containing the *Escherichia coli* cytosine deaminase gene to provide local activation of 5-fluorocytosine to suppress the growth of colon carcinoma metastatic to liver. Hum Gene Ther 7:1567-1576, 1996

109. Miller CR, Williams CR, Buchsbaum DJ, et al: Intratumoral 5-fluorouracil produced by cytosine deaminase/5-fluorocytosine gene therapy is effective for experimental human glioblastomas. Cancer Res 62:773-780, 2002

110. Pandha HS, Martin LA, Rigg A, et al: Genetic prodrug activation therapy for breast cancer: A phase I clinical trial of *erb*B-2-directed suicide gene expression. J Clin Oncol 17:2180-2189, 1999

111. Breitling F, Dubel S, Seehaus T, et al: A surface expression vector for antibody screening. Gene 104:147-153, 1991

112. Fuchs P, Dubel S, Breitling F, et al: Recombinant human monoclonal antibodies. Basic principles of the immune system transferred to E. coli. Cell Biophys 21:81-91, 1992

113. Hu S-z, Shively L, Raubitschek A, et al: Minibody: A novel engineered anti-carcinoembryonic antigen antibody fragment (single-chain Fv-C_H3) which exhibits rapid, high-level targeting of xenografts. Cancer Res 56:3055-3061, 1996

114. Holliger P, Prospero T, Winter G: "Diabodies": Small bivalent and bispecific antibody fragments. Proc Natl Acad Sci U S A 90:6444-6448, 1993

115. Wu AM, Williams LE, Zieran L, et al: Anti-carcinoembryonic antigen (CEA) diabody for rapid tumor targeting and imaging. Tumor Targeting 4:47-58, 1999

116. Yazaki PJ, Wu AM, Tsai SW, et al: Tumor targeting of radiometal labeled anti-CEA recombinant T84.66 diabody and t84.66 minibody: comparison to radioiodinated fragments. Bioconjug Chem 12:220-228, 2001

117. Wu AM, Yazaki PJ, Tsai S, et al: High-resolution microPET imaging of carcinoembryonic antigen-positive xenografts by using a copper-64-labeled engineered antibody fragment. Proc Natl Acad Sci U S A 97:8495-8500, 2000

118. Adams GP, Schier R, McCall AM, et al: High affinity restricts the localization and tumor penetration of single-chain fv antibody molecules. Cancer Res 61:4750-4755, 2001

119. Buchsbaum DJ, Curiel DT: Gene therapy for the treatment of cancer. Cancer Biother Radiopharm 16:275-288, 2001

120. Rogers BE, Zinn KR, Buchsbaum DJ: Gene transfer strategies for improving radiolabeled peptide imaging and therapy. Q J Nucl Med 44:208-223, 2000

121. Rogers BE, Zinn KR, Lin C-Y, et al: Targeted radiotherapy with [^{90}Y]-SMT 487 in mice bearing human non-small cell lung tumor xenografts induced to express human somatostatin receptor subtype 2 with an adenoviral vector. Cancer 94:1298-1305, 2002

122. Zinn KR, Buchsbaum DJ, Chaudhuri T, et al: Noninvasive monitoring of gene transfer using a reporter receptor imaged with a high affinity peptide radiolabeled with ^{99m}Tc or ^{188}Re. J Nucl Med 41:887-895, 2000

123. Manchanda R, Azure M, Lister-James J, et al: Tumor regression in rat pancreatic (AR42J) tumor-bearing mice with Re-188 P2045—A somatostatin analog. Clin Cancer Res 5:3769s, 1999

124. Chaudhuri TR, Rogers BE, Buchsbaum DJ, et al: A noninvasive reporter system to image adenoviral-mediated gene transfer to ovarian cancer xenografts. Gynecol Oncol 83:432-438, 2001

125. Zinn KR, Chaudhuri TR, Krasnykh VN, et al: Gamma camera dual imaging with a somatostatin receptor and thymidine kinase after gene transfer with a bicistronic adenovirus. Radiology 223:417-425, 2002

126. Chaudhuri TR, Krasnykh VN, Belousova N, et al: An Ad-based strategy for imaging, radiotherapy, and enhanced tumor killing. Mol Ther 3:S25, 2001

127. Liang Q, Gotts J, Satyamurthy N, et al: Noninvasive, repetitive, quantitative measurement of gene expression from a bicistronic message by positron emission tomography, following gene transfer with adenovirus. Mol Ther 6:73-82, 2002

128. Tjuvajev JG, Doubrovin M, Akhurst T, et al: Comparison of radiolabeled nucleoside probes (FIAU, FHBG, and FHPG) for PET imaging of HSV1-*tk* gene expression. J Nucl Med 43:1072-1083, 2002

129. Blasberg RG: Molecular imaging and cancer. Mol Cancer Ther 2:335-343, 2003

Adenovirus-mediated cytosine deaminase/5-fluorocytosine gene therapy of experimental human prostate cancer is enhanced by uracil phosphoribosyltransferase

Christopher R. Williams, Donald J. Buchsbaum, and C. Ryan Miller

Departments of Radiation Oncology and Surgery, Divisions of Radiation Biology, Neurosurgery, and Urology, University of Alabama at Birmingham, Birmingham, Alabama

Running Title: CDUPRT/5-FC/XRT therapy of prostate cancer

Address Correspondence To:

C. Ryan Miller, Ph.D.

Departments of Radiation Oncology and Surgery

Divisions of Radiation Biology and Neurosurgery

Wallace Tumor Institute Room 678

1824 Sixth Avenue South

Birmingham, Alabama 35294-3300

Phone: 205-934-6293

Fax: 205-975-7060

Email: rmiller@uab.edu

SUMMARY

Adenovirus (Ad) mediated cytosine deaminase/5-fluorocytosine (CD/5-FC) enzyme/prodrug therapy (VDEPT) is a promising approach for enhancing local control of prostate cancer (CaP) by ionizing radiation (XRT). We evaluated the efficacy of two CD-based chemoradiation systems *in vitro* and *in vivo* involving either CD alone or coexpression of CD and uracil phosphoribosyltransferase (UPRT), an enzyme known to potentiate 5-fluorouracil (5-FU) cytotoxicity. Ad-mediated gene transfer efficiency (AdCMVGFP) to human CaP cell lines (PC-3, DU145, and LNCaP) and their expression of Ad receptors (coxsackie-Ad receptor (CAR) and $\alpha v\beta 3$ and $\alpha v\beta 5$ integrins) were quantified by flow cytometry. Ad gene transfer efficiency correlated strongly with both CAR and $\alpha v\beta 5$, but not $\alpha v\beta 3$, integrin expression. Following infection of CaP cells with Ad expressing CD (AdCMVCD) or a CDUPRT fusion protein (AdCMVCDUPRT), 5-FU and 5-FC cytotoxicity were examined *in vitro* by a tetrazolium reduction assay. While both viruses expressing CD displayed a viral dose-dependent increase in 5-FC cytotoxicity, AdCMVCDUPRT was 6-125 fold more potent than AdCMVCD. In addition, AdCMVCDUPRT, but not AdCMVCD, markedly increased 5-FU cytotoxicity 20-156 fold, presumably secondary to increased intratumoral 5-FU anabolism. Efficacy of both CD and CDUPRT VDEPT with and without XRT was tested in nude mice bearing subcutaneous DU145 human CaP xenografts. While AdCMVCDUPRT/5-FC/XRT-treated xenografts grew slower than those receiving XRT alone or AdCMVCD/5-FC/XRT, no significant differences in time to tumor doubling were evident relative to untreated control tumors. Thus, although CDUPRT coexpression enhances Ad-mediated CD/5-FC cytotoxicity, further refinements are necessary to adequately assess the impact of this strategy on local control in experimental animal models of CaP.

Keywords: adenovirus, prostate cancer, cytosine deaminase, uracil phosphoribosyltransferase, coxsackie-adenovirus receptor, 5-fluorouracil

INTRODUCTION

Adenocarcinoma of the prostate (CaP) is now a treatable disease in most cases, primarily due to early detection and low clinical stage at the time of diagnosis. This early detection has largely been attributed to more aggressive screening measures in the overall population, with particular emphasis placed on evaluation of prostate specific antigen (PSA). Still, for the year 2001, CaP is predicted to be the second leading cause of cancer-related deaths and the cancer with the highest incidence in men.[1] Management options for localized CaP include watchful waiting, radical prostatectomy, radiation therapy (XRT), hormonal therapy, and newer strategies such as cryotherapy, photodynamic therapy, and laser therapy.[2] Despite acceptable cure rates, the active treatment options for localized CaP may result in substantial morbidity, including impotence and incontinence, urinary and bowel irritative symptoms, and stricture and fistula formation.[2] Hence, further development of novel treatment strategies that are efficacious and minimize complications are necessary for localized CaP.

Molecular chemotherapy refers to use of gene-directed enzyme/prodrug therapy (GDEPT) systems to achieve similar goals as conventional chemotherapy, maximizing the therapeutic index. The main advantages of GDEPT over traditional systemic chemotherapy are increased local (intracellular and intratumoral) production of a chemotherapeutic drug from a non-toxic, systemically delivered prodrug and reduced systemic toxicity to normal tissues.[3] In addition, GDEPT elicits a potent bystander effect on surrounding, untreated cancer cells. This effect is important to the overall efficacy of GDEPT, potentially compensating for the inherently low gene transfer efficiency of current gene delivery systems.[4]

The most extensively studied GDEPT system is herpes simplex virus thymidine kinase/ganciclovir (HSV-TK/GCV). HSV-TK/GCV has been investigated in preclinical animal

models of a variety of tumor types as well as in numerous clinical trials, including CaP. While HSV-TK/GCV GDEPT is promising for CaP, other more attractive alternatives have been described.[5] A particularly promising approach utilizes the *E. coli* enzyme cytosine deaminase (CD, EC 3.5.4.1). CD converts the nontoxic prodrug 5-fluorocytosine (5-FC) into the toxic agent 5-fluorouracil (5-FU). 5-FC is non-toxic to humans due to the absence of CD.[6] We have previously utilized a replication-defective Ad vector encoding the *E. coli* CD (AdCMVCD) in animal models of gastrointestinal (GI) malignancies,[7-10] tumors for which 5-FU is a clinically important chemotherapeutic agent, particularly in combination with external beam XRT.[11-14] In this system, termed virus-directed enzyme/prodrug therapy (VDEPT), intratumoral injection of AdCMVCD results in localized, intratumoral CD expression, which enzymatically converts the systemically administered, nontoxic 5-FC into intratumoral 5-FU. Ad-mediated CD/5-FC VDEPT offers several distinct advantages over HSV-TK/GCV, including a bystander effect that does not require cell-cell contact through gap junctions,[15-18] proteins known to be down-regulated in CaP,[19] and the capacity of 5-FU to sensitize cells to the effects of ionizing XRT.[12, 13]

A major factor limiting 5-FU-based therapy and potentially CD/5-FC GDEPT for localized CaP is 5-FU resistance, which is due in part to intratumoral 5-FU catabolism to inactive metabolites by the enzyme dihydropyrimidine dehydrogenase (DPD).[20-23] One strategy to overcome high intratumoral expression of DPD involves expression of the enzyme uracil phosphoribosyltransferase (UPRT). This enzyme, a homologue of human orotate phosphoribosyltransferase expressed only in bacteria and yeast, converts 5-FU to 5-fluorouracil monophosphate (5-FUMP), the next metabolite in the 5-FU anabolism pathway. Expression of UPRT has been shown to overcome 5-FU resistance in human stomach cancer cells,[24] presumably due to shunting of 5-FU down the anabolic pathway, away from DPD-mediated

catabolism. Moreover, coexpression of CD and UPRT as a fusion protein (CDUPRT) has been shown to sensitize *E. coli*[25] and human tumor cells[26] to both 5-FC and 5-FU *in vitro*, and to greatly augment CD/5-FC efficacy *in vivo*.[26]

Based upon the facts that Ad vectors have shown utility in animal models of CaP and are currently being investigated in clinical trials,[27] the advantages of CD/5-FC over HSV-TK/GCV, the potentially superior cytotoxicity facilitated by coexpression of CD and UPRT, the clinical utility of external beam or intersitital XRT in the management of localized CaP, and the known radiosensitizing effects of 5-FU, [11-14] we hypothesized that Ad-mediated CD or CDUPRT/5-FC VDEPT may be useful as an adjunct to XRT in the management of localized CaP. Previous work by Anello et al. demonstrated that Ad-mediated expression of CD sensitized mouse RM-1 CaP cells to 5-FC and 5-FC/XRT *in vitro*.[28] Blackburn et al. demonstrated that Ad-mediated expression of a CD/HSV-TK fusion gene sensitized human PC-3 CaP cells to both 5-FC and GCV, and that this combination also potentiated XRT sensitivity.[29] Yoshimura et al. recently reported efficacy of CD/5-FC in cultured LNCaP cells, but did not address its affect on radiosensitization.[30]

While these studies demonstrate the potential of CD/5-FC VDEPT for radiosensitization of CaP, its efficacy in animal models of CaP has yet to be evaluated. In this report, Ad gene transfer efficiency (AdCMVGFP) and Ad receptor expression profiles of three common human CaP cell lines (DU145, LNCaP, PC-3) were determined and their correlation assessed. The effects of Ad-mediated expression of either CD or CDUPRT on 5-FC and 5-FU were determined *in vitro*. The first studies on the efficacy of CD and CDUPRT/5-FC VDEPT and XRT in a nude mouse subcutaneous xenograft model of DU145 human CaP are then presented.

RESULTS

Ad receptor expression. CAR and αv integrin expression was assessed by indirect immunofluorescence as previously described.[31] CAR, αvβ3 and αvβ5 integrin expression was variable on the 3 CaP cell lines tested (Table 1). DU145 cells expressed the highest level of both CAR and αvβ3 integrins, while αvβ5 expression was similar in all three cell lines.

Ad gene transfer efficiency. AdCMVGFP-mediated gene transfer to all 3 CaP cell lines was efficient, but variable (Fig. 1A). DU145 were the most transducible, while PC-3 cells were the least (MOI_{50} 4.0 and 39.2, respectively, $p<0.001$). An intermediate but significantly lower level of transduction was seen with LNCaP cells (MOI_{50} 8.0) compared to DU145 cells ($p<0.05$). With all 3 CaP cell lines, there was a significant dose-dependent increase in GFP expression with increasing AdCMVGFP MOI (Fig. 1B, $R^2>0.85$, $p<0.0001$ for each individual cell line). As shown in Fig. 1C, AdCMVGFP transduction (AdCMVGFP MOI_{50}) correlated strongly with the composite index of Ad receptor expression ($RMFI_{AdR}$, R^2 0.71), and with CAR ($RMFI_{CAR}$, R^2 0.95) and αvβ5 ($RMFI_{\alpha v\beta 5}$, R^2 0.79) expression levels but not αvβ3 ($RMFI_{\alpha v\beta 3}$, R^2 0.09). However, lack of sufficient sample size (n=3 cell lines) precluded assessment of the significance of these relationships.

AdCMVCD versus AdCMVCDUPRT-mediated 5-FC cytotoxicity. 5-FC cytotoxicity to cells infected with either AdCMVCD or AdCMVCDUPRT at various MOI (10-300) was determined after 5 days of continuous exposure. As shown in Table 2, 5-FC cytotoxicity to the 3 CaP cell lines after viral infection was variable. LNCaP cells were the most susceptible to 5-FC after infection with either AdCMVCD or AdCMVCDUPRT, PC-3 cells displayed an

intermediate level of sensitivity, and DU145 cells were the least sensitive. However, in all 3 cells lines, coexpression of CD and UPRT from AdCMVCDUPRT rendered cells much more sensitive to 5-FC (range 6-125 fold) than CD expression alone from AdCMVCD. The magnitude of enhancement in 5-FC sensitivity between AdCMVCDUPRT and AdCMVCD varied among cell lines, with LNCaP>PC-3>DU145 cells in order of decreasing sensitivity (increasing IC_{50}). While a trend towards a dose-dependent increase in 5-FC sensitivity was apparent with both LNCaP and DU145 cells, a significant relationship between AdCMVCD or AdCMVCDUPRT dose and 5-FC cytotoxicity existed only with PC-3 cells ($R^2>0.97$, $p<0.01$ for both viruses, Fig. 2). Taken together, these data demonstrate a significant enhancement in 5-FC cytotoxicity to CaP cells after Ad-mediated expression of CDUPRT versus CD alone.

AdCMVCDUPRT-mediated 5-FU cytotoxicity. 5-FU sensitivities of the 3 CaP cell lines tested were found to be remarkably similar (Table 3, IC_{50} 0.17-0.39 μg/ml, $p>0.05$). Moreover, 5-FU sensitivity levels with these CaP cells did not significantly differ from levels determined with cells derived from GI malignancies (human colon and pancreas), as previously described ($p>0.05$).[32] To determine whether the AdCMVCDUPRT-mediated enhancement of 5-FC cytotoxicity was due to UPRT expression, 5-FU cytotoxicity to PC-3 cells was determined after infection with AdCMVCDUPRT versus AdCMVCD. As shown in Fig. 3, compared to treatment with 5-FU alone, no change in 5-FU sensitivity was seen after infection with a high dose of AdCMVCD (100 pfu/cell, IC_{50} 0.22 versus 0.15, $p>0.05$). However, a significant decrease in 5-FU cytotoxicity was apparent after infection with either 10 or 30 pfu/cell of AdCMVCDUPRT (IC_{50} 0.005 versus 0.003, respectively, $p<0.001$). These data suggest that the

enhanced cytotoxicity of CDUPRT/5-FC was due to UPRT mediated conversion of 5-FU to its downstream toxic metabolite 5-FUMP.

AdCMVCD versus AdCMVCDUPRT and 5-FC/XRT therapy in nude mice bearing DU145 xenografts. The efficacy of AdCMVCDUPRT/5-FC/XRT therapy in local tumor control was assessed using a subcutaneous xenograft model of DU145 CaP in nude mice. Tumors were established (63±8 mm^2, range 16-168 mm^2, p=0.97 among groups) and animals randomized to receive a single intratumoral injection of either saline, 10^9 pfu AdCMVCD or AdCMVCDUPRT, followed by either 5-FC alone or 5-FC plus 6 Gy XRT. As shown in Fig. 4A, therapy with AdCMVCDUPRT/5-FC without XRT caused marginal growth delay compared to saline/5-FC over the first 6 weeks of therapy, but no significant difference in TTD was apparent (76 ± 13 vs. 69 ± 9 days, respectively, $p>0.05$). While combined therapy with AdCMVCDUPRT/5-FC/XRT achieved a greater level of tumor growth inhibition (TTD 91 ± 8 days) relative to animals treated with AdCMVCDUPRT/5-FC alone, this difference was not statistically significant ($p>0.05$). Moreover, the treatment effects of neither AdCMVCDUPRT-containing regimen significantly differed from that obtained by saline/5-FC/XRT (TTD 75 ± 12 days, $p>0.05$).

The effect of coexpression of CD and UPRT was assessed by comparing the efficacy of AdCMVCD/5-FC versus AdCMVCDUPRT/5-FC with or without XRT (Fig. 4B). In general, AdCMVCDUPRT-containing regimens achieved an increased level of growth inhibition compared to AdCMVCD-containing regimens. In addition, while concurrent XRT increased the tumor growth inhibition of AdCMVCD/5-FC therapy without XRT (68 ± 13 versus 56 ± 6 days, respectively), neither treatment regimen with this virus enhanced local tumor control relative to

saline/5-FC/XRT ($p>0.05$). One-way ANOVA of experimental endpoint mean ± SEM surface areas confirmed that no differences existed across all 6 treatment groups (data not shown, $p>0.18$). Taken together, these results indicate that, under the conditions examined, infection with neither AdCMVCD nor AdCMVCDUPRT significantly increased local tumor control over that obtained in the absence of viral infection.

DISCUSSION

GDEPT involves the intratumoral transduction of genes encoding foreign enzymes into cancer cells and concurrent systemic prodrug therapy. Expression of these enzymes within transduced cells results in localized metabolism of the nontoxic prodrug and thus accumulation of a high intratumoral concentration of the cytotoxic metabolite. Since production is localized, this system has the capacity to avoid systemic chemotherapy-induced toxicity. Thus, GDEPT represents an alternative drug delivery platform through which well-known chemotherapeutic agents that have been clinically abandoned due to unacceptable therapeutic indices may be re-evaluated.[33]

A number of GDEPT systems have been described, with HSV-TK in combination with the antiherpetic nucleoside analogue GCV and CD/5-FC being the two most actively investigated. Recent studies have suggested that the CD/5-FC system may be the better potential clinical treatment modality.[34-36] In contrast to phosphorylated GCV, which requires intercellular gap junctions to elicit a bystander effect, converted 5-FU freely diffuses from cells expressing CD and thus mediates a gap junction-independent bystander effect.[17, 34, 35] In addition, 5-FU is a potent XRT sensitizer[7, 8, 37, 38] and has been a component of standard-of-care multimodality therapy for several cancers.[39]

Systemic 5-FU, both alone and in combination with other cytotoxic agents, has been evaluated in numerous clinical trials over the last thirty years for localized, locally advanced, and metastatic CaP. Few have reported sufficient therapeutic indicies to warrant its routine clinical use. Given the advantages of GDEPT, we evaluated CD/5-FC-based VDEPT both *in vitro* and in a preclinical animal model for radiosensitization of CaP. We first assessed the transduction efficiency of 3 commonly investigated human CaP cell lines (DU145, LNCaP, PC-3).

Transducibility, as quantitatively determined by monitoring GFP expression from AdCMVGFP,[32] was variable among the 3 cell lines, with DU145>LNCaP>>PC-3 (Fig. 1A and 1B). Ad gene transfer has been shown to depend upon expression of the cell surface receptors necessary for Ad entry, CAR[40, 41] and αv integrins.[42] Lack of expression of CAR or αv integrins on primary tumor cells from different tissues significantly limits Ad gene transfer.[43-45] Ad receptor expression, quantified on CaP cells by indirect immunofluorescence as previously described,[31, 46] was variable (Table 1). The overall level of Ad receptor expression, as defined by the composite $RMFI_{AdR}$, directly correlated with AdCMVGFP transducibility (inversely with MOI_{50}, R^2>0.71). This correlation was largely due to CAR, the individual receptor of the three that most strongly correlated with MOI_{50} (R^2>0.95, Fig. 1C). These results demonstrate the importance of CAR expression levels on Ad gene transfer efficiency and suggest that targeted Ad vectors capable of CAR-independent gene transfer[47] may be utilized in future Ad-based CD vectors to overcome the problem of low CAR expression on CaP cells.

Three reports have previously investigated Ad-mediated CD/5-FC VDEPT of CaP *in vitro* using murine RM-1,[28] human PC-3,[29] and human LNCaP cells.[30] This report is the first to evaluate the cytotoxicity of AdCMVCD/5-FC in multiple human CaP cell lines *in vitro* and to evaluate the potential enhancement produced by its expression in fusion with UPRT. While the magnitude of enhancement varied, data presented in Table 2 demonstrate that both AdCMVCD and AdCMVCDUPRT greatly sensitized all 3 human CaP cell lines to 5-FC. Furthermore, this effect was dependent on viral dose (Fig. 2). These data suggest that CD/5-FC-based VDEPT may be efficacious in heterogeneous tumors composed of cells with distinct genetic, morphologic and phenotypic properties and emphasize the importance of Ad gene transfer efficiency in the level of response.

Competition for 5-FU anabolism within tumors cells by the catabolic enzyme DPD is a key limitation to 5-FU cytotoxicity.[48] Exogenous expression of UPRT has been shown to overcome 5-FU resistance and greatly augment its cytotoxicity, presumably due to its increased conversion to 5-FUMP.[25] Thus, UPRT expression may be utilized to overcome high intratumoral levels of DPD expression or inefficient anabolism of 5-FU to its downstream metabolites. Results presented in Table 2 and Fig. 2 are consistent with this hypothesis. In general, expression of CDUPRT rendered cells significantly (1-2 orders of magnitude) more sensitive to 5-FC than CD alone. Analyzing its effect on 5-FU cytotoxicity validated the effect of UPRT expression on CD/5-FC cytotoxicity. As shown in Fig. 3, AdCMVCDUPRT infection significantly enhanced 5-FU cytotoxicity to PC-3 cells at MOI 10 and 30 ($p<0.001$), while AdCMVCD infection at a higher MOI (100) had no effect ($p>0.05$). These results are consistent with previous reports[25, 26] and suggest that the enhanced efficacy of CDUPRT/5-FC *in vitro* was due to further anabolism of 5-FU produced from CD/5-FC to its downstream metabolite, 5-FUMP. Further work is necessary to determine the impact of DPD expression on 5-FU cytotoxicity in CaP and the potential of CDUPRT coexpression to overcome its effect.

Finally, we present the first report on the efficacy of CD and CDUPRT/5-FC VDEPT in an animal model of CaP. While there was a distinct trend towards slowing tumor growth acutely (<6 weeks), treatment of nude mice bearing subcutaneous DU145 xenografts with intratumoral AdCMVCD or AdCMVCDUPRT and systemic 5-FC with 6 Gy external beam XRT did not significantly delay tumor growth compared to animals receiving saline/5-FC/XRT (TTD 68 ± 13, 91 ± 8 and 75 ± 12 days, respectively, $p>0.05$). These results contrast with our previous work demonstrating a significantly enhanced therapeutic effect of AdCMVCD/5-FC/XRT on human SK-ChA-1 bile duct[7] and WiDr colon[9] tumor xenografts.

Obvious causes of these disappointing results may include tumor-, virus-, drug-, or XRT-related issues. The most straightforward explanation is sampling bias. DU145 cells were the most refractory cells of the 3 tested to both AdCMVCD/5-FC and AdCMVCDUPRT/5-FC *in vitro* (Table 2). These cells were chosen for *in vivo* studies based upon the desire to utilize the most stringent animal model available. Studies are currently ongoing to evaluate whether LNCaP tumors, the most sensitive of the 3 cell lines tested, respond more robustly to CD/5-FC-based VDEPT.

Alternatively, the inherent biology of CaP in general, and DU145 cells specifically, may be responsible. Growth of CaP is largely androgen-related and most tumors grow fairly slowly relative to tumors from other organs.[2] Since its effects are cell-cycle dependent, 5-FU cytotoxicity and radiosensitization are maximal in rapidly proliferating tumors.[39] DU145 cells are known to be androgen-independent, as are most human CaP cell lines, and grow slowly in nude mice.[49] We have previously shown that the group of 3 human prostate cancer cell lines included in the present study (DU145, LNCaP, PC-3) are equally sensitive as human colon tumor cell lines (LS174T, WiDr) to 5-FU-mediated cytotoxicity *in vitro*.[34] However, Smalley et al. found that 5-FU-mediated radiosensitization of DU145 cells was significantly less than with HT-29 human colon cancer cells.[50] The human colon carcinoma cell line WiDr was derived from HT-29,[51] grows rapidly as subcutaneous xenografts in nude mice, is equally sensitive as DU145 cells to 5-FU *in vitro*, and responds well to AdCMVCD/5-FC-mediated radiosensitization both *in vitro* and *in vivo*.[9] Thus, DU145 tumors may be inherently less sensitive to 5-FU-mediated radiosensitization than human colon xenografts based solely upon their relatively slow growth *in vivo*. Preliminary results demonstrating that clonogenic survival of DU145 cells after infection with AdCMVCDUPRT at 30 pfu/cell and treatment with 5-50 μg/ml 5-FC and 8 Gy XRT is

decreased over two orders of magnitude compared to 5-FC/XRT alone and one order of magnitude greater than that achieved by AdCMVCD/5-FC/XRT would support this hypothesis (data not shown). Work comparing the radiosensitizing effect of AdCMVCD and AdCMVCDUPRT/5-FC on DU145 with other human CaP and colon cancer cells both *in vitro* and *in vivo* is currently underway.

Secondly, the above studies were conducted with a single intratumoral injection of AdCMVCD and AdCMVCDUPRT. It is well established that intratumoral Ad gene transfer is limited to the area around the needle track in subcutaneous animal models of cancer, presumably due to poor diffusion secondary to the high interstitial pressure within the tumor.[52] Therefore, to maximize intratumoral transgene expression and thus efficacy, further optimization of the intratumoral Ad dosing regimen is necessary. We are currently evaluating a strategy previously shown to be efficacious in animal models of cholangio- and colon carcinomas, whereby 3 doses of intratumoral AdCMVCD were given at days –2, 0, and 2 relative to XRT.[7, 9] An alternative approach we are also pursuing involves construction of a conditionally replicative Ad encoding CDUPRT, since it has been previously shown that replicative Ad vectors are capable of lateral infection throughout the tumor mass.[53]

Thirdly, inefficient intratumoral 5-FU metabolism may be responsible for the lack of CD and CDUPRT/5-FC radiosensitization *in vivo*. Three anabolic pathways have been described for 5-FU metabolism. In GI tumors, 5-FU-mediated cytotoxicity and radiosensitization occurs predominantly through its conversion into 5-fluorodeoxyuridine-monophosphate (5-FdUMP).[50] In combination with reduced intracellular folates or analogs such as leucovorin, 5-FdUMP forms a ternary complex with and reversibly inhibits thymidylate synthase (TS), a key enzyme in DNA synthesis. This effect can be reversed with exogenous thymidine, providing a method by which

TS-directed 5-FU effects may be investigated. Thus, in colon cancer cells, 5-FU-mediated radiosensitization occurs predominantly via DNA-directed effects.[54] Finally, downstream 5-FU metabolites may also be incorporated into RNA, where they inhibit RNA processing and translation. Little is known about the relative importance of these three mechanisms of cytotoxicity in CaP cells. Further studies involving biochemical modulation with leucovorin and thymidine rescue of CD and CDUPRT/5-FC-mediated cytotoxicity and radiosensitization in CaP cells will help delineate between these mechanisms and guide future optimization efforts.

Lastly, the timing of external beam XRT relative to 5-FU administration is known to affect 5-FU radiosensitization.[55] Recent data have indicated that progression of cells into S phase after 5-FU-induced alterations in intracellular deoxynucleotide triphosphate pools, primarily the dATP:dTTP ratio, is essential to 5-FU-mediated radiosensitization.[56] These results suggest that therapeutic levels of intratumoral 5-FU prior to XRT exposure is necessary to achieve maximal radiosensitization. The treatment regimen described in this report consisted of 7 days of systemic 5-FC (500 mg/kg b.i.d. delivered i.p.) on days 2-9 post-infection, with single-dose XRT on day 2 post-infection. Since only a single i.p. dose of 5-FC was administered prior to XRT, sufficient intratumoral 5-FU levels were unlikely to be achieved with this regimen. Studies combining multiple intratumoral vector injections and fractionated XRT after sufficient systemic 5-FC preloading are currently underway to optimize any CD or CDUPRT/5-FC-mediated radiosensitizing effects *in vivo*. Based upon the encouraging *in vitro* results and the number of readily identifiable tumor-, virus-, drug-, and XRT-related areas for future treatment optimization *in vivo*, we conclude that CD and CDUPRT/5-FC VDEPT still holds promise for CaP radiosensitization.

MATERIALS AND METHODS

Tumor cells, viruses and mAbs. Human prostate (DU145, LNCaP, PC-3) carcinoma cell lines (American Type Culture Collection, Manassas, VA) were maintained in RPMI (Mediatech, Herndon, VA) containing 10% FBS (Summit Biotechnology, Ft. Collins, CO) and 2 mM glutamine. Cells were cultured at 37°C in a 5% CO_2 atmosphere without antibiotics and passaged less than 12 times during the course of these experiments.

AdCMVGFP, a first-generation E1-, E3-deleted vector expressing green fluorescent protein (GFP) from the cytomegalovirus (CMV) immediate-early promoter, was obtained from Corey Goldman (Cleveland Clinic, Cleveland, OH). The construction and characterization of AdCMVCD has been previously described.[7] To construct an identical virus encoding CDUPRT, cDNA encoding a fusion protein between CD and UPRT[25] was PCR amplified from pGT65 (Invivogen, San Diego, CA) using the following primers: upstream primer 5'-GCAGAATTCGCCATC**ATG**GTG-TCGAATAAC-3' containing an EcoRI site (underlined) and an ATG start codon (bold); and downstream primer 5'-GCAGGATCCCGACAAGCTTA**TTT**CGTACCA-3' containing a BamHI site (underlined) and the original CDUPRT stop codon (bold). The PCR fragment was digested with EcoRI/BamHI and subcloned into EcoRI/BamHI-digested pAcCMVCD[7] to generate pAcCDUPRT. Recombinant virus (AdCMVCDUPRT) was obtained by homologous recombination in 293 cells using pJM17 rescue vector as previously described for the construction of AdCMVCD.[7] DNA sequencing using an ABI Prism 377 sequencer (Applied Biosystems, Foster City, CA) at the University of Alabama at Birmingham Center for AIDS Research DNA Sequencing Core Facility and comparison to GenBank sequence L37432 confirmed the integrity of the CDUPRT insert. Viruses were propagated and plaque titered on permissive 293 cells and purified twice by

centrifugation on CsCl gradients. All virus aliquots were maintained at -80°C until use. A single batch of each individual virus was used for all studies reported. Anti-CAR RmcB mAb was purified from ascites produced from RmcB hybridoma cells (ATCC). Murine mAbs LM609 to αvβ3 integrin and P1F6 to αvβ5 integrin were purchased from Chemicon (Temecula, CA).

Indirect immunofluorescence. Receptor expression was analyzed by indirect immunofluorescence as previously described.[31] Briefly, subconfluent cells were harvested with versene and resuspended at 1-2 x 10^6 cells/ml in phosphate buffered saline (PBS) containing 0.1% BSA and 0.1% sodium azide. Cells were then incubated for 1 hour at 4°C with primary mAbs at a final concentration of 5 μg/ml. After washing with buffer, cells were stained for 30 min at 4°C with Alexa 488-conjugated goat-anti-mouse IgG secondary antibody (Molecular Probes, Eugene, OR) also at 5 μg/ml. Cells (10^4 per sample) were then analyzed on a Becton-Dickinson FACSVantage at the UAB Rheumatology FACS Core Facility. Percent positive cells was calculated by setting at 1% the cells incubated in the absence of primary mAb (mock) as positive. $RMFI_{Receptor}$ (relative mean fluorescence intensity of a given receptor) was calculated as the ratio of the MFI of the sample of interest ($RMFI_{CAR}$, $RMFI_{\alpha v\beta 3}$, and $RMFI_{\alpha v\beta 5}$ for CAR, αvβ3 and αvβ5, respectively) to the MFI for the corresponding mock (no primary antibody) sample of each individual cell line. Composite Ad receptor expression ($RMFI_{AdR}$) was calculated as the product of the 3 $RMFI_{Receptor}$ values.

Quantitation of Ad transducibility. Ad gene transfer efficiency was quantitated by monitoring expression of GFP in AdCMVGFP-infected cells as previously described.[46] Cells ($0.5\text{-}1x10^6$) were plated in 6-well plates (Corning, Corning, NY), allowed to adhere overnight,

and subsequently infected with AdCMVGFP at various multiplicities of infection (MOI, 0-500 plaque forming units (pfu) per cell) in 0.6 ml of OptiMEM (Invitrogen, Carlsbad, CA) for 1 hour at 37°C with continuous rocking. Twenty-four hours post-infection, cells were harvested with 0.25% trypsin/EDTA (Mediatech), washed with buffer (PBS, 0.1% sodium azide, 0.1% BSA) and resuspended at 1-2x10^6 cells/ml. Cells (10^4 per sample) were analyzed by flow cytometry as described above. MOI_{50} values, defined as the AdCMVGFP MOI required to produce detectable GFP in 50 percent of cells, were determined for each cell line by fitting the data plotted as the logarithm of AdCMVGFP MOI versus percent GFP-positive cells to the sigmoidal dose-response function with variable slope (Hill equation) using GraphPad Prism 3.01 (GraphPad Software, San Diego, CA). MOI_{50} were then compared by one-way ANOVA. To assess the AdCMVGFP dose-response, the $RMFI_{GFP}$ was calculated as the ratio of the MFI at each individual MOI versus the MFI of uninfected cells. Linear regression analysis was then performed on logarithmically converted MOI and $RMFI_{GFP}$ values using Prism 3.01. Correlations of MOI_{50} with Ad receptor expression ($RMFI_{Receptor}$) was determined by linear regression analysis on logarithmically converted data.

5-FC and 5-FU cytotoxicity. Confluent cell monolayers were harvested with 0.25% trypsin/EDTA, plated (5,000 cells in 100 µl/well) in 96-well tissue culture plates, and allowed to adhere overnight at 37°C. Ten serial half-log dilutions of 5-FC or 5-FU (six replicates per dilution) were made and 100 µl of drug-containing media was added directly to cells to achieve final concentrations of 0-200 µg/ml. Cells were incubated at 37°C for 5 days and cellular metabolism determined by tetrazolium reduction assay using 3-(4,5-dimethylthiazol-2-yl)-5-(3-carboxymethoxyphenyl)-2-(4-sulfophenyl)-2H-tetrazolium (MTS, Promega, Madison, WI) as

per the manufacturer's protocol. Fractional cell survival at each drug concentration was calculated as the ratio of absorbance at 490 nm of cells incubated in the presence versus absence of drug, corrected for background absorbance of media alone. Fractional cell survival data from n separate experiments for each cell line was plotted against the logarithm of drug concentration and the data fit by nonlinear regression to a sigmoidal dose-response function with variable slope using Prism 3.01. LOG IC_{50} values, defined as the logarithm of the drug concentration producing 50% reduction in corrected absorbance, were then determined. To ensure quality control, a correlation coefficient of $R^2 \geq 0.85$ was necessary for each cell line in each separate experiment. Verified data consisting of n times 30 drug concentration-fractional cell survival (x,y) datapoints were then pooled for each cell line, the data fit to the sigmoidal dose-response function as described above, and the mean ± SEM LOG IC_{50} determined. Mean LOG IC_{50} values for each cell line were then compared by one-factor ANOVA with Tukey's multiple pairwise comparison post-test using Prism 3.01.

For AdCMVCD or AdCMVCDUPRT drug cytotoxicity experiments, cells were harvested from confluent monolayers and plated at 1.5-3x10^6 cells/well in T25 flasks (Corning) overnight at 37°C. Cells were infected with varying amounts of virus (0-300 pfu/cell) in 2 ml of OptiMEM (Invitrogen) for 1 hour at 37°C with continuous rocking. Twenty-four hours post-infection, cells were harvested with 0.25% trypsin/EDTA, plated into 96-well tissue culture plates at 5,000 cells/well in 100 µl complete media, and allowed to adhere overnight at 37°C. One hundred µl of media supplemented with serial dilutions of drug (5-FC or 5-FU) was added and drug cytotoxicity (IC_{50}) determined at 5 days as described above.

Subcutaneous DU145 xenograft animal studies. Therapy studies were conducted as previously described.[7] Briefly, DU145 human CaP xenograft tumors were established subcutaneously in the right flanks of nu/nu mice (NCI Frederick, Frederick, MD) by injecting $5x10^6$ cells in 50 µl of sterile RPMI medium and allowing growth for approximately 14 days. Mice were then randomized to 6 treatment arms consisting of intratumoral injection of 10^9 pfu AdCMVCD or AdCMVCDUPRT in 50 µl sterile saline on day 0, systemic therapy with intraperitoneal 5-FC at 400 mg/kg bid for 7 days (days 2-9 post-infection), and either XRT or not with 6 Gy from a ^{60}Co source on day 2 post-infection. Tumor growth was then monitored 3 times per week until the mice died or the tumor caused ulceration of the overlying skin. Tumor surface area was calculated (length x width) and data plotted as the percent increase in tumor surface area versus time. Mean ± SEM initial (before treatment), time-to-tumor doubling (TTD), and endpoint surface areas were then determined and analyzed by one-way ANOVA across treatment groups using GraphPad Prism v3.01.

ACKNOWLEDGEMENTS

The authors thank Sheila Bright, Scott Chiz, Debbie Della Manna, Charlotte Hammond, Synethia Kidd, and Barbara Krum for technical assistance and Yancey Gillespie, William Grizzle, and Martin Johnson for fruitful discussions and critical reading of the manuscript. This work was supported by an award from the Pediatric Brain Tumor Foundation of the United States (C.R.M.) and NIH Grant CA73636 (D.J.B.).

REFERENCES

1. Greenlee RT, Hill-Harmon MB, Murray T, Thun M. Cancer statistics, 2001. CA Cancer J Clin 2001;**51**:15-36.

2. Kirby R. Treatment options for early prostate cancer. Urology 1998;**52**:948-962.

3. Wallace PM, MacMaster JF, Smith VF, Kerr DE, et al. Intratumoral generation of 5-fluorouracil mediated by an antibody-cytosine deaminase conjugate in combination with 5-fluorocytosine. Cancer Res 1994;**54**:2719-2723.

4. Kuriyama S, Masui K, Sakamoto T, Nakatani T, et al. Bystander effect caused by cytosine deaminase gene and 5-fluorocytosine in vitro is substantially mediated by generated 5-fluorouracil. Anticancer Res 1998;**18**:3399-3406.

5. Springer CJ, Niculescu-Duvaz I. Prodrug-activating systems in suicide gene therapy. J Clin Invest 2000;**105**:1161-1167.

6. Vermes A, Guchelaar HJ, Dankert J. Flucytosine: a review of its pharmacology, clinical indications, pharmacokinetics, toxicity and drug interactions. J Antimicrob Chemother 2000;**46**:171-179.

7. Pederson LC, Buchsbaum DJ, Vickers SM, Kancharla SR, et al. Molecular chemotherapy combined with radiation therapy enhances killing of cholangiocarcinoma cells in vitro and in vivo. Cancer Res 1997;**57**:4325-4332.

8. Pederson LC, Vickers SM, Buchsbaum DJ, Kancharla SR, et al. Combined cytosine deaminase expression, 5-fluorocytosine exposure, and radiotherapy increases cytotoxicity to cholangiocarcinoma cells. J Gastrointest Surg 1998;**2**:283-291.

9. Stackhouse MA, Pederson LC, Grizzle WE, Curiel DT, et al. Fractionated radiation therapy in combination with adenoviral delivery of the cytosine deaminase gene and 5-fluorocytosine enhances cytotoxic and antitumor effects in human colorectal and cholangiocarcinoma models. Gene Ther 2000;7:1019-1026.

10. Miller CR, Buchsbaum DJ, Williams CW, Kiss P, et al. Cytosine deaminase/5-fluorocytosine therapy for gastrointestinal (GI) and non-GI malignancies. Proc Am Assoc Cancer Res 2001;**42**:28.

11. Tepper JE. Combined radiotherapy and chemotherapy in the treatment of gastrointestinal malignancies. Semin Oncol 1992;**19**:96-101.

12. Lowy AM, Leach SD. Adjuvant/neoadjuvant chemoradiation for gastric and pancreatic cancer. Oncology (Huntingt) 1999;**13**:121-130.

13. Rich TA. Infusional chemoradiation for rectal and anal cancers. Oncology (Huntingt) 1999;**13**:131-134.

14. Grem JL. 5-Fluorouracil: forty-plus and still ticking. A review of its preclinical and clinical development. Invest New Drugs 2000;**18**:299-313.

15. Elshami AA, Saavedra A, Zhang H, Kucharczuk JC, et al. Gap junctions play a role in the 'bystander effect' of the herpes simplex virus thymidine kinase/ganciclovir system in vitro. Gene Ther 1996;**3**:85-92.

16. Dilber MS, Abedi MR, Christensson B, Bjorkstrand B, et al. Gap junctions promote the bystander effect of herpes simplex virus thymidine kinase in vivo. Cancer Res 1997;**57**:1523-1528.

17. Lawrence TS, Rehemtulla A, Ng EY, Wilson M, et al. Preferential cytotoxicity of cells transduced with cytosine deaminase compared to bystander cells after treatment with 5-flucytosine. Cancer Res 1998;**58**:2588-2593.

18. Touraine RL, Ishii-Morita H, Ramsey WJ, Blaese RM. The bystander effect in the HSVtk/ganciclovir system and its relationship to gap junctional communication. Gene Ther 1998;**5**:1705-1711.

19. Hossain MZ, Jagdale AB, Ao P, LeCiel C, et al. Impaired expression and posttranslational processing of connexin43 and downregulation of gap junctional communication in neoplastic human prostate cells. Prostate 1999;**38**:55-59.

20. Diasio RB. The role of dihydropyrimidine dehydrogenase (DPD) modulation in 5-FU pharmacology. Oncology (Huntingt) 1998;**12**:23-27.

21. Diasio RB. Clinical implications of dihydropyrimidine dehydrogenase inhibition. Oncology (Huntingt) 1999;**13**:17-21.

22. Diasio RB. Dihydropyrimidine dehydrogenase and resistance to 5-fluorouracil. Prog Exp Tumor Res 1999;**36**:115-123.

23. Milano G, McLeod HL. Can dihydropyrimidine dehydrogenase impact 5-fluorouracil-based treatment? Eur J Cancer 2000;**36**:37-42.

24. Inaba M, Sawada H, Sadata A, Hamada H. Circumvention of 5-fluorouracil resistance in human stomach cancer cells by uracil phosphoribosyltransferase gene transduction. Jpn J Cancer Res 1999;**90**:349-354.

25. Tiraby M, Cazaux C, Baron M, Drocourt D, et al. Concomitant expression of E. coli cytosine deaminase and uracil phosphoribosyltransferase improves the cytotoxicity of 5-fluorocytosine. FEMS Microbiol Lett 1998;**167**:41-49.

26. Erbs P, Regulier E, Kintz J, Leroy P, et al. In vivo cancer gene therapy by adenovirus-mediated transfer of a bifunctional yeast cytosine deaminase/uracil phosphoribosyltransferase fusion gene. Cancer Res 2000;**60**:3813-3822.

27. Shalev M, Thompson TC, Kadmon D, Ayala G, et al. Gene therapy for prostate cancer. Urology 2001;**57**:8-16.

28. Anello R, Cohen S, Atkinson G, Hall SJ. Adenovirus mediated cytosine deaminase gene transduction and 5-fluorocytosine therapy sensitizes mouse prostate cancer cells to irradiation. J Urol 2000;**164**:2173-2177.

29. Blackburn RV, Galoforo SS, Corry PM, Lee YJ. Adenoviral transduction of a cytosine deaminase/thymidine kinase fusion gene into prostate carcinoma cells enhances prodrug and radiation sensitivity. Int J Cancer 1999;**82**:293-297.

30. Yoshimura I, Suzuki S, Tadakuma T, Hayakawa M. Suicide gene therapy on LNCaP human prostate cancer cells. Int J Urol 2001;**8**:S5-8.

31. Miller CR, Buchsbaum DJ, Reynolds PN, Douglas JT, et al. Differential susceptibility of primary and established human glioma cells to adenovirus infection: targeting via the epidermal growth factor receptor achieves fiber receptor-independent gene transfer. Cancer Res 1998;**58**:5738-5748.

32. Williams CW, Miller CR, Buchsbaum DJ. Uracil phosphoribosyltransferase potentiates 5-fluorouracil and cytosine deaminase/5-fluorocytosine cytotoxicity in prostate cancer. Proc Am Assoc Cancer Res 2001;**42**:455.

33. Miller CR, Williams CW, Buchsbaum DJ, Gillespie GY. Intratumoral 5-fluorouracil produced by cytosine deaminase/5-fluorocytosine gene therapy is effective for experimental human glioblastomas. Cancer Res 2002;**62**:773-780.

34. Denning C, Pitts JD. Bystander effects of different enzyme-prodrug systems for cancer gene therapy depend on different pathways for intercellular transfer of toxic metabolites, a factor that will govern clinical choice of appropriate regimes. Hum Gene Ther 1997;**8**:1825-1835.

35. Paillard F. Bystander effects in enzyme/prodrug gene therapy. Hum Gene Ther 1997;**8**:1733-1735.

36. Shirakawa T, Gardner TA, Ko SC, Bander N, et al. Cytotoxicity of adenoviral-mediated cytosine deaminase plus 5- fluorocytosine gene therapy is superior to thymidine kinase plus acyclovir in a human renal cell carcinoma model. J Urol 1999;**162**:949-954.

37. Khil MS, Kim JH, Mullen CA, Kim SH, et al. Radiosensitization by 5-fluorocytosine of human colorectal carcinoma cells in culture transduced with cytosine deaminase gene. Clin Cancer Res 1996;**2**:53-57.

38. Gabel M, Kim JH, Kolozsvary A, Khil M, et al. Selective in vivo radiosensitization by 5-fluorocytosine of human colorectal carcinoma cells transduced with the E. coli cytosine deaminase (CD) gene. Int J Radiat Oncol Biol Phys 1998;**41**:883-887.

39. Schmoll HJ, Buchele T, Grothey A, Dempke W. Where do we stand with 5-fluorouracil? Semin Oncol 1999;**26**:589-605.

40. Bergelson JM, Cunningham JA, Droguett G, Kurt-Jones EA, et al. Isolation of a common receptor for Coxsackie B viruses and adenoviruses 2 and 5. Science 1997;**275**:1320-1323.

41. Tomko RP, Xu R, Philipson L. HCAR and MCAR: the human and mouse cellular receptors for subgroup C adenoviruses and group B coxsackieviruses. Proc Natl Acad Sci U S A 1997;**94**:3352-3356.

42. Wickham TJ, Mathias P, Cheresh DA, Nemerow GR. Integrins alpha v beta 3 and alpha v beta 5 promote adenovirus internalization but not virus attachment. Cell 1993;**73**:309-319.

43. Bergelson JM. Receptors mediating adenovirus attachment and internalization. Biochem Pharmacol 1999;**57**:975-979.

44. Nemerow GR, Stewart PL. Role of alpha(v) integrins in adenovirus cell entry and gene delivery. Microbiol Mol Biol Rev 1999;**63**:725-734.

45. Nemerow GR. Cell receptors involved in adenovirus entry. Virology 2000;**274**:1-4.

46. Miller CR, Kelly FJ, Williams CW, Curiel DT, et al. A quantitative method for determining adenovirus gene transfer efficiency with established and primary human tumor cell cultures. Mol Ther 2001;**3**:S165.

47. Krasnykh VN, Douglas JT, van Beusechem VW. Genetic targeting of adenoviral vectors. Mol Ther 2000;**1**:391-405.

48. Beck A, Etienne MC, Cheradame S, Fischel JL, et al. A role for dihydropyrimidine dehydrogenase and thymidylate synthase in tumour sensitivity to fluorouracil. Eur J Cancer 1994;**10**:1517-1522.

49. Navone NM, Logothetis CJ, von Eschenbach AC, Troncoso P. Model systems of prostate cancer: uses and limitations. Cancer Metastasis Rev 1998;**17**:361-371.

50. Smalley SR, Kimler BF, Evans RG. 5-Fluorouracil modulation of radiosensitivity in cultured human carcinoma cells. Int J Radiat Oncol Biol Phys 1991;**20**:207-211.

51. Chen TR, Drabkowski D, Hay RJ, Macy M, et al. WiDr is a derivative of another colon adenocarcinoma cell line, HT-29. Cancer Genet Cytogenet 1987;**27**:125-134.

52. Stohrer M, Boucher Y, Stangassinger M, Jain RK. Oncotic pressure in solid tumors is elevated. Cancer Res 2000;**60**:4251-4255.

53. Heise C, Kirn DH. Replication-selective adenoviruses as oncolytic agents. J Clin Invest 2000;**105**:847-851.

54. Lawrence TS, Davis MA, Maybaum J. Dependence of 5-fluorouracil-mediated radiosensitization on DNA- directed effects. Int J Radiat Oncol Biol Phys 1994;**29**:519-523.

55. Pu AT, Robertson JM, Lawrence TS. Current status of radiation sensitization by fluoropyrimidines. Oncology (Huntingt) 1995;**9**:707-714; discussion 714, 717-708, 721.

56. Hwang HS, Davis TW, Houghton JA, Kinsella TJ. Radiosensitivity of thymidylate synthase-deficient human tumor cells is affected by progression through the G1 restriction point into S-phase: implications for fluoropyrimidine radiosensitization. Cancer Res 2000;**60**:92-100.

Table 1 *CAR and αv integrin expression on human prostate cancer cells*

Cell Line	CAR		αvβ3		αvβ5	
	%	RMFI	%	RMFI	%	RMFI
DU145	97.9	13.7	64.6	3.4	72.2	3.4
LNCaP	75.4	6.7	5.3	1.7	67.7	4.7
PC-3	44.0	3.3	24.4	2.4	66.6	5.3

Receptor expression determined by indirect immunofluorescence as described in Materials and Methods. Data from 1-2 separate experiments presented as the percent of cells gated positive (%) and the relative mean fluorescence intensity (RMFI) of cells incubated in the presence versus the absence of primary anti-receptor antibody.

Table 2 *AdCMVCD versus AdCMVCDUPRT mediated 5-FC cytotoxicity to human prostate cancer cells in vitro*

Cell Line	MOI (pfu/cell)	5-FC IC_{50} (μg/ml)		Enhancement
		AdCMVCD	AdCMVCDUPRT	
DU145	10	>200	20.3 ± 1.6 (3)	>10
	100	24.8 ± 0.6 (3)	0.7 ± 0.7 (4)	34
	300	15.4 ± 15.4 (2)	0.3 ± 0.01 (2)	56
LNCaP	1	15.8 (1)	ND	
	10	3.9 ± 0.7 (3)	0.03 ± 0.01 (4)	125
	100	1.0 ± 0.4 (3)	0.01 ± 0.001 (4)	108
PC-3	1	>200	34.4 (1)	>6
	10	26.6 ± 0.02 (2)	1.6 ± 0.7 (3)	17
	100	5.7 ± 1.9 (4)	0.2 ± 0.2 (3)	24
	300	4.6 ± 1.5 (2)	0.1 (1)	46

Mean ± SEM 5-FC IC_{50} determined by piecewise linear regression from log-linear dose-response curves (6 replicates at 10 separate drug concentrations) from 1-4 separate experiments. ND, not determined.

Table 3 *5-FU cytotoxicity to human prostate cancer cells in vitro*

Cell Line	5-FU IC_{50} (μg/ml)
DU145	0.39 ± 0.17
LNCaP	0.18 ± 0.04
PC-3	0.17 ± 0.07

Mean ± SEM 5-FU IC_{50} determined by piecewise linear regression from log-linear dose-response curves (6 replicates at 10 separate drug concentrations) from 3 separate experiments. Differences in means not statistically significant at 0.05.

TITLES AND LEGENDS TO FIGURES

Fig. 1. AdCMVGFP gene transfer to human CaP cells *in vitro*. Cells were infected with various MOI of AdCMVGFP and GFP expression determined 24 hours post-infection. Data presented as (A) percent transduction and (B) relative mean fluorescence intensity (RMFI) compared to uninfected control cells. MOI_{50} values compared by one factor ANOVA. The relationships between MOI_{50} and Ad receptor expression determined by linear regression analysis on log-log converted MOI_{50} and $RMFI_{Receptor(s)}$ values (C). AdCMVGFP MOI_{50} correlated strongly with $RMFI_{CAR}$, $RMFI_{\alpha v\beta 5}$, and the composite $RMFI_{AdR,}$ but not with $RMFI_{\alpha v\beta 3}$.

Fig. 2. Dose-response of 5-FC cytotoxicity to PC-3 cells upon infection with AdCMVCD (open circles) or AdCMVCDUPRT (closed circles) *in vitro*. Cells were infected for 1 hour at various MOI (1-300 pfu/cell). Twenty-four hours post infection, cells were treated with varying concentrations of 5-FC and cytotoxicity (IC_{50}, μg/ml) determined at day 5. Data plotted as log Ad MOI vs. log 5-FC IC_{50} and linear regression analysis performed. A significant linear relationship ($p=0.01$) existed for both AdCMVCD/5-FC and AdCMVCDUPRT/5-FC.

Fig. 3. 5-FU cytotoxicity to PC-3 cells after infection with AdCMVCD or AdCMVCDUPRT *in vitro*. Cells were infected for 1 h, treated with varying concentrations of 5-FU 24 hours post-infection, and cytotoxicity (IC_{50}, μg/ml) determined 5 days later. AdCMVCD infection at MOI 100 did not significantly affect 5-FU cytotoxicity relative to uninfected cells (IC_{50} 0.22 vs. 0.15 μg/ml, respectively, $p>0.05$). AdCMVCDUPRT infection significantly enhanced 5-FU cytotoxicity 50- and 75-fold at MOI 10 and 30, respectively (IC_{50} 0.005 and 0.003 μg/ml, respectively, $p<0.001$).

Fig. 4. AdCMVCD vs. AdCMVCDUPRT plus systemic 5-FC and XRT therapy of subcutaneous human DU145 prostate xenografts in nu/nu mice. Flank tumors were established (63±8 mm^2, range 20-168 mm^2, p=0.97 among groups) and treated with a single injection of no virus (saline), 10^9 pfu AdCMVCD or 10^9 pfu AdCMVCDUPRT. Animals in the XRT groups received 6 Gy 2 days post-infection. Either saline or 400 mg/kg 5-FC was given bid for 7 days beginning at 2 days post-infection. Data presented as the mean percent change in initial tumor area (n = 5 per group). A representative of 2 separate experiments is shown comparing saline vs. AdCMVCDUPRT regimens (A) and AdCMVCDUPRT vs. AdCMVCD regimens (B).

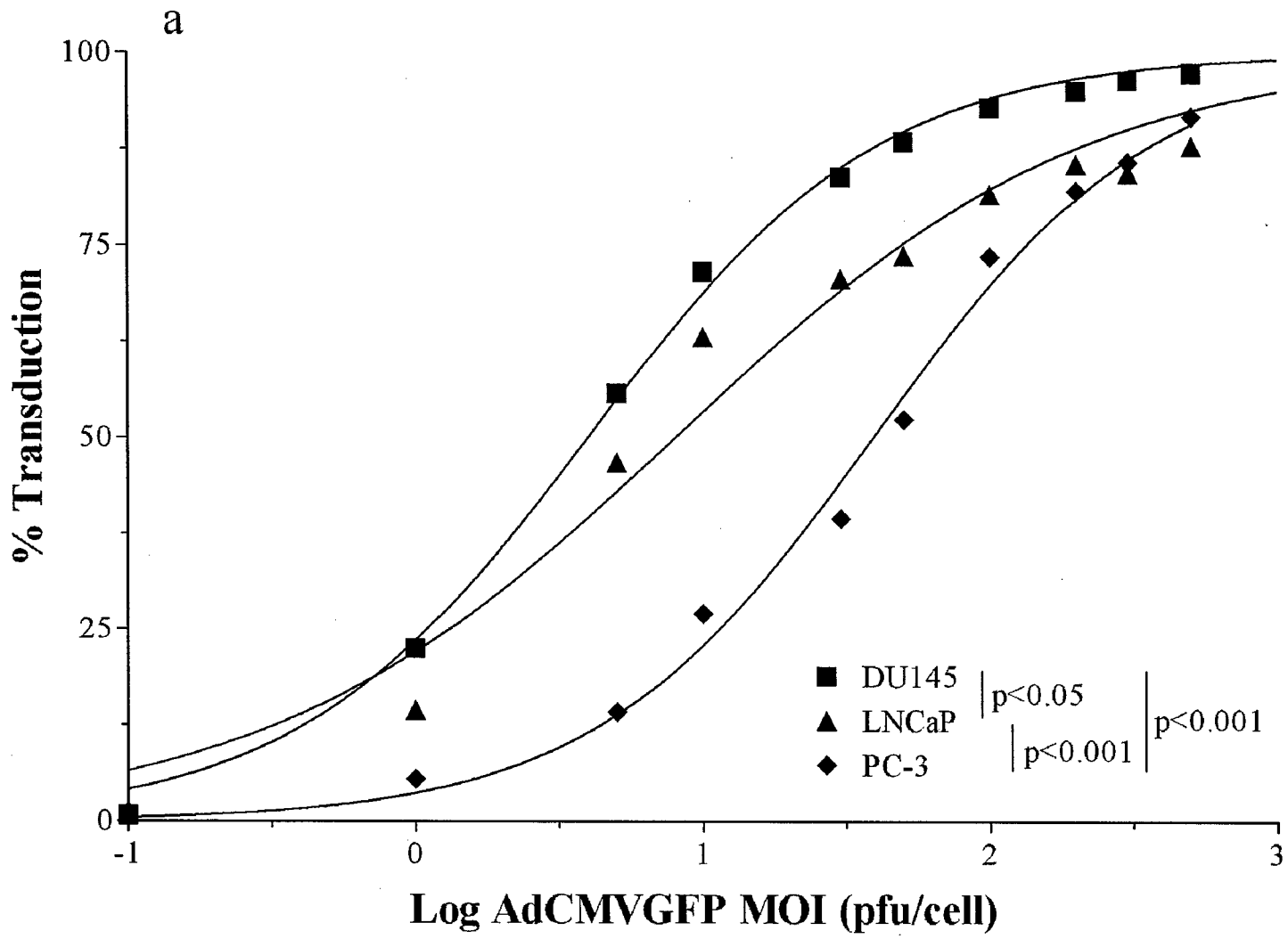
a
100
75
50
25
0
% Transduction
-1
0
1
2
3
Log AdCMVGFP MOI (pfu/cell)
DU145
LNCaP
PC-3
p<0.05
p<0.001
p<0.001

b

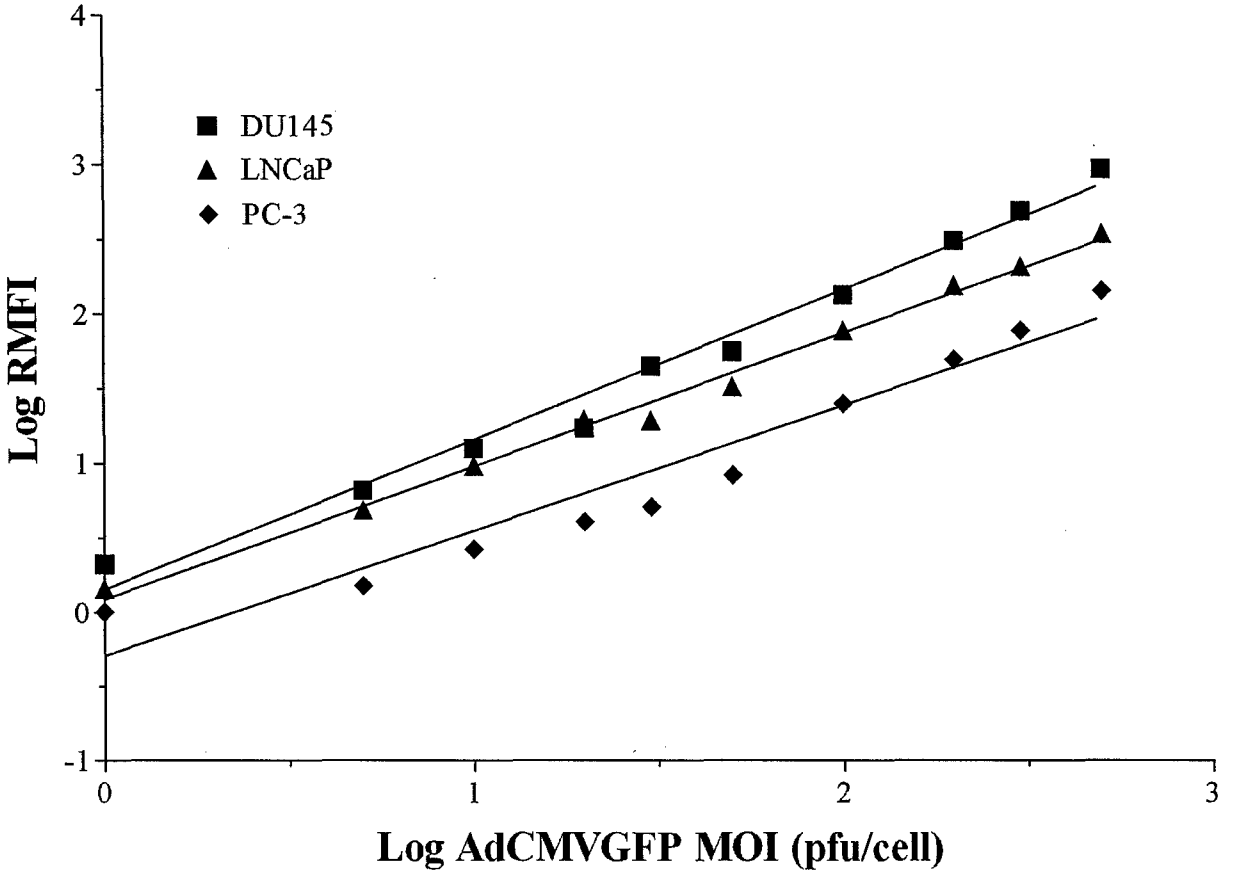
DU145
LNCaP
PC-3
Log RMFI
4
3
2
1
0
-1
0
1
2
3
Log AdCMVGFP MOI (pfu/cell)

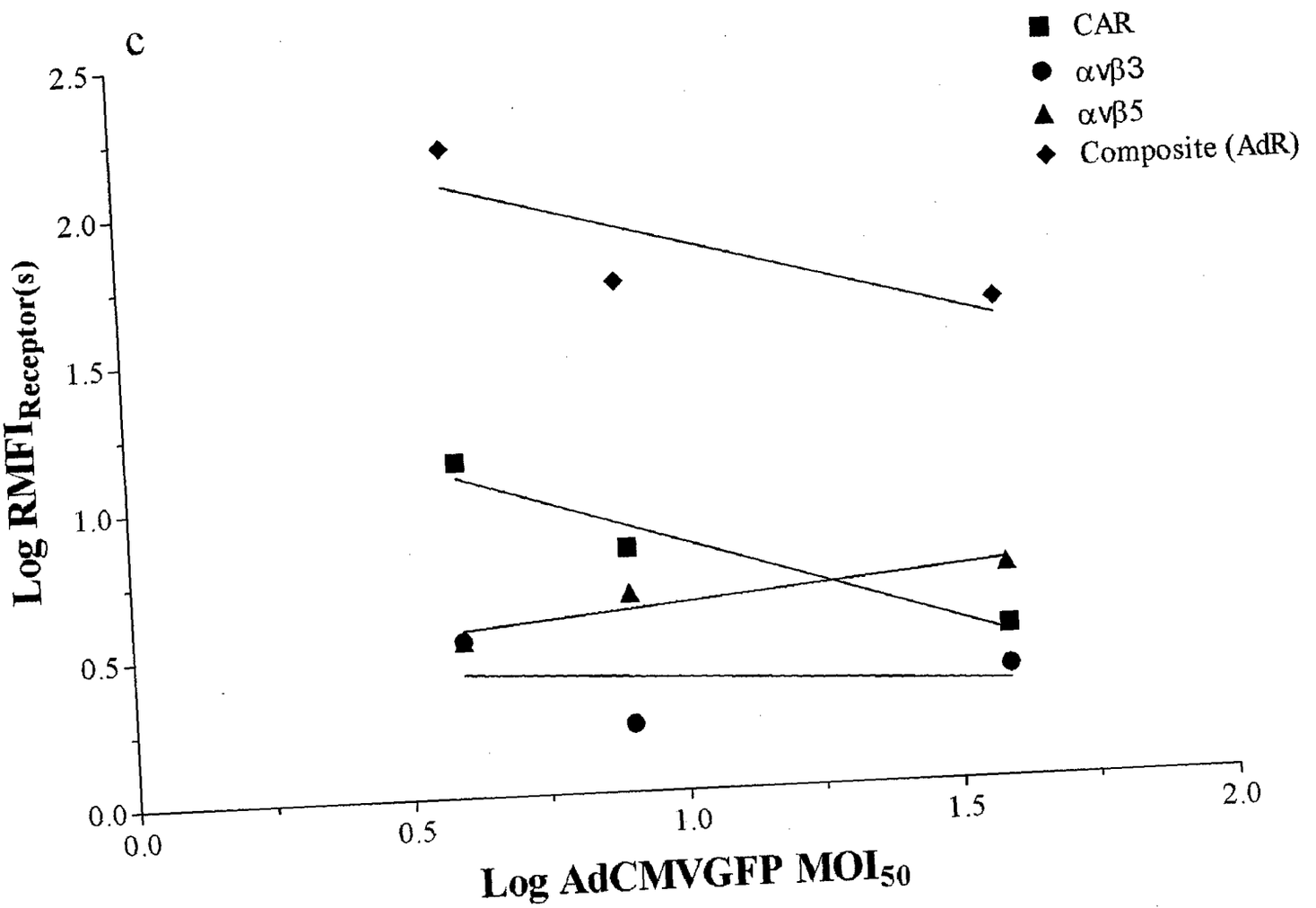
C
CAR
αvβ3
αvβ5
Composite (AdR)
Log RMFI Receptor(s)
Log AdCMVGFP MOI50
2.5
2.0
1.5
1.0
0.5
0.0
0.0
0.5
1.0
1.5
2.0

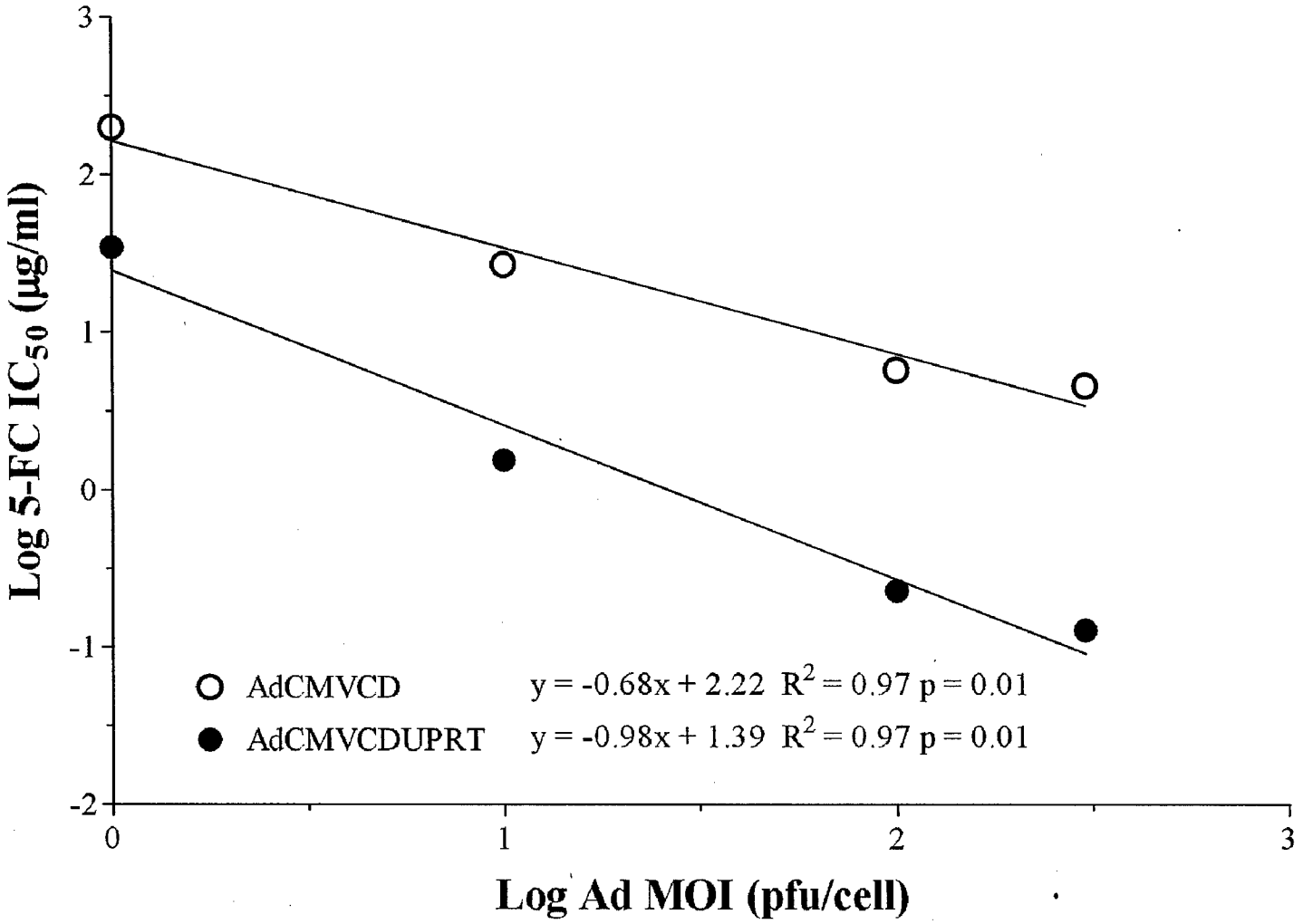
Log 5-FC IC50 (µg/ml)
3
2
1
0
-1
-2
0
1
2
3
Log Ad MOI (pfu/cell)
AdCMVCD
y = -0.68x + 2.22 R2 = 0.97 p = 0.01
AdCMVCDUPRT
y = -0.98x + 1.39 R2 = 0.97 p = 0.01

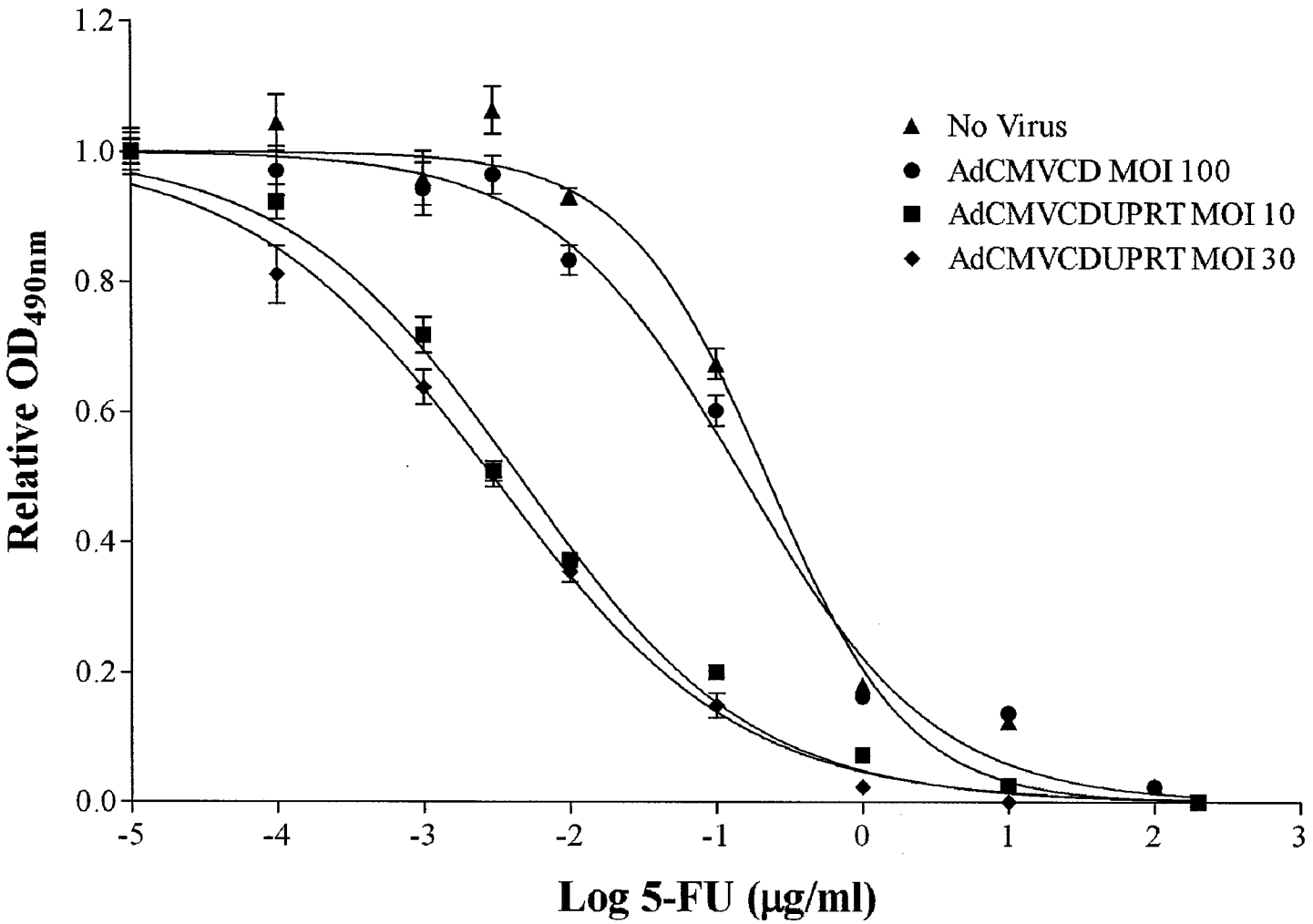
1.2
1.0
0.8
0.6
0.4
0.2
0.0
Relative OD490nm
-5
-4
-3
-2
-1
0
1
2
3
Log 5-FU (µg/ml)
No Virus
AdCMVCD MOI 100
AdCMVCDUPRT MOI 10
AdCMVCDUPRT MOI 30

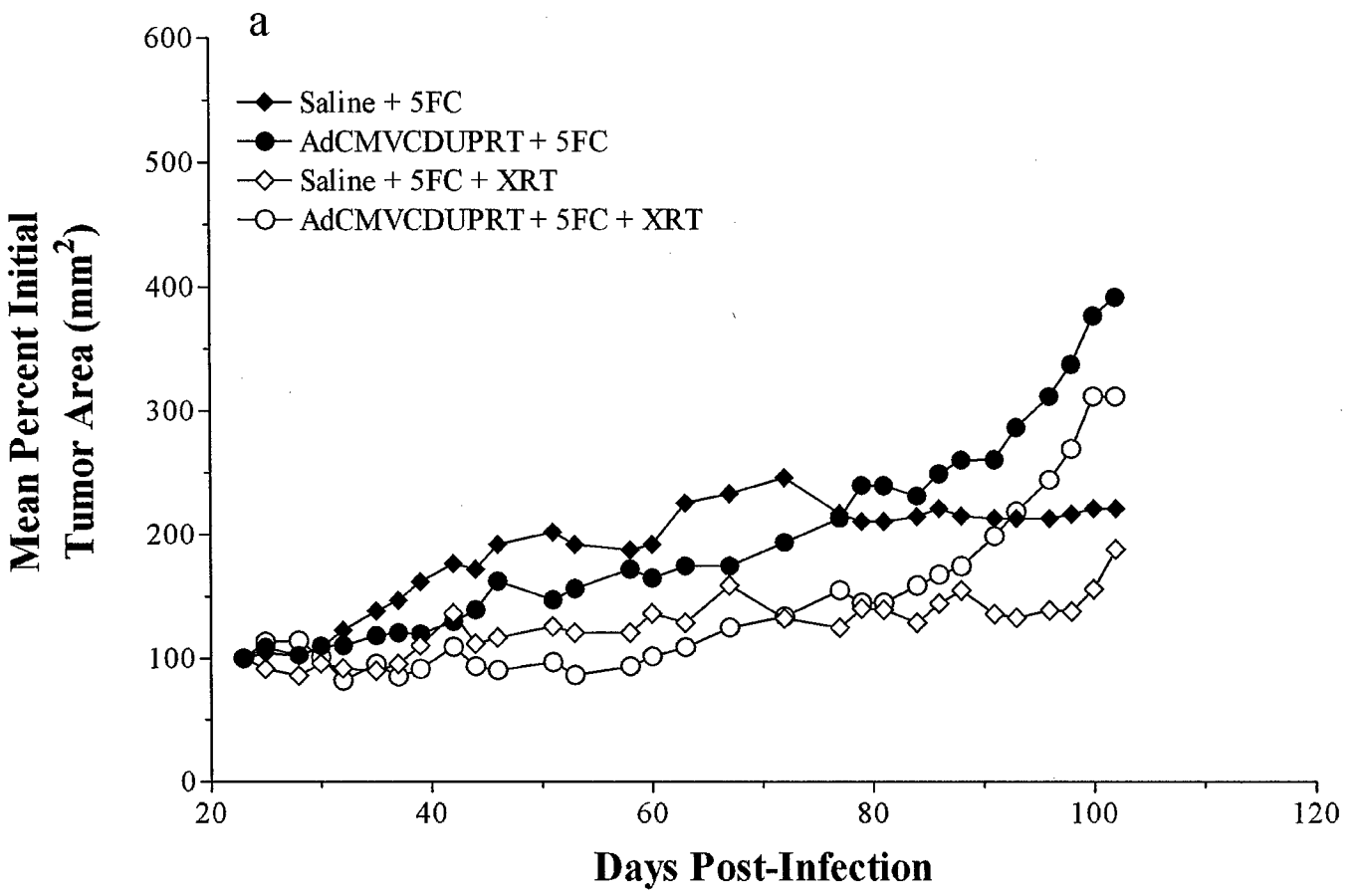
a
Saline + 5FC
AdCMVCDUPRT + 5FC
Saline + 5FC + XRT
AdCMVCDUPRT + 5FC + XRT
Mean Percent Initial Tumor Area (mm²)
600
500
400
300
200
100
0
20
40
60
80
100
120
Days Post-Infection

b

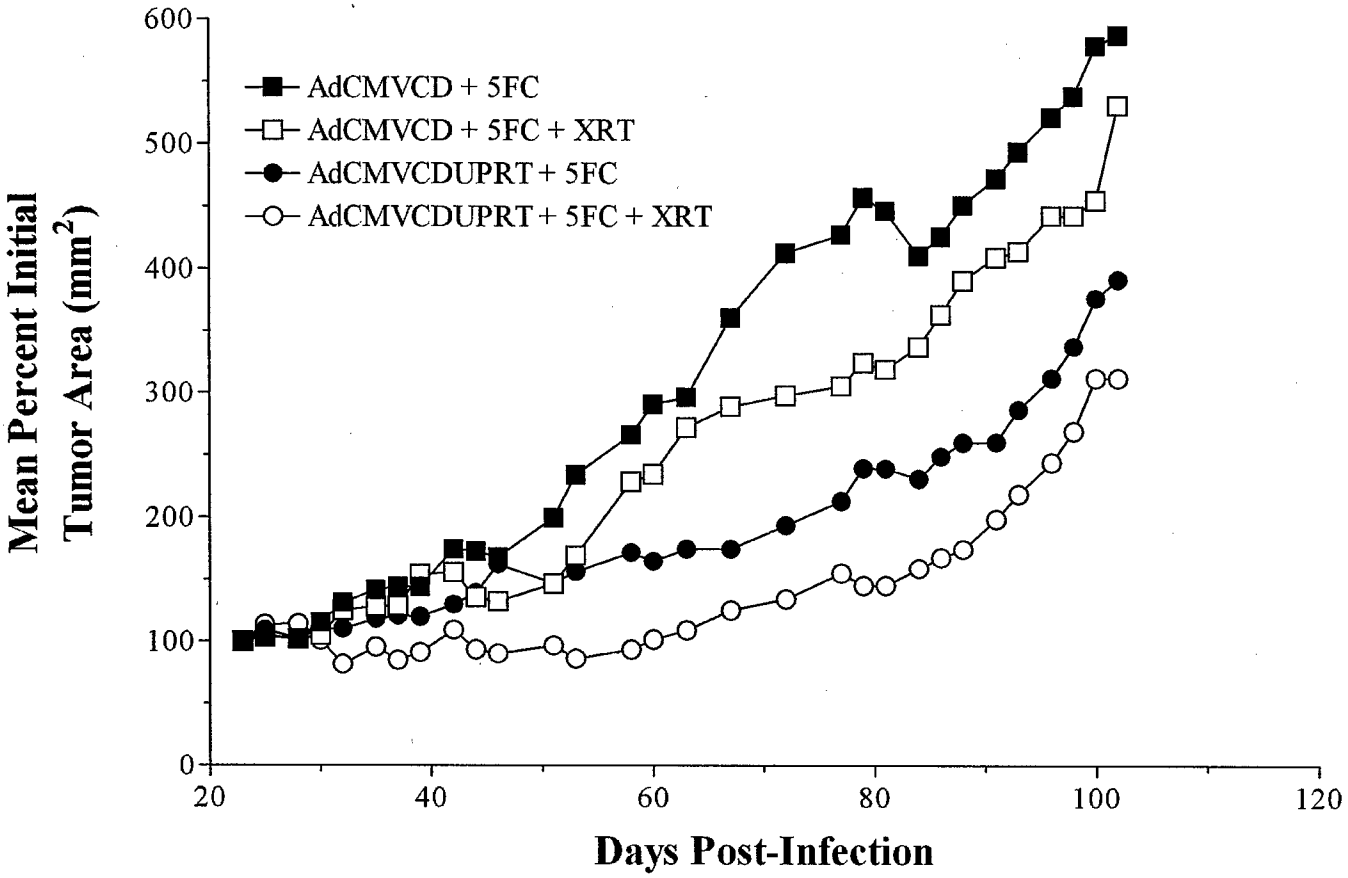
AdCMVCD + 5FC
AdCMVCD + 5FC + XRT
AdCMVCDUPRT + 5FC
AdCMVCDUPRT + 5FC + XRT
Mean Percent Initial Tumor Area (mm2)
0
100
200
300
400
500
600
20
40
60
80
100
120
Days Post-Infection